TABLE OF CONTENTS

LIST OF TABLES

Page

LIST OF FIGURES

LIST OF ALGORITHMS

LIST OF ABREVIATIONS

AAS	arbitrary antenna selection
AWGN	additive white Gaussian noise
BB	branch and bound
BD	block diagonalization
BFS	brute-force search
BS	base station
C-RAN	cloud radio access networks
CB	conjugate beamforming
CSI	channel state information
DL	downlink
DP	dynamic programming
DPC	dirty paper coding
ERP	equal received power
HetNets	heterogenous networks
IAS	iterative antenna selection
i.i.d.	independent and identically distributed
IPM	interior point method
MBS	macro base station
MILP	mixed-integer linear program

MIMO	multiple-input multiple-output
MINLP	mixed-integer nonlinear problem
MMSE	minimum mean square error
MRC	maximal ratio combining
MRT	maximal ratio transmission
OPA	optimal power allocation
RRH	remote radio heads
RTDD	reverse time division duplex
SBS	small base station
SET	spectral efficiency tradeoff
SINR	signal-to-interference-plus-noise ratio
SLNR	signal-to-leakage-plus-noise ratio
SNR	signal-to-noise ratio
TDD	time division duplex
UL	uplink
ZF	zero forcing
ZFB	zero forcing beamforming

LISTE OF SYMBOLS AND UNITS OF MEASUREMENTS

Symbols Common to Chapters

σ^2	noise variance
ν	path loss exponent
p_c	fixed power consumed by each activated RF chain
γ_{th}	minimum received SINR
ξ	reliability of channel estimation
B	bandwidth
$\lfloor . \rfloor$	floor function
$\lceil . \rceil$	ceiling function
$(x)^+$	$\max(0,x)$
$(.)^H$	Hermitian of a matrix
$(.)^T$	transpose of a matrix
$\mathbf{C}_N^S$	binomial coefficient $\frac{N!}{(N-S)!S!}$
$\mathbf{Tr}\{.\}$	trace of a square matrix
$\mathbf{E}\{.\}$	expectation
$\mid . \mid$	Euclidean norm of a vector
$\mathbf{I}_S$	identity matrix with trace S
$\| . \|_F$	Frobenius norm of a matrix
$\mathbf{0}_{M\times N}$	$M \times N$ matrix with zero entries

Symbols of Chapter 2

N	number of antennas
K	number of users
$\widehat{\mathbf{h}}_k$	estimated channel vector of user k
Σ	spatial correlation between transmit antennas
$\mathbf{g}_k$	small-scale fading channel vector of user k
β_k	large-scale fading component of user k
d_k	distance between the BS and user k
p_k	portion of power allocated to user k
α_n	antenna index that is set to 1 if antenna n is activated and to 0 otherwise
S	cardinality of the set of selected antennas
$\mathbf{W}(\alpha)$	beamforming matrix
p_{max}	power available at the BS
χ_k	user index that is set to 1 if user k is scheduled and to 0 otherwise
Λ	set of activated antennas
Ω	set of scheduled users

Symbols of Chapter 3

N	number of RRHs
K	number of users
L	number of frames

$\mathbf{g}_k(i)$	channel vector for user k at frame i
$h_{n,k}(i)$	small-scale fading channel coefficient at frame i
$\beta_{n,k}$	large-scale fading channel coefficient between user k and RRH n
$\mathbf{w}_k(i)$	beamforming vector for user k at frame i
$p_{n,k}(i)$	power allocated for user k on RRH n at frame i
B_{max}	maximal battery capacity
$A_n(i)$	amount of harvested energy at RRH n during frame i
$X_n(i)$	mount of consumed energy at RRH n during frame i
Ω	set of possible amount of harvested energy
$Q(\omega_m, \omega_j)$	state transition probability
$p^e_{n,k}(i)$	power drawn from the energy harvesting source
$p^g_{n,k}(i)$	power drawn from the grid
E_{fix}	fixed required energy
$E^e_n(i)$	energy drawn from the energy harvesting
$E^g_n(i)$	energy drawn from the grid source
$X^e_n(i)$	total energy drawn from the energy harvesting source by RRH n at frame i
T	duration of downlink transmission phase
$B_n(i)$	battery level of RRH n at frame i
$\alpha_{n,i}$	grid power weight factor
Δ_{tot}	total grid power consumption

Ω	set of removed links
p_{max}	max transmit power per-RRH
$\overline{\Gamma}$	set of RRHs to be activated
$\widehat{A}_n(i)$	predicted energy at RRH n during frame i

Symbols of Chapter 4

N	number of antennas at the MBS
M_s	number of antennas at SBS s
S	number of SBSs
Λ_s	set of users associated with SBS s
p_{max}^{mbs}	maximal transmit power of the MBS
p_{max}^{sbs}	maximal transmit power of the SBSs
$p^{ac,ul}$	transmit power of each user
$p_s^{bh,dl}, p_s^{bh,ul}$	portion of power allocated to SBS s on DL and UL respectively
$p_{s,k}^{ac,dl}$	power allocated for user k associated with SBS s
$\mathbf{H}_s$	channel matrix between the MBS and SBS s
$\mathbf{g}_{s,k}$	channel vector between user $k \in \Lambda_s$ and SBS s
λ	time splitting parameter
$r_{s,k}^{ac,ul}, r_{s,k}^{ac,dl}$	rate for user $k \in \Lambda_s$ on UL and DL respectively
$r_s^{bh,ul}, r_s^{bh,dl}$	rate for SBS s on UL and DL respectively

INTRODUCTION

The global mobile data traffic is growing exponentially due to the emergence of new wireless devices and applications. The mobile data traffic is various and composed of: video, web, games, VoIP, mobile to mobile and file sharing. Moreover, according to some projections, the number of connected devices may reach 50 billion in the next decade Gupta & Jha (2015). Hence, the design of new systems that support this large number of wireless devices is vital. In particular, these systems must support the traffic of the data exchanged while taking into account the energy efficiency of the proposed solutions. The challenge of designing future generations of cellular networks is to support the exponential increase in mobile data traffic. The researchers are in the process of designing the 5th generation (5G) cellular networks. Several guidelines are established to evolve 4G. Thus, some technologies will be adopted in the design of 5G cellular networks. A powerful strategy is to adopt large-scale multiple-input multiple-output (MIMO) systems (also known as massive MIMO) in 5G cellular networks Gupta & Jha (2015); Boccardi *et al.* (2014); Nam *et al.* (2013); Andrews *et al.* (2014); Larsson *et al.* (2014); Zheng *et al.* (2015); Yang & Hanzo (2015) which is the focus of this dissertation.

The organization of this thesis is as follows. The dissertation consists of 4 chapters. The first one presents the state of the art, the research domain, the objectives and the methodology. The three remaining chapters present each an article that has been published or under revision in a peer-reviewed journal. Chapter 2 presents the first article, which investigates the downlink of large-scale MIMO systems while considering non-negligible circuit power consumption. The optimal number of activated RF chains is derived considering both conjugate beamforming (CB) and zero forcing (ZF) and efficient antenna selection, user scheduling and power allocation algorithms that maximize the instantaneous sum-rate are devised. Chapter 3 presents the second article, which investigates a distributed large-scale MIMO system powered by hybrid energy sources. In order to minimize the total grid power cost, off-line and on-line energy management schemes are proposed. In addition, the problem feasibility is solved by proposing

a link removal algorithm. The energy efficiency is enhanced by investigating the remote radio head (RRH) on/off operation. Finally, chapter 4 presents the third article, which proposes a new transmission technique for heterogeneous networks with large-scale MIMO systems. The resource allocation problem is investigated under the proposed transmission technique. This technique is shown to be more efficient in terms of transmit power consumption than the conventional reverse time division duplex (RTDD) with bandwidth splitting.

Efficient resource allocation solutions related to system power are proposed in this thesis for wireless networks that incorporate large-scale MIMO systems under different assumptions and network architectures. The results in this thesis can be expanded when investigating further research problem given at the end of the dissertation.

CHAPTER 1

RESEARCH PROBLEM

1.1 Large-Scale MIMO Systems for Next Generation Wireless Networks

Large-scale MIMO is based on using few hundreds of antennas simultaneously to serve tens of users in the same time-frequency resource. The diversity of large number of antennas implies quasi-orthogonality between the users' channels in consequence of the law of large numbers. Hence, linear transmitters and receivers based on spatial multiplexing achieve high performance Boccardi *et al.* (2014). The benefits of large-scale MIMO systems are summarized in Gupta & Jha (2015); Zheng *et al.* (2015):

- Enhance the spectral efficiency and the energy efficiency.
- Implement low power and low cost RF chains.
- Reduce the latency.
- Simplify the access layer.

Now, we discuss the impact of large-scale antenna systems compared to conventional MIMO systems Gupta & Jha (2015). First, large-scale MIMO systems inherit the benefits of conventional MIMO systems. The introduction of a large number of antennas implies a quasi-orthogonality of the channels. Thus, maximum ratio transmission (MRT) and maximum ratio combiner receiver (MRC) are suitable as transmit and receive techniques while its performances are limited for conventional MIMO systems. In addition, the channel is no longer frequency selective. The transmission can be done on the same time-frequency resources. The increase in the number of transmit antennas requires more resources but the consumed power per antenna decreases. Thus, we may deploy low power RF chains with reduced complexity. On the other hand, deploying all the antennas on the same base station is practically difficult and distributed antenna systems are required. Channel estimation is very challenging in large-scale MIMO systems. In conventional MIMO systems, the base station sends pilot symbols to users. Users estimate the channels and send the estimated channel coefficients to the base

station. This is no longer feasible for large-scale MIMO systems due to the large number of antennas that will result in an increase of the size of control packets and the dominance of pilot contamination impact. Existing solutions of resource allocation in conventional MIMO systems become complex for a large number of antennas. Also, as the number of antennas becomes large, the power consumed by the circuit of RF chains is no longer neglected. Therefore, the consumed circuit power must be taken into consideration when optimizing system performance.

1.2 Motivation & Impact

In Andrews *et al.* (2014), the authors confirm that large-scale MIMO systems achieve the primary goal of 5G, which is the increase of the throughput. In addition, it can coexist with other 5G technologies especially mmWave systems and heterogeneous networks. Thus, the investigation of new interference management scheme is vital. Larsson *et al.* (2014) presents large-scale MIMO technology as a potential candidate for interconnecting Internet of Things systems since it reduce the latency. Furthermore, large-scale MIMO systems provide excellent performance with low-complexity transmit and receive systems Rusek *et al.* (2013); Yang & Marzetta (2013); Ngo *et al.* (2013b). In Pitarokoilis *et al.* (2012), the authors show that spatial multiplexing in large-scale MIMO systems allows to obtain a uniform channel gain coefficient. Thus, this technology eliminates the frequency selectivity of the propagation channel. Therefore, the transmission of data symbols can be done on a single carrier with near-optimal performance. Thus, this technique allows to considerably simplify the media access control layer.

The deployment of a large number of antennas at the same base station is challenging in practice, although this deployment offers the best performance. In Nam *et al.* (2013), the authors propose to deploy the antennas in a 3 diemntionnal grid and they modeled the propagation channel geometrically by a spatial channel model for several antenna configurations. New architectures based on a distributed deployment of the antennas have to be investigated. In Wang *et al.* (2014), the authors investigated the architectures and technologies of cellular networks that can be adopted in 5G. Specifically, they considered that large-scale MIMO systems could

be implemented in a distributed way, antennas will be deployed on several transmit devices in order to improve the spectral efficiency and energy efficiency with simple linear precoder.

The channel estimation in large-scale MIMO systems is usually done in time division duplex (TDD). Based on channel reciprocity, the channel gains are assumed to be the same at uplink and downlink. As a result, channel estimation proceeds by sending pilot symbols from users to the base station on uplink. Furthermore, since the number of orthogonal pilot symbol sequences is limited, there will be a reuse of the same pilot symbols in the adjacent cells. This generates an interference phenomenon between pilot symbols called *pilot contamination*, specially when the number of antennas is large. Overcoming this problem is challenging and is the subject of several research works Jose *et al.* (2011); Ngo *et al.* (2013a). Also, channel estimation in frequency division duplex (FDD) large-scale MIMO systems is very challenging.

The emergence of wireless communicating systems and their applications in several areas has sparked my interest in wireless communication research. Researchers and engineers are in the process of designing the next generation of cellular networks. Some challenges need to be addressed when designing 5G cellular networks. Some techniques are proposed to achieve the objectives defined by 5G. One of the major technologies is large-scale MIMO. These systems allow to increase the spectral efficiency as well as the energy efficiency. This has aroused interest on work on large-scale MIMO systems especially since several resource allocation problems are unachieved. This research direction is very timely. Large-scale MIMO systems may be deployed in a distributed manner and per-antenna power consumption is reduced. Thus, antennas can be powered by renewable energy sources. As a result, energy-efficient resource allocation solutions will be very useful for designing future wireless networks that respect the environment. Thus, this thesis proposes algorithmic solutions for resource allocation in large-scale MIMO systems of 5G cellular networks. These solutions can be implemented or can provide guiding ideas and insights for 5G network developers.

1.3 State of the Art and Its Limitations

Large-scale MIMO systems offer several gains needed by 5G cellular networks. These gains cannot be fully exploited without adequate resource allocation strategies. Thus, we present in this section the state of art of resource allocation problem in large-scale MIMO systems under different assumptions and network architectures. The following discussion includes the state of art and its limitations related to the specific problems in the articles that constitute chapters 2,3 and 4. More recent articles related to the general resource allocation problem in large-scale MIMO systems are included.

The research has investigated this resource allocation issue under different network architectures and assumptions. In Makki *et al.* (2016), the authors derive the minimum number of transmit/receive antennas satisfying outage probability constraint in point-to-point massive MIMO systems. The problems of antenna selection, user scheduling and power allocation were the focus of Benmimoune *et al.* (2015); Liu & Lau (2014); Gkizeli & Karystinos (2014); Guozhen *et al.* (2014); Gao *et al.* (2013); Amadori & Masouros (2016); Makki *et al.* (2017); Amadori & Masouros (2017); Garcia-Rodriguez *et al.* (2017). In Benmimoune *et al.* (2015), a joint antenna selection and user scheduling strategy is introduced for downlink massive MIMO systems assuming limited number of RF chains. In Liu & Lau (2014), the authors designed a joint antenna selection and power allocation scheme that maximizes the sum-rate in large cloud radio access networks. A polynomial time algorithm is proposed in Gkizeli & Karystinos (2014) to optimize the beamforming vector and select the set of antennas with maximum signal-to-noise ratio (SNR). Distributed massive MIMO systems with limited backhaul capacity are investigated in Guozhen *et al.* (2014). The antenna selection problem under limited number of RF chains is also investigated in Gao *et al.* (2013) for measured massive MIMO channels. In Amadori & Masouros (2016), a low complexity antenna selection algorithm is designed based on constructive interference for throughput maximization considering matched filter receiver in downlink massive MIMO systems. Also, Amadori & Masouros (2017) proposed sub-optimal antenna selection techniques by exploiting the constructive interference. In Makki *et al.* (2017), an efficient antenna selection method was developed based on genetic

algorithms. Finally, the authors of Garcia-Rodriguez *et al.* (2017) enhance the energy efficiency by including the switching connectivity based on antenna selection schemes.

Furthermore, resource allocation in large-scale MIMO was investigated considering the impact of pilot contamination in Nguyen *et al.* (2015); Ngo *et al.* (2014); Liu *et al.* (2017a); Zhang *et al.* (2015a); Zuo *et al.* (2017). In Nguyen *et al.* (2015), the authors proposed near-optimal solutions for power allocation and pilot assignment that maximize the spectral efficiency. Also, the spectral effciecny was optimzed in Ngo *et al.* (2014); Zhang *et al.* (2015a) by deriving the optimal training duration in Ngo *et al.* (2014) and tracktable expressions of the power allocation in Zhang *et al.* (2015a). Whereas, the energy efftciecny was optimzed in Zuo *et al.* (2017) by deriving the optimal number of activated antennas and of scheduled users. In Zuo *et al.* (2017), the authors investigate the optimal power splitting between pilot and data by including an efficient scheduling strategy.

Systems with co-located antennas suffer from highly-correlated channels and identical large-scale fading coeffcient. Also, the deployment of large number of antennas on the same base station presents many technical and implementation challenges Larsson *et al.* (2014). Alternatively, distributed large-scale MIMO systems can mitigate large-scale fading due to heterogeneous path-loss conditions. They are also shown to be more energy efficient than co-located antenna systems when taking exclusively into account the energy consumption of transmit and receive units He *et al.* (2014). A distributed large-scale MIMO system consists of a set of remote radio heads (RRHs) distributed over a large area. Each RRH contains single or multiple antennas and RF chains and is reliably connected to a central unit. Such systems may be also seen as the so-called cloud radio access networks (C-RAN) Saxena *et al.* (2016). The gains offered by distributed large-scale MIMO systems cannot be extracted without adequate resource management strategies as shown in Liu & Lau (2014); Joung *et al.* (2014); Van Chien *et al.* (2016); Feng *et al.* (2016). In Liu & Lau (2014), the sum-rate is maximized using an efficient joint antenna selection and power allocation scheme in large C-RAN. The authors in Joung *et al.* (2014) investigate the energy efficiency in distributed large-scale antenna systems and propose efficient power control, antenna selection and user clustering algorithms.

In Van Chien *et al.* (2016), the problem of transmit power minimization and user association is optimally solved for downlink multi-cell large-scale MIMO systems. Finally, antenna selection based on geometric programming was the focus of Feng *et al.* (2016).

We trust that because of the high number of antennas, the power consumed by the circuits of RF chains cannot be neglected anymore in the design of such systems. The literature proposes different circuit power consumption models, such as data rate dependent circuit power consumption model Ng *et al.* (2012b). However, related works consider a data rate independent circuit power consumption model and investigate the energy efficiency or the channel capacity Li *et al.* (2014); Ha *et al.* (2013); Ng *et al.* (2012a); Bjornson *et al.* (2014); Wang *et al.* (2016b); Pei *et al.* (2012); Ng & Schober (2012); Liu *et al.* (2017b). In Li *et al.* (2014), antennas are selected to maximize the energy efficiency for the downlink of massive MIMO systems. This work is extended to include multi-cell and multi-user case in Ha *et al.* (2013). In Ng *et al.* (2012a), the authors propose iterative resource allocation algorithm for energy efficiency maximization considering imperfect channel state information (CSI). The authors in Bjornson *et al.* (2014) study the impact of RF circuit imperfection on energy efficiency of massive MIMO systems and derive the achievable user rate in such systems. In Wang *et al.* (2016b), the energy efficiency is optimized in frequency division duplexing massive MIMO systems by deriving the training duration, training power and data power. The authors of Pei *et al.* (2012); Ng & Schober (2012) investigate the channel capacity for point-to-point transmission assuming MRT precoding when the RF circuit power consumption is not neglected. It was shown in Pei *et al.* (2012) that the capacity is not always maximized by activating all the RF chains. In Ng & Schober (2012), the authors study the optimal transmit power allocation and the number of transmit antennas based on an asymptotic approximation of the average capacity over channel realizations. Finally, tradeoff between the spectral efficiency and energy efficiency for massive MIMO systems with transmit antenna selection was investigated in Liu *et al.* (2017b).

Previous work that investigate large-scale MIMO systems with circuit power consumption seek to optimize the energy efficiency for different network architectures. Due to the lack of spectral

efficiency optimization in the literature, novel resource allocation schemes that optimize the system sum-rate have to be proposed. It is more efficient but challenging to optimize the instantaneous sum-rate for multi-user system over each channel realization.

Large-scale MIMO systems could be powered by energy harvesting which is a promising key technology for greening future wireless networks since it reduces network operation costs and carbon footprints Ku *et al.* (2016). Therefore, these systems can be powered by both energy harvested from renewable sources such as thermal, wind or solar Prasad *et al.* (2017) and energy bought from the electrical grid. In Zhou *et al.* (2014), a co-located point-to-point large-scale MIMO system powered by a single hybrid source was considered and an off-line energy management strategy is given. The design of energy efficient communication systems is challenging when considering large-scale MIMO powered by energy harvesting due to the large number of antennas and to the intermittent characteristics of renewable energy sources. Even though resource allocation was extensively investigated for large-scale MIMO systems or for energy harvesting systems, very little attention was given to the design of energy management schemes that implement both technologies.

The coexistence of large-scale MIMO, HetNets and wireless backhaul is a promising research direction since large-scale MIMO is a suitable solution to enable wireless backhauling Zhang *et al.* (2015b). The gains offered by the coexistence between the two technologies require adequate resource allocation and interference management strategies. Specifically, it is very challenging to manage the interference between the wireless backhaul links and the access links.

In HetNets with wireless backhaul, reverse time division duplex with bandwidth splitting was investigated in Sanguinetti *et al.* (2015); Wang *et al.* (2016a); Xia *et al.* (2017); Niu *et al.* (2018); Feng & Mao (2017) for managing interference between backhaul and access links. A large system analysis is performed in Sanguinetti *et al.* (2015) to find the asymptotic power allocation and beamforming vectors. An efficient cell association and bandwidth allocation algorithm that maximizes wireless backhaul link sum-rate was proposed in Wang *et al.* (2016a).

In Xia *et al.* (2017), the authors optimize the bandwidth division between access and backhaul links based on statistical channel information. An efficient iterative resource allocation algorithm that maximizes the throughput based on primal decomposition is developed in Niu *et al.* (2018). In Feng & Mao (2017), the authors proposed a distributed pilot allocation and user association algorithm that maximizes the sum rate of all users. Other works Li *et al.* (2015); Tabassum *et al.* (2016); Chen *et al.* (2016b) investigated wireless backhauling enabled by full duplex SBSs where the backhaul as well as the access links share the same spectrum band. In Li *et al.* (2015), the authors demonstrate that these systems have the potential to improve the sum-rate. In Tabassum *et al.* (2016), the portion of SBSs working on full duplex mode is optimized in order to improve several performance metrics. In addition of considering wireless backhaul communication enabled by full duplex, the authors of Chen *et al.* (2016b) assume that the SBSs are powered by energy harvesting sources. Efficient power allocation and user association algorithms are proposed in order to optimize the energy efficiency. Unfortunately, full duplex communication systems may suffer from self interference which lead to poor system performance, unless implementing high complexity interference cancellation techniques. Also, the access and backhaul spectrum bands could be separated in order to eliminate the inter-tier interference which was the focus of Zhao *et al.* (2015). The authors proposed efficient iterative algorithms to manage the inter-SBS interference and hence to maximize the number of active SBSs. Moreover, millimeter wave systems were incorporated in HetNets in order to eliminate the inter-tier interference Gao *et al.* (2015). An architecture based on millimeter wave communications is proposed in Hao & Yang (2018) and an efficient iterative power allocation algorithm is designed. However, these systems are vulnerable to severe pathloss attenuation compared to conventional spectrum band.

The interference in HetNets between the access links and the backhaul should be efficiently managed especially when the wireless backhaul is using large-scale MIMO. Moreover, to ensure an energy efficient network operation Li *et al.* (2016), novel energy efficient inter-tier interference management schemes have to be designed.

Large-scale MIMO may coexist with various 5G wirless technologies specifically physical layer security Chen *et al.* (2017, 2016a). Large-scale MIMO have been proposed to improve secrecy performance via exploiting spatial degrees of freedom. Moreover, resource allocation in secure wireless systems is a promising research direction. The problem of joint power and time allocation for secure communications is investigated in Chen *et al.* (2016a) by deriving tractable expressions of the allocated power.

Large-scale MIMO may also coexist with wireless energy transfer systems Yuan *et al.* (2015); Yang *et al.* (2015) which generate many challenging resource allocation problems. Specifically, the authors proposed an efficient transmission scheme that enable these systems and optimal power allocated is derived.

1.4 Research Domain, Objectives & Methodology

1.4.1 Research Domain

Next generation wireless networks are being designed to provide better performance while minimizing energy consumption. Large-scale MIMO systems offer various gains including increase in spectral efficiency and energy efficiency. Thus, these systems will be adopted in the 5G cellular networks. These gains can not be fully exploited without an optimal and adequate resource allocation. These resources, including antenna selection, user scheduling, power allocation, are directly related to energy consumption. Thus, optimal or nea-optimal resource allocation solutions may be proposed to improve the system performance while minimizing the network energy consumption. In addition, since the number of antennas is large in large-scale MIMO systems, the energy consumed in the RF channels is no longer neglected. Existing solutions for resource allocation in large-scale MIMO systems do not consider the energy consumed by the circuit. Perfect channel estimation is difficult to achieve in large-scale MIMO systems. Also, increasing the size of control messages significantly reduces the spectral efficiency. Thus, the proposed solutions must take into account imperfect channel estimation. The introduction of a large number of antennas on the same base station is challenging in practice.

Thus, a distributed deployment of antennas may be considered while the antennas are powered by renewable energy sources. Consequently, near-optimal algorithmic solutions with reduced complexity have to be proposed for this resource management problem. Furthermore, large-scale MIMO is a good candidate to enable wireless backhauling in heterogeneous networks and designing new interference management for these systems is vital.

1.4.2 Objectives

The main objectives of this thesis is to propose energy-aware resource allocation techniques for wireless networks that incorporate large-scale MIMO systems. The different network architectures and assumptions that are investigated, are summarized in the following items:

- The large number of antennas in large-scale MIMO systems involves that the power consumed by the circuit of RF chains is no longer negligible and the sum-rate is not maximized when activating all RF chains. Thus, the optimal number of activated RF chains that maximizes the system performance have to be investigated. Moreover, the objective is to find the optimal balance between the power consumed by the circuit of RF chains and the transmit power. In addition, efficient power allocation, antenna selection and user scheduling algorithms adapted to large-scale MIMO systems have to be designed. Imperfect channel estimation may be taken into consideration in the system model and analysis. Also, fairness may be investigated by assuming equal receive power among users.
- The deployment of large number of antennas on the same base station presents many technical and implementation challenges. Thus, a distributed large-scale antenna system have to be investigated. They may also incorporate energy harvesting that is a promising key technology for greening future wireless networks. Also, The grid energy source may compensate for the randomness and intermittency of the harvested energy. Hence, the objective is to design adequate resource management strategies for these systems. Specifically, on-line and off-line energy management solutions have to be proposed.

- The coexistence of large-scale MIMO, HetNets and wireless backhauling is a promising research direction since large-scale MIMO is a suitable solution to enable wireless backhauling. The interference management between the wireless backhaul links and the access links is very challenging. Thus, novel energy efficient inter-tier interference management schemes have to be designed. Moreover, the novel transmission technique may be more efficient in term of power consumption than the conventional reverse time division duplex with bandwidth splitting. Also, adequate resource allocation strategies have to be devised for these systems.

The above items represent the main objectives of this thesis. Each objective is addressed in a publication and presented in a unique chapter.

1.4.3 Methodology

The benefits of large-scale MIMO systems compared to conventional MIMO systems is the deployment of a very large number of antennas at the base station which allows to enhance significantly the spectral efficiency. An exhaustive bibliographic study of large-scale MIMO systems have to be completed. Also, a detailed study of the existing solutions for resource allocation problem in conventional MIMO systems have to be carried out. These studies allow to formulate challenging resource allocation problem in large-scale MIMO systems: antenna selection, user scheduling, power allocation, determination of the number of activated RF chains. Indeed, the implementation of a large-scale antenna system raises several challenges such as: channel estimation, pilot contamination, high complex resource allocation algorithms, complex transmit/receive techniques and non-negligible circuit power consumption.

Solving the formulated problems requires mathematical and algorithmic tools. In the first place, optimization theory is vital in order to be able to solve resource allocation problems specially convex optimization. Iterative algorithms may be proposed to solve joint optimization problems (i.e. power allocation and antenna selection). Since the optimal antenna selection and user scheduling problems are combinatorial and can be obtained with high complex brute-force and specially for antenna selection when the number of antennas is large, we use approximation

and heuristic algorithms to provide near-optimal solutions. In addition, we use dynamic programming, linear programming, greedy algorithm. Dynamic programming is based on solving sub-problems in an optimal way iteratively, the optimal global solution of the problem is obtained from these local solutions Puterman (2014). Linear programs can be effciently solved using interior point method Boyd & Vandenberghe (2004). The greedy algorithm solves the problem locally at each iteration of the algorithm. It is very useful for combinatorial optimization. Thus, it is used for antenna selection and user scheduling problems. The incorporation of energy harvesting in wireless networks requires on-line scheduling tools and probability theory due to the randomness of the harvested energy.

Simple beamforming techniques such as MRT and ZF may be considered in the system model since they allow to achieve high performance with reduced complexity. Practical propagation conditions are considered mainly the channel estimation errors and correlation between the channels.

Computer simulations, using tools such as MATLAB and CPLEX, are done to evaluate the system performance and validate the theoretical results.

1.5 Summary of Publications

- Joint optimal number of RF chains and power allocation for downlink massive MIMO systems

  This paper was published in the proceedings of IEEE Vehicular Technology Conference (VTC Fall), 2015 Hamdi & Ajib (2015a).
- Sum-rate maximizing in downlink massive MIMO systems with circuit power consumption

  This paper was published in the proceedings of IEEE International Conference on Wireless and Mobile Computing, Networking and Communications (WiMob), 2015 Hamdi & Ajib (2015b).
- Large-scale MIMO systems with practical power constraints

This paper was published in the proceedings of IEEE Vehicular Technology Conference (VTC Fall), 2016 Hamdi *et al.* (2016b).

- Resource allocation in downlink large-scale MIMO systems

  This article was published in IEEE Access in November 2016 Hamdi *et al.* (2016a).

- Energy management in large-scale MIMO systems with per-antenna energy harvesting

  This paper was published in the proceedings of IEEE International Conference on Communications (ICC), 2017 Hamdi *et al.* (2017a).

- Energy management in hybrid energy large-scale MIMO systems

  This article was published in IEEE Transactions on Vehicular Technology in September 2017 Hamdi *et al.* (2017b).

- On the resource allocation for HetNets with massive MIMO wireless backhaul

  This paper was published in the proceedings of IEEE Vehicular Technology Conference (VTC Fall), 2018 Hamdi *et al.* (2018).

- New efficient transmission technique for HetNets with massive MIMO wireless backhaul

  This article was submitted to IEEE Transactions on Wireless Communications in December 2017 and revised (Major revision) in April 2018.

CHAPTER 2

RESOURCE ALLOCATION IN DOWNLINK LARGE-SCALE MIMO SYSTEMS

Rami Hamdi[1,2], Elmahdi Driouch[1], Wessam Ajib[1]

[1] Department of Computer Science, Université du Québec à Montréal (UQÀM), QC, Canada
[2] École de Technologie Supérieure,
1100 Notre-Dame Ouest, Montréal, Québec, Canada H3C 1K3

This article was published in IEEE Access in November 2016 Hamdi *et al.* (2016a).

2.1 Abstract

This paper investigates the downlink of a single-cell base station (BS) equipped with a large-scale antenna array system while taking into account a non-negligible transmit circuit power consumption. This consumption involves that activating all RF chains does not always necessarily achieve the maximum sum-rate when the total BS transmit power is limited. This paper formulates a sum-rate maximization problem when a low complexity linear precoder such as conjugate beamforming or zero forcing beamforming, is used. The problem is first relaxed by assuming arbitrary antenna selection. In this case, we derive analytically the optimal number of activated RF chains that maximizes the sum-rate under either optimal power allocation or equal received power constraint for all users. Also, user scheduling algorithms are proposed when users require a minimum received signal-to-interference-plus-noise ratio. Two iterative user scheduling algorithms are designed. The first one is efficient in terms of fairness and the second one achieves the optimal performance. Next, the antenna selection is investigated and we propose iterative antenna selection algorithms that are efficient in terms of instantaneous sum-rate. Simulation results corroborate our analytical results and demonstrate the efficiency of the proposed algorithms compared to arbitrary and optimal brute force search antenna selection.

2.2 Introduction

It is widely accepted that large-scale multiple-input multiple-output (MIMO) (also known as massive MIMO) is a key technology to increase the spectral efficiency by several orders of magnitude, as requested for future 5G wireless networks and beyond Larsson *et al.* (2014); Zheng *et al.* (2015); Yang & Hanzo (2015). Large-scale MIMO is based on using few hundreds antennas simultaneously to serve tens of users in the same time-frequency resource. The diversity of large number of antennas implies quasi-orthogonality between the users' channels in consequence of the law of large numbers. Hence, linear transmitters and receivers such as zero forcing (ZF), maximal ratio transmission (MRT) and maximal ratio combining (MRC) achieve high performance Rusek *et al.* (2013); Yang & Marzetta (2013); Ngo *et al.* (2013b).

Large-scale MIMO systems offers Zheng *et al.* (2015) higher energy efficiency, higher spectral efficiency, lower latency and simpler access layer. These gains cannot be fully exploited without adequate resource allocation strategies. Hence, the research have investigated this resource allocation issue under different network architectures and assumptions. In Makki *et al.* (2016), the authors derive the minimum number of transmit/receive antennas satisfying outage probability constraint in point-to-point massive MIMO systems. The problems of antenna selection, user scheduling and power allocation were the focus of Benmimoune *et al.* (2015); Liu & Lau (2014); Gkizeli & Karystinos (2014); Guozhen *et al.* (2014); Gao *et al.* (2013); Amadori & Masouros (2016). In Benmimoune *et al.* (2015), a joint antenna selection and user scheduling strategy is introduced for downlink massive MIMO systems assuming limited number of RF chains. In Liu & Lau (2014), the authors designed a joint antenna selection and power allocation scheme that maximizes the sum-rate in large cloud radio access networks. A polynomial time algorithm is proposed in Gkizeli & Karystinos (2014) to optimize the beamforming vector and select the set of antennas with maximum signal-to-noise ratio (SNR). Distributed massive MIMO systems with limited backhaul capacity are investigated in Guozhen *et al.* (2014). The antenna selection problem under limited number of RF chains is also investigated in Gao *et al.* (2013) for measured massive MIMO channels. In Amadori & Masouros (2016), a low complexity antenna selection algorithm is designed based on constructive inter-

ference for throughput maximization considering matched filter receiver in downlink massive MIMO systems.

We trust that because of the high number of antennas, the power consumed by the circuits of RF chains cannot be neglected anymore in the design of such systems. The literature proposes different circuit power consumption models, such as data rate dependent circuit power consumption model Ng *et al.* (2012b). However, related works consider a data rate independent circuit power consumption model and investigate the energy efficiency or the channel capacity Li *et al.* (2014); Ha *et al.* (2013); Ng *et al.* (2012a); Bjornson *et al.* (2014); Wang *et al.* (2016b); Pei *et al.* (2012); Ng & Schober (2012). In Li *et al.* (2014), antennas are selected to maximize the energy efficiency for the downlink of massive MIMO systems. This work is extended to include multi-cell and multi-user case in Ha *et al.* (2013). In Ng *et al.* (2012a), the authors propose iterative resource allocation algorithm for energy efficiency maximization considering imperfect channel state information (CSI). The authors in Bjornson *et al.* (2014) study the impact of RF circuit imperfection on energy efficiency of massive MIMO systems and derive the achievable user rate in such systems. In Wang *et al.* (2016b), the energy efficiency is optimized in frequency division duplexing massive MIMO systems by deriving the training duration, training power and data power. The authors of Pei *et al.* (2012); Ng & Schober (2012) investigate the channel capacity for point-to-point transmission assuming MRT precoding when the RF circuit power consumption is not neglected. It was shown in Pei *et al.* (2012) that the capacity is not always maximized by activating all the RF chains. In Ng & Schober (2012), the authors study the optimal transmit power allocation and the number of transmit antennas based on an asymptotic approximation of the average capacity over channel realizations.

Previous work that investigate large-scale MIMO systems with circuit power consumption seek to optimize the energy efficiency for different network architectures. Due to the lack of spectral efficiency optimization in the literature, this paper proposes novel resource allocation schemes that optimize the system sum-rate. It is more efficient but challenging to optimize the instantaneous sum-rate for multi-user system over each channel realization. Hence, we derive

in Hamdi & Ajib (2015a) the optimal number of RF chains and the optimal power allocation that maximize the sum-rate considering conjugate beamforming (CB) and assuming random antenna selection. In this paper, the main contributions can be summarized as follows:

- The problem of sum-rate maximization under circuit power consumption constraint in massive MIMO is formulated as a mixed integer nonlinear program.
- Assuming an arbitrary antenna selection (AAS), the optimal power allocation (OPA) is derived for both CB and zero forcing beamforming (ZFB). Next, the approximation of the optimal number of RF chains is analytically found under either OPA or equal received power (ERP) constraint.
- User scheduling algorithms, with AAS, are also proposed in order to improve the achievable sum-rate when ERP constraint is used.
- Iterative antenna selection (IAS) algorithms that are efficient in terms of instantaneous sum-rate are proposed for both CB and ZFB. The proposed algorithms jointly compute the number of RF chains to be activated, select the best antennas and allocate power among users. Hence, they allow determining the near-to-optimal balance between the amount of power consumed at RF chains and the amount of power used for transmission.
- Simulations validate the analytical results and show the efficiency of proposed algorithms.

The rest of the paper is organized as follows. In Section 2.3, the system model is presented. The joint optimization problem is formulated in Section 2.4. Assuming arbitrary antenna selection in Section 2.5, the system sum-rate is maximized for both cases when allocating power optimally among users and when assuming equal received power per user. Then, iterative antenna selection and power allocation algorithms are proposed in Section 2.6 to maximize the instantaneous system sum-rate. Computational complexity of different algorithms are calculated in Section 2.7. Numerical and simulation results are shown and discussed in Section 2.8. Finally, we conclude and discuss the main findings in Section 2.9.

2.3 System Model

2.3.1 Channel and Signal Model

The downlink of a single cell large-scale MIMO system shown in Fig. 2.1 is investigated. The base station (BS) is equipped with a large number of antennas N serving K single-antenna users with $N \gg K$. Let $\mathbf{g}_k \in \mathbb{C}^{N\times 1}$ denotes the small-scale fading channel vector for user k, that is assumed to be quasi-static Gaussian independent and identically distributed (i.i.d.) slow fading channel. Since users are assumed to be spatially separated, matrix Σ describes the spatial correlation only between transmit antennas, the well-known Kronecker correlation model is considered Chuah *et al.* (2002). The channel vector $\mathbf{h}_k \in \mathbb{C}^{1\times N}$ is given by $\mathbf{h}_k^T = \Sigma^{\frac{1}{2}}\mathbf{g}_k$. Assuming that the BS has imperfect channel state information (CSI), the minimum mean square error (MMSE) estimated channel vector satisfies Rusek *et al.* (2013):

$$\widehat{\mathbf{h}}_k^T = \Sigma^{\frac{1}{2}}(\xi\mathbf{g}_k + \sqrt{1-\xi^2}\mathbf{e}), \tag{2.1}$$

where $0 \leq \xi \leq 1$ denotes the reliability of the estimate and $\mathbf{e}$ is an error vector with Gaussian i.i.d. entries with zero mean and unit variance.

The antenna array is sufficiently compact so that the distances between a particular user and the BS antennas are assumed equal. Considering only path loss, the large-scale fading component is expressed as $\beta_k = \zeta\frac{d_k^{-\nu}}{d_0^{-\nu}}$, where ν is the path loss exponent, d_k is the distance between the BS and user k, d_0 is the reference distance and ζ is a constant related to the carrier frequency and reference distance. Vector $\mathbf{p} = [p_1, p_2, ..., p_K]$ denotes the portions of power allocated to the K users. As discussed before, this work deals with the practical case of non negligible circuit power consumption. Hence, the system performance can no longer be maximized by activating all the transmit antennas. Therefore, this work seeks to optimize the number of activated RF chains where only a subset of antennas is activated. We define α_n as an antenna index that is set to 1 if antenna n is activated and to 0 otherwise and we define the vector $\alpha = [\alpha_1\alpha_2...\alpha_N]$. We also define $S = \sum_{n=1}^{N}\alpha_n$ as the cardinality of the set of selected antennas. In consequence,

the downlink channel matrix between the selected antennas and the K users can be defined as $\mathbf{H}(\alpha) = [\mathbf{h}_1(\alpha), \mathbf{h}_2(\alpha), ..., \mathbf{h}_K(\alpha)]$ where $\mathbf{h}_k(\alpha)^T = \Sigma(\alpha)^{\frac{1}{2}}\mathbf{g}_k(\alpha)$. The beamforming matrix is defined as $\mathbf{W}(\alpha) = [\mathbf{w}_1(\alpha)\mathbf{w}_2(\alpha)...\mathbf{w}_K(\alpha)]$, where $\mathbf{w}_k(\alpha) = [w_{s,k}(\alpha)]_{s=1:S} \in \mathbb{C}^{S\times 1}$ is the k^{th} beamforming vector for user k. Hence, the signal received by user k can be written as:

$$y_k = \sqrt{p_k}\sqrt{\beta_k}\mathbf{h}_k(\alpha)\mathbf{w}_k(\alpha)s_k + n_k + \sum_{i=1, i\neq k}^{K} \sqrt{p_i}\sqrt{\beta_k}\mathbf{h}_k(\alpha)\mathbf{w}_i(\alpha)s_i, \tag{2.2}$$

where s_k is a data symbol with unit energy and n_k is assumed to be additive white Gaussian noise (AWGN) with zero mean and variance σ^2. Hence, the received signal-to-interference-plus-noise ratio (SINR) at user k is expressed as:

$$\gamma_k(\mathbf{p}, \alpha) = \frac{p_k\beta_k \mid \mathbf{h}_k(\alpha)\mathbf{w}_k(\alpha) \mid^2}{\sum_{i=1, i\neq k}^{K} p_i\beta_k \mid \mathbf{h}_k(\alpha)\mathbf{w}_i(\alpha) \mid^2 + \sigma^2}. \tag{2.3}$$

The sum-rate is given as:

$$R(\mathbf{p}, \alpha) = \sum_{k=1}^{K} B\log_2(1 + \gamma_k(\mathbf{p}, \alpha)), \tag{2.4}$$

where B is the bandwidth.

The optimal precoding to achieve the sum-rate in MIMO systems is dirty paper coding (DPC) Caire & Shamai (2003). Since DPC implementation is impractical due to its high complexity, we consider two linear beamforming strategies: ZFB and CB.

2.3.1.1 Conjugate Beamforming (CB)

The CB matrix is given by $\mathbf{W}^{CB}(\alpha) = \frac{\widehat{\mathbf{H}}(\alpha)^H}{\eta_{CB}(\alpha)}$, where the normalization factor is defined as $\eta_{CB}(\alpha) = \| \widehat{\mathbf{H}}(\alpha)^H \|_F$. Hence, the received SINR at user k is given by:

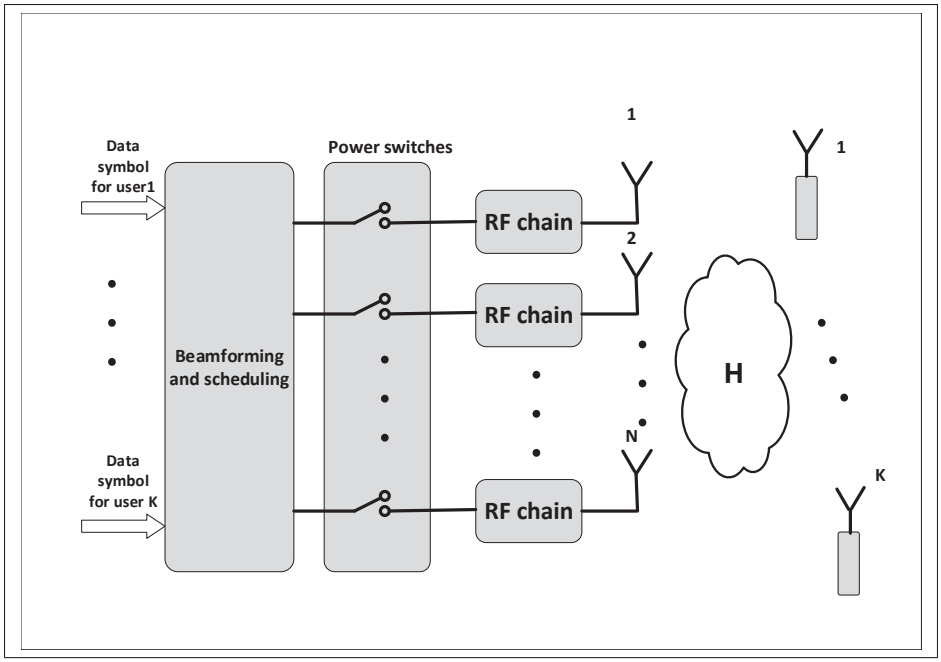

Figure 2.1 Large-scale MIMO system with transmit antenna selection.

$$\gamma_k^{CB}(\mathbf{p},\alpha) = \frac{p_k \frac{\beta_k}{\eta_{CB}(\alpha)^2} \mid \mathbf{h}_k(\alpha)\widehat{\mathbf{h}}_k(\alpha)^H \mid^2}{\sum_{i=1,i\neq k}^{K} p_i \frac{\beta_k}{\eta_{CB}(\alpha)^2} \mid \mathbf{h}_k(\alpha)\widehat{\mathbf{h}}_i(\alpha)^H \mid^2 + \sigma^2}. \tag{2.5}$$

2.3.1.2 Zero Forcing Beamforming (ZFB)

The zero forcing beamforming matrix is expressed as $\mathbf{W}^{ZF}(\alpha) = \frac{\widehat{\mathbf{H}}(\alpha)^H(\widehat{\mathbf{H}}(\alpha)\widehat{\mathbf{H}}(\alpha)^H)^{-1}}{\eta_{ZF}(\alpha)}$, where the normalization factor is defined as $\eta_{ZF}(\alpha) = \sqrt{\mathbf{Tr}\{(\widehat{\mathbf{H}}(\alpha)\widehat{\mathbf{H}}(\alpha)^H)^{-1}\}}$. The received SINR at user k is given by:

$$\gamma_k^{ZF}(\mathbf{p},\alpha) = \frac{p_k\beta_k \mid \mathbf{h}_k(\alpha)\mathbf{w}_k^{ZF}(\alpha) \mid^2}{\sum_{i=1,i\neq k}^{K} p_i\beta_k \mid \mathbf{h}_k(\alpha)\mathbf{w}_i^{ZF}(\alpha) \mid^2 + \sigma^2}. \tag{2.6}$$

2.3.2 Circuit Power Consumption Model

A circuit power consumption model similar to the one used in Li *et al.* (2014); Ha *et al.* (2013); Ng *et al.* (2012a); Bjornson *et al.* (2014); Ng & Schober (2012); Pei *et al.* (2012); Kumar & Gurugubelli (2011) is adopted in this paper. The circuit power consumption is expressed in function of the sum of consumptions of different analog and digital components as:

$$p_{cp} = p_{fix} + \sum_{n=1}^{N} \alpha_n.(p_{dac} + p_{mix} + p_{fil}) + p_{syn} + p_{out}/\delta, \tag{2.7}$$

where p_{fix} is a constant consumed power for the base-band unit, $p_c = p_{dac} + p_{mix} + p_{fil}$ denotes the fixed power consumed by each activated RF chain (the sum of the powers consumed by the digital to analog converter, mixer and filter), p_{syn} denotes the power consumed by the frequency synthesizer, $p_{out} = \sum_{k=1}^{K} p_k$ is the output transmit power and δ is the efficiency of the power amplifier.

Hence, the power consumption constraint can be expressed as:

$$\sum_{k=1}^{K} p_k/\delta + \sum_{n=1}^{N} \alpha_n.p_c \leq p_{max} - p_{fix} - p_{syn}, \tag{2.8}$$

where p_{max} denotes the power available at the BS.

2.4 Problem Formulation

The aim of this work is to maximize the system sum-rate. Since the total available power at BS is limited, the circuit power consumption implies that activating all RF chains does not achieve the maximum sum-rate. Hence, an adequate antenna selection strategy should be designed in order to maximize the sum-rate. Moreover, the available power should be optimally divided into a portion that is dedicated to RF chains, and a second one used for transmission. The system sum-rate is maximized when the power allocated for transmission p_{out} is optimally

allocated among users. Hence, regardless of the used beamformer the main problem can be formulated as:

$$\begin{aligned} \underset{\mathbf{p},\alpha}{\text{maximize}} \quad & R(\mathbf{p},\alpha) \\ \text{subject to} \quad & C1: \sum_{k=1}^{K} p_k/\delta + S\cdot p_c \leq p_{max} - p_{fix} - p_{syn}, \\ & C2: S \geq K, \\ & C3: \alpha_n \in \{0,1\}, n = 1..N. \end{aligned} \tag{2.9}$$

The formulated problem is in general a mixed-integer nonlinear problem (MINLP) because of its combinatorial nature and the non-linearity of the objective function. Antenna selection in MIMO wireless communication is known to be an NP-hard problem Dua *et al.* (2006); Luo & Zhang (2008). Consequently, the problem is combinatorial with exponential complexity growth in N.

Under conjugate beamforming, the objective function is non-convex due to multi-user interference. Hence even when α is fixed, the formulated problem is still non-convex and the well known water-filling algorithm does not lead to optimal power allocation among users Driouch & Ajib (2012), (Boyd & Vandenberghe, 2004, sec. 5.5.3). However, under ZFB and for a given set of selected antennas, water-filling gives the optimal power allocation among users for perfect CSI scenario.

Fairness may be investigated by imposing the constraint of equal received power at each user. The following constraint may be added to problem (2.9) in order to obtain a fair optimization:

$$C4: \gamma_k(\mathbf{p},\alpha) = \gamma_p(\mathbf{p},\alpha), \quad \forall (k,p) \in \{1,...,K\}^2. \tag{2.10}$$

Moreover, complete fairness may lead to low sum-rate and hence scheduling users with minimum received SINR becomes of significant importance. Thus, it has to be investigated in order to enhance system performance.

2.5 Arbitrary Antenna Selection (AAS)

Due to the large number of antennas at the BS, optimal antenna selection is computationally very complex. Therefore, we first study a low complexity antenna selection, namely arbitrary antenna selection (AAS) that works as follows: the index of the first activated antenna n_0 is chosen randomly in $\{1 : \lfloor N/S \rfloor\}$. The rest of $S-1$ activated antennas are chosen such that each two successive antennas have the same footstep $\lfloor N/S \rfloor$. The set of activated antennas can be analytically expressed as $\Lambda = \{n_0 + \lfloor N/S \rfloor \cdot s, s = 0 : S-1\}$. This way of choosing arbitrary antennas implies that each two activated antennas are distant enough to lower the transmit spatial correlation. Hence, the analytical derivations presented in this section assume that $\Sigma(\alpha) \rightarrow \mathbf{I}_S$ and hence the estimated channel vector for user k is given by $\widehat{\mathbf{h}}_k^T = (\xi \mathbf{g}_k + \sqrt{1-\xi^2}\mathbf{e})$.

First, we derive analytically the optimal power allocation among users for both CB and ZFB. Then, the achieved sum-rate averaged over channel realizations is expressed in function of S the number of activated RF chains. Based on that, the optimal value of S can be derived iteratively. Next, we consider the sum-rate maximization problem under a fairness constraint by assuming equal received power. The received SINR is derived analytically, which allows to determine analytically the optimal number of RF chains maximizing the sum-rate. Since the fairness constraint leads to low sum-rate because some users may require high transmit power, we propose user scheduling algorithms in order to select users that respect a minimum received SINR constraint and maximize the system sum-rate.

The whole AAS procedure can be summarized in the following three steps:

- compute the optimal number of activated RF chains S^* maximizing the average sum rate;
- select S^* antennas arbitrary as explained above;
- perform an optimal or near-optimal power allocation.

It is to be noted that with OPA and ERP, all users are served; whereas, user scheduling algorithms serve only the subset of users that achieve the required SINR constraint.

2.5.1 Optimal Power Allocation (OPA)

As AAS is assumed, the sum-rate $\widetilde{R}(\mathbf{p},S)$ can be maximized by activating the optimal number of RF chains and applying the optimal power allocation. The problem in (2.9) becomes:

$$\begin{aligned} \underset{\mathbf{p},S}{\text{maximize}} \quad & \widetilde{R}(\mathbf{p},S) \\ \text{subject to} \quad & C1, C2. \end{aligned} \tag{2.11}$$

2.5.1.1 CB

Under CB, the sum-rate is a non-convex function due to the multi-user interference term. The interference term can be asymptotically approximated when K and S are large but finite, Zhao *et al.* (2013) as:

$$\begin{aligned} \sum_{i=1,i\neq k}^{K} p_i \mid \mathbf{h}_k(\alpha)\widehat{\mathbf{h}}_i(\alpha)^H \mid^2 &\rightarrow p_{out}\mathbf{E}\{\mid \mathbf{h}_k(\alpha)\widehat{\mathbf{h}}_i(\alpha)^H \mid^2\} \\ &\approx S p_{out}. \end{aligned} \tag{2.12}$$

Hence, the sum-rate can be approximated by:

$$\widetilde{R}^{CB}(\mathbf{p},S) \approx \sum_{k=1}^{K} B\log_2\left(1+\frac{p_k\beta_k \mid \mathbf{h}_k(\alpha)\widehat{\mathbf{h}}_k(\alpha)^H \mid^2}{\beta_k S p_{out}+\sigma^2\eta_{CB}(\alpha)^2}\right). \tag{2.13}$$

The sum-rate function becomes concave in $\mathbf{p}$ and the power allocation among users can be given by water-filling:

$$p_{k,CB} = \left(\frac{1}{\ln(2)\mu_{CB}} - \frac{\beta_k S p_{out}+\sigma^2\eta_{CB}(\alpha)^2}{\beta_k \mid \widehat{\mathbf{h}}_k(\alpha)\widehat{\mathbf{h}}_k(\alpha)^H \mid^2}\right)^+, \tag{2.14}$$

where μ_{CB} is the water level.

The closed-form expression for the optimal number of RF chains S^*_{CB} is intractable due to the complex expression of $\widetilde{R}^{CB}$. However, it can be numerically determined by an iterative search over the set $\{K,...,\min(N_{RF},N)\}$. This search terminates when the sum-rate averaged over channel realizations $\widetilde{R}^{CB}$ starts decreasing.

It is to be noted that $N_{RF} = \lfloor (p_{max} - p_{fix} - p_{syn})/p_c \rfloor > K$ represents the maximum number of RF chains that can be powered (assuming no transmit power) by the system.

2.5.1.2 ZFB

Considering ZFB, the sum-rate function is convex in $\mathbf{p}$ for perfect CSI scenario when $\xi \to 1$ and the transmit power can be optimally shared among users using the water-filling algorithm as:

$$p^0_{k,ZF} = \left(\frac{1}{\ln(2)\mu_{ZF}} - \frac{\sigma^2 \eta_{ZF}(\alpha)^2}{\beta_k} \right)^+, \tag{2.15}$$

where μ_{ZF} is the water level.

For imperfect CSI scenario, the interference term can be asymptotically approximated when K and S are large but finite as:

$$\tau = \sum_{i=1, i\neq k}^{K} p_i \mid \mathbf{h}_k(\alpha)\mathbf{w}_i^{ZF}(\alpha) \mid^2 \to p_{out}\mathbf{E}\{\mid \mathbf{h}_k(\alpha)\mathbf{w}_i^{ZF}(\alpha) \mid^2\} \approx p_{out}\frac{1-\xi^2}{K}. \tag{2.16}$$

Therefore, the portion of power allocated to user k can be adequately given by:

$$p_{k,ZF} = \left(\frac{1}{\ln(2)\mu_{ZF}} - \frac{(\beta_k \tau + \sigma^2)\eta_{ZF}(\alpha)^2}{\xi^2 \beta_k} \right)^+. \tag{2.17}$$

The achieved sum-rate can be approximated in order to determine analytically the number of activated RF chains. By assuming that all users are served with transmit power $p_k = \frac{1}{\ln(2)\mu_{ZF}} - \frac{(\beta_k \tau + \sigma^2)\eta_{ZF}(\alpha)^2}{\xi^2 \beta_k}$. Hence, the water level can be derived from $C1$ as:

$$\frac{1}{\ln(2)\mu_{ZF}} = \frac{1}{K} \left(p_{out} + \frac{\eta_{ZF}(\alpha)^2}{\xi^2} (K\tau + \sigma^2 \sum_{j=1}^{K} \frac{1}{\beta_j}) \right). \tag{2.18}$$

The term $\eta_{ZF}(\alpha)^2$ is approximated Rusek *et al.* (2013); Yang & Marzetta (2013); Ngo *et al.* (2013b), when K and S are large but finite, as follows:

$$\frac{1}{\eta_{ZF}(\alpha)^2} \approx \frac{S}{K} - 1. \tag{2.19}$$

Theses approximations are validated later by simulations. Hence, the sum-rate averaged over the channel realizations can be approximated as:

$$\widetilde{R}^{ZF} \approx \sum_{k=1}^{K} B \cdot \log_2 \left(\frac{\beta_k \xi^2}{\beta_k \tau + \sigma^2} \left(\frac{p_{out}}{K^2}(S-K) + \tau + \frac{\sigma^2}{K} \sum_{j=1}^{K} \frac{1}{\beta_j} \right) \right). \tag{2.20}$$

The expression of $\widetilde{R}^{ZF}$ is concave in S. However, the closed-form expression for the optimal number of RF chains S^*_{ZF} is intractable due to the complex expression of $\widetilde{R}^{ZF}$ but can be numerically determined by an iterative search over the set $\{K, ..., \min(N_{RF}, N)\}$. This search terminates when the sum-rate averaged over channel realizations $\widetilde{R}^{ZF}$ starts decreasing.

For perfect CSI scenario when $\xi \to 1$ and $\tau \to 0$, the optimal number of RF chains can be derived analytically:

$$S_{ZF}^{*} \approx \begin{cases} \lfloor \phi_{ZF} \rfloor, & \text{if } \overline{R}^{ZF}(\lfloor \phi_{ZF} \rfloor) > \overline{R}^{ZF}(\lceil \phi_{ZF} \rceil) \\ & \text{or } \lfloor \phi_{ZF} \rfloor = N_{RF} \\ \lceil \phi_{ZF} \rceil, & \text{otherwise.} \end{cases} \tag{2.21}$$

where

$$\phi_{ZF} = \frac{p_{max} - p_{fix} - p_{syn} + K.p_c}{2p_c}. \tag{2.22}$$

2.5.2 Equal Received Power (ERP)

This section discusses the case of complete fairness between users by having equal received power at each user, or more precisely equal SINR. The following constraint is imposed:

$$\gamma_k(\mathbf{p}, S) = \gamma_p(\mathbf{p}, S), \quad \forall (k,p) \in \{1, ..., K\}^2. \tag{2.23}$$

The problem becomes the same as in (2.11) in addition to the constraint given in (2.23). The transmit power allocated to each user is derived for both CB and ZFB and the optimal number of RF chains maximizing the average sum-rate is derived analytically.

2.5.2.1 CB

Considering CB, the transmit power allocated to user k under fairness constraint is derived by solving (2.23). It is given by:

$$p_{k,CB} = \frac{p_{out}}{a_k \sum_{j=1}^{K} \frac{1}{a_j}}, \tag{2.24}$$

where $a_k = \frac{\beta_k |\widehat{\mathbf{h}}_k(\alpha)\widehat{\mathbf{h}}_k(\alpha)^H|^2}{\beta_k S p_{out} + \sigma^2 \eta_{CB}(\alpha)^2}, k \in \{1,...,K\}$.

As the transmit power is derived, the sum-rate averaged over channel realizations should be evaluated in order to derive analytically the optimal number of RF chains. The normalization factor $\eta_{CB}(\alpha)^2$ can be approximated as $\eta_{CB}(\alpha)^2 \approx K.S$ as in Rusek *et al.* (2013), $\mathbf{E}\{|\widehat{\mathbf{h}}_k(\alpha)\widehat{\mathbf{h}}_k(\alpha)^H|^2\} = S^2$ and $\mathbf{E}\{|\mathbf{h}_k(\alpha)\widehat{\mathbf{h}}_k(\alpha)^H|^2\} = \xi^2 S^2$. These approximations will be validated later by simulations. Hence, the sum-rate averaged over the channel realizations can be approximated as:

$$\widetilde{R}^{CB} \approx K \cdot B \cdot \log_2 \left(1 + \frac{1}{K} \frac{\xi^2 S}{1 + \frac{\sigma^2}{p_{out}} \sum_{j=1}^{K} \frac{1}{\beta_j}} \right). \tag{2.25}$$

The optimal number of RF chains can be analytically derived as:

$$S^*_{CB} \approx \begin{cases} \lfloor \phi_{CB} \rfloor, & \text{if } \widetilde{R}^{CB}(\lfloor \phi_{CB} \rfloor) > \widetilde{R}^{CB}(\lceil \phi_{CB} \rceil) \\ & \text{or } \lfloor \phi_{CB} \rfloor = N_{RF} \\ \lceil \phi_{ZF} \rceil, & \text{otherwise.} \end{cases} \tag{2.26}$$

where

$$\phi_{CB} = \frac{\delta \cdot (p_{max} - p_{fix} - p_{syn}) + \sigma^2 \sum_{j=1}^{K} \frac{1}{\beta_j} - \kappa 1}{\delta \cdot p_c} \tag{2.27}$$

and

$$\kappa 1 = \sqrt{\sigma^2 \sum_{j=1}^{K} \frac{1}{\beta_j} . (\delta \cdot (p_{max} - p_{fix} - p_{syn}) + \sigma^2 \sum_{j=1}^{K} \frac{1}{\beta_j})}. \tag{2.28}$$

2.5.2.2 ZFB

Here, the optimal number of RF chains under ERP constraint is investigated considering ZFB. Since users are assumed to have equal received power, the transmit power allocated for user k can be expressed as:

$$p_{k,ZF} = \frac{p_{out}}{b_k \sum_{j=1}^{K} \frac{1}{b_j}}, \tag{2.29}$$

where $b_k = \frac{\beta_k}{\beta_k p_{out} \frac{1-\xi^2}{K} + \sigma^2}, k \in \{1, ..., K\}$.

Hence, using $\mathbf{E}\{| \mathbf{h}_k(\alpha)\mathbf{w}_k^{ZF}(\alpha) |^2\} = \xi^2 \frac{S-K}{K}$ the sum-rate averaged over the channel realizations can be expressed as:

$$\widetilde{R}^{ZF} \approx K \cdot B \cdot \log_2 \left(1 + \frac{1}{K} \frac{\xi^2 (S-K)}{1 - \xi^2 + \frac{\sigma^2}{p_{out}} \sum_{j=1}^{K} \frac{1}{\beta_j}} \right). \tag{2.30}$$

In consequence, the optimal number of RF chains that maximizes the average sum-rate over channel realizations can be derived as:

$$S_{ZF}^{*} \approx \begin{cases} \lfloor \phi_{ZF} \rfloor, & \text{if } \widetilde{R}^{ZF}(\lfloor \phi_{ZF} \rfloor) > \widetilde{R}^{ZF}(\lceil \phi_{ZF} \rceil) \\ & \text{or } \lfloor \phi_{ZF} \rfloor = N_{RF} \\ \lceil \phi_{ZF} \rceil, & \text{otherwise.} \end{cases} \tag{2.31}$$

where

$$\phi_{ZF} = \frac{\varpi \cdot (p_{max} - p_{fix} - p_{syn}) + 1 - \kappa 2}{\varpi \cdot p_c}, \tag{2.32}$$

$$\kappa 2 = \sqrt{1 - \varpi \cdot (K p_c - p_{max} + p_{fix} + p_{syn})} \tag{2.33}$$

and $\varpi = \delta \frac{1-\xi^2}{\sigma^2 \sum_{j=1}^{K} \frac{1}{\beta_j}}$.

2.5.3 User Scheduling

Imposing the stringent constraint of ERP, although achieving a complete fairness, may lead to low sum-rate performance since some 'bad' users can require high amount of transmit power to achieve the ERP constraint. If the users require a minimum received SINR γ_{th}, then only a subset of users can be scheduled and the previously mentioned case can not happen since 'bad' users will not be scheduled.

We define χ_k as a user index that is set to 1 if user k is scheduled and to 0 otherwise and we define the vector $\chi = [\chi_1 \chi_2 ... \chi_K]$. The problem is reformulated as:

$$\begin{aligned} \underset{\mathbf{p},S,\chi}{\text{maximize}} \quad & \widetilde{R}(\mathbf{p},S,\chi) \\ \text{subject to} \quad & C1, C2, \\ & C5 : \chi_p \cdot \gamma_k(\mathbf{p},S) = \chi_k \cdot \gamma_p(\mathbf{p},S), \\ & \qquad \forall (k,p) \in \{1,...,K\}^2, \\ & C6 : \gamma_k(\mathbf{p},S) \geq \chi_k \cdot \gamma_{th}, k = 1..K, \\ & C7 : \chi_k \in \{0,1\}, k = 1..K. \end{aligned} \tag{2.34}$$

Constraint $C5$ ensures that the scheduled users have equal received power and constraint $C6$ imposes a minimum received SINR to the scheduled users.

In consequence, considering CB, the scheduled users must satisfy the following constraint:

$$\sum_{k=1}^{K} \frac{1}{a_k} \chi_k \leq \frac{\xi^2 p_{out}}{\gamma_{th}} \tag{2.35}$$

and considering ZFB, the scheduled users must satisfy the following constraint:

$$\sum_{k=1}^{K} \frac{1}{b_k} \chi_k \leq \frac{\xi^2 p_{out}}{\gamma_{th} \cdot \eta_{ZF}(\alpha, \chi)^2}. \tag{2.36}$$

In order to solve problem (2.34), we propose two heuristic user scheduling algorithms described in Algorithm 2.1 and Algorithm 2.2. The first algorithm aims to schedule the maximum number of users. It proceeds by eliminating the 'worst' users one by one until the minimum required received SINR constraint becomes satisfied. The worst user is defined as the one that requires the highest amount of power. The second algorithm eliminates the 'worst' users iteratively and schedules the best set of users in order to maximize the system sum-rate. Hence, the second algorithm is supposed to achieve higher performance in terms of system sum-rate. On the other hand, the first algorithm is expected to provide higher fairness since it aims to schedule the maximum number of scheduled users.

Algorithm 2.1 and Algorithm 2.2 are described considering CB, they can be easily formulated for ZFB by having the constraint (2.36) instead of (2.35) and parameter b_k instead of a_k.

Algorithm 2.1 Heuristic user scheduling algorithm I

$\chi_k \leftarrow 1, k = 1:K$, initialization (all users are scheduled) ;
$\Omega \leftarrow \{k, k = 1:K\}$, set of scheduled users ;
while *(2.35) is not satisfied* **do**
    $k^* \leftarrow \underset{k \in \Omega}{\operatorname{argmax}} \frac{1}{a_k}$, find the worst user k^*;
    $\chi_{k^*} \leftarrow 0$;
    $\Omega \leftarrow \Omega \setminus \{k^*\}$;
end
Sum-rate computation;

2.6 Iterative Antenna Selection (IAS)

In this section, antennas are not arbitrarily selected any more. Hence, efficient algorithms are proposed to heuristically solve problem (2.9). They jointly find the set of antennas α and provide a power allocation $\mathbf{p}$ among users that approaches the maximum sum-rate. The

Algorithm 2.2 Heuristic user scheduling algorithm II

$\chi_k \leftarrow 1, k = 1 : K$, initialization (all users are scheduled);
$\Omega \leftarrow \{k, k = 1 : K\}$, set of scheduled users;
Initial sum-rate computation R_{max};
for $j = 1 : K - 1$ **do**
    $k^* \leftarrow \underset{k \in \Omega}{\operatorname{argmax}} \frac{1}{a_k}$, find the worst user k^*;
    $\chi_{k^*} \leftarrow 0$;
    $\Omega \leftarrow \Omega \setminus \{k^*\}$;
    Sum-rate computation R;
    if $R > R_{max}$ **then**
        $R_{max} \leftarrow R$;
    end
end

optimal antenna selection for ZFB can be obtained using a brute-force search (BFS) algorithm but suffers from very high computational complexity. For CB, it can be obtained using a branch and bound (BB) algorithm which highly improves the meantime complexity of the BFS, but still suffers from exponential complexity in the worst case.

2.6.1 CB

A greedy antenna selection and power allocation algorithm is described in Algorithm 2.3. At each iteration, the best antenna n^*, the one that maximizes the sum-rate, is determined among the set of non selected antennas Λ. Once the selected antennas are found, the power can be allocated among users using (2.14). The proposed algorithm allows to determine the number of activated RF chains, the selected antennas and the power allocated among users.

It is to be noted that even without taking into consideration the circuit power consumption, the system sum-rate considering CB is not always maximized when activating all antennas. Specifically, 'bad' antennas (those experiencing poor channel gains) may cause high interference and decrease the system performance. Hence, based on this property, a second low complexity greedy algorithm is proposed. The new algorithm takes at each iteration the antenna with maximum average channel gain. It verifies if the correspondent antenna allows to

Algorithm 2.3 CB-IAS algorithm

$\alpha_n \leftarrow 0, n = 1 : N$, initialization;
$\Lambda \leftarrow \{n, n = 1 : N\}$, set of non-selected antennas;
for $s = 1 : min(N_{RF}, N)$ **do**
    for $n \in \Lambda$ **do**
        $\alpha_n \leftarrow 1$, activate antenna n;
        compute p_k using (2.14);
        compute R^{CB} using (2.4);
        if $R^{CB} > R^{CB}_{max}$ **then**
            $R^{CB}_{max} \leftarrow R^{CB}$;
            $n^* \leftarrow n$;
        end
        $\alpha_n \leftarrow 0$, deactivate antenna n;
    end
    $\alpha_{n^*} \leftarrow 1$, select antenna n^*;
    $\Lambda \leftarrow \Lambda \setminus \{n^*\}$;
end

increase the sum-rate. If this is the case, the antenna is activated; otherwise, it is considered as a 'bad' antenna and it is discarded. The details of the low complexity greedy algorithm are given in Algorithm 2.4.

The two proposed algorithms can be easily adapted in order to ensure the fairness constraint discussed in Section 2.5.2. In fact, instead of computing the p_k's using (2.14), they have to be computed using (2.24). Also, algorithms can be slightly modified to incorporate the user scheduling.

2.6.2 ZFB

Here, we propose a reverse greedy algorithm that is able to determine the set of antennas and power allocation among users that maximizes the instantaneous sum-rate for ZFB. The optimal set of antennas minimizes the normalization factor, that is, we have:

Algorithm 2.4 CB low complexity IAS algorithm

$\alpha_n \leftarrow 0, n = 1 : N$, initialization;
$\Upsilon \leftarrow \{n, n = 1 : N\}$,;
while $\Upsilon \neq \emptyset$ *and* $\sum_{n=1}^{N} \alpha_n < min(N_{RF}, N)$ **do**
    $n^* \leftarrow \underset{n \in \Upsilon}{\text{argmax}} \frac{1}{K} \sum_{k=1}^{K} | \widehat{h}_{k,n} |^2$, find antenna n^* with maximum average channel gain;
    $\Upsilon \leftarrow \Upsilon \setminus \{n^*\}$;
    $\alpha_{n^*} \leftarrow 1$, activate antenna n^*;
    compute p_k using (2.14);
    compute R^{CB} using (2.4);
    if $R^{CB} > R^{CB}_{max}$ **then**
        $R^{CB}_{max} \leftarrow R^{CB}$;
    else
        $\alpha_{n^*} \leftarrow 0$, deactivate antenna n^*;
    end
end

$$\underset{\alpha}{\text{argmax}} \quad R^{ZF} = \underset{\alpha}{\text{argmin}} \quad \eta_{ZF}(\alpha)^2. \tag{2.37}$$

Equation (2.37) allows to build a greedy algorithm where the best antenna is selected with no need for power or sum-rate computation. Since the normalization factor $\eta_{ZF}(\alpha)^2$ is infinite for $S < K$ and the beamforming matrix $\mathbf{W}^{ZF}(\alpha)$ cannot be calculated in this case, the reverse greedy algorithm is initialized by selecting all antennas. Then, the worst antenna is deactivated at each iteration. The worst antenna is defined as the one that the sum-rate is maximized when it is deactivated (i.e. the normalization factor is minimized). Hence, we have

$$n^* = \underset{n \in \Lambda}{\text{argmin}} \quad \eta_{ZF}(\alpha)^2, \tag{2.38}$$

where Λ is the set of activated antennas.

The computation of the normalization factor at each iteration requires a matrix inversion. When the spatial correlation between antennas is low enough, the complexity of the algorithm can be reduced. A low complexity method based on matrix theory was proposed in Lütkepohl;

Gaur & Ingram (2005) to compute the normalization factor iteratively. Let $\widehat{\mathbf{H}}_s$, the matrix formed by the selected antennas at iteration s and $\mathbf{D}_{s-1} = (\widehat{\mathbf{H}}_{s-1}\widehat{\mathbf{H}}_{s-1}^H)^{-1}$. When the antenna corresponding to the n^{th} column of the channel matrix $\widehat{\mathbf{H}}$ denoted $\widehat{\mathbf{v}}_n$ is deactivated, the expression of the updated trace of $\mathbf{D}_{s-1}$ can be simplified as:

$$\lambda_{s-1} = \lambda_s + \frac{|\ \widehat{\mathbf{v}}_n^H \mathbf{D}_s\ |^2}{1 - \widehat{\mathbf{v}}_n^H \mathbf{D}_s \widehat{\mathbf{v}}_n}. \tag{2.39}$$

Hence, the worst antenna is the one that when deactivated at step $s-1$ minimizes the normalization factor and is derived as:

$$n^* = \underset{n\in\Lambda}{\operatorname{argmin}} \quad \frac{|\ \widehat{\mathbf{v}}_n^H \mathbf{D}_s\ |^2}{1 - \widehat{\mathbf{v}}_n^H \mathbf{D}_s \widehat{\mathbf{v}}_n}. \tag{2.40}$$

In consequence, the matrix inversion is done only once and the normalization factor is updated with low complexity.

The number of activated RF chains must be less than N_{RF}. Once the transmit antennas are selected, the transmit power can be optimally shared among users using the water filling algorithm.

The convergence is obtained when the sum-rate starts decreasing. A pseudo code of the proposed algorithm is given in Algorithm 2.5.

Similarly to CB, Algorithm 2.5 can also be slightly modified to ensure the fairness constraint discussed in Section 2.5. Therefore, instead of using (2.17) to compute the p_k's, they are computed using (2.29). Also, it can be easily adapted to incorporate the user scheduling.

2.7 Complexity Analysis

In this section, the worst case computational complexity of the algorithms proposed in Section 2.6 is computed asymptotically. For the brute-force search optimal algorithm under ZFB,

Algorithm 2.5 ZFB-IAS algorithm

$\alpha_n \leftarrow 1, n = 1:N$, initialization (all antennas are activated);
$\Lambda \leftarrow \{n, n = 1:N\}$, set of selected antennas;
while $R^{ZF} > R^{ZF}_{max}$ **do**
    $R^{ZF}_{max} \leftarrow R^{ZF}$;
    $n^* \leftarrow \underset{n\in\Lambda}{\operatorname{argmin}} \quad \eta_{ZF}(\alpha)^2$, find the worst antenna n^*;
    $\alpha_{n^*} \leftarrow 0$, deactivate the antenna n^*;
    $\Lambda \leftarrow \Lambda \setminus \{n^*\}$;
    if $s \leq N_{RF}$ **then**
        compute p_k using (2.17);
        compute R^{ZF} using (2.4);
    end
end

the number of possible combinations of sets of antennas is $\sum_{s=K}^{N_{RF}} \mathbf{C}_N^s$. While for the ZFB-IAS algorithm, the number of combinations of sets of antennas is given by $\sum_{s=K}^{N} s$.

For each selected set of antennas, the coefficient $\eta_{ZF}(\alpha)^2$ is calculated using one matrix multiplication with a complexity of $O(sK^2)$ and one matrix inversion with a complexity of $O(K^3)$. Also, the water filling power allocation complexity is $O(K^3)$. Hence, the computational complexity of the optimal BFS algorithm under ZFB is given by:

$$C_{ZF}^{OAS} = O\left(\sum_{s=K}^{N_{RF}} \mathbf{C}_N^s (sK^2 + K^3)\right). \tag{2.41}$$

For the ZFB-IAS algorithm, the complexity order of the normalization factor computation is simplified to $O(K^2)$. Hence, the overall complexity is given by:

$$\begin{aligned} C_{ZF}^{IAS} &= O\left(\sum_{s=K}^{N} sK^2 + \sum_{s=K}^{N_{RF}} K^3\right) \\ &= O(K^2N^2). \end{aligned} \tag{2.42}$$

Now, we investigate the complexity of CB. For the optimal BB algorithm, the number of possible combinations of the antennas in the worst case is $\sum_{s=1}^{N_{RF}} \mathbf{C}_N^s$. For each selected set of antennas, the coefficient $\eta_{CB}(\alpha)^2$ is calculated, which includes one matrix multiplication. Hence, the computational complexity of the optimal BB algorithm under CB is given by:

$$C_{CB}^{OAS} = O\left(\sum_{s=K}^{N_{RF}} \mathbf{C}_N^s (sK^2 + K^3)\right). \tag{2.43}$$

For the CB-IAS algorithm, the number of combinations of antennas is given by $\sum_{s=1}^{N_{RF}} N - s + 1$. The update of the normalization factor at each iteration can be simplified using (2.39). Hence, its computational complexity is given by:

$$\begin{aligned} C_{CB}^{IAS1} &= O\left(\sum_{s=1}^{N_{RF}} (N - s + 1)(K^2 + K^3)\right) \\ &= O(N_{RF} K^3 N). \end{aligned} \tag{2.44}$$

Finally, we investigate the complexity of the proposed CB low complexity IAS algorithm. The complexity of order of sorting the antenna coefficients is $O(N \log_2(N))$. Hence, the complexity order of this algorithm is given by:

$$\begin{aligned} C_{CB}^{IAS2} &= O\left(\sum_{n=1}^{N} (K^2 + K^3) + N \log_2(N)\right) \\ &= O((K^3 + \log_2(N))N). \end{aligned} \tag{2.45}$$

The optimal antenna selection can be obtained with very high complexity whereas the proposed efficient algorithms are polynomial time at most quadratic on N. The computational complexities of these algorithms are evaluated for different values of N in Table 2.1 considering $K = 10$.

Table 2.1 Computational Complexity of the proposed iterative and optimal algorithms.

Complexity order	C_{CB}^{OAS}	C_{CB}^{IAS1}	C_{CB}^{IAS2}	C_{ZF}^{OAS}	C_{ZF}^{IAS}
$N = 64, N_{RF} = 32$	2.10^{21}	2.10^{6}	6.10^{4}	2.10^{21}	4.10^{6}
$N = 128, N_{RF} = 64$	2.10^{40}	8.10^{6}	2.10^{5}	2.10^{40}	2.10^{7}

2.8 Numerical Results

In this section, Monte Carlo simulations show the efficiency of the proposed algorithms and validate the analytical results.

The correlation among the BS transmit antennas is following the Kronecker spatial correlation model represented by $\Sigma[i, j] = \theta^{|i-j|}, \forall i, j = 1...N$, where θ is a correlation coefficient such that $\theta = 0$ (resp. $\theta = 1$) corresponds to the uncorrelated (resp. fully correlated) conditions Makki *et al.* (2016).

We consider that the BS is equipped with 256 antennas serving 10 users. The users are assumed to be randomly distributed within a circular cell of radius $d_{max} = 500$ m. Simulation parameters are summarized in Table 2.2.

2.8.1 Arbitrary Antenna Selection

Fig. 2.2 shows the average sum-rate as a function of the number of activated RF chains assuming AAS and OPA. Clearly, the maximum achievable sum-rate is not obtained when activating all RF chains. At low p_{max}, the performance given by CB is higher than ZFB whereas ZFB outperforms CB for higher p_{max} due to the increasing impact of multi-user interference.

The optimal number of activated RF chains with AAS is shown in Fig. 2.3. Simulation results confirm the analytical expressions of the optimal number of activated RF chains. It can be noticed that ERP requests the activation of less RF chains compared to OPA for both beamforming techniques.

Table 2.2 Simulation Parameters.

Symbol	Description	Value
K	number of users	10
N	number of antennas	256
p_c	circuit power per activated RF chain	1 W Kumar & Gurugubelli (2011)
p_{syn}	power consumed by frequency synthesizer	2 W Kumar & Gurugubelli (2011)
p_{fix}	fixed power consumption	18 W Kumar & Gurugubelli (2011)
δ	power amplifier efficiency	0.8
ξ	reliability of the estimate	0.9
ν	path loss exponent	3.7 Zhao *et al.* (2013)
θ	correlation coefficient	0.25 Makki *et al.* (2016)
B	bandwidth	200 KHz
f_c	carrier frequency	2.5 GHz Ng *et al.* (2012a)
d_0	reference distance	1 m
d_{max}	cell radius	500 m
γ_{th}	minimum received SINR	10 dB
	noise PSD	-174 dBm/Hz Pei *et al.* (2012)

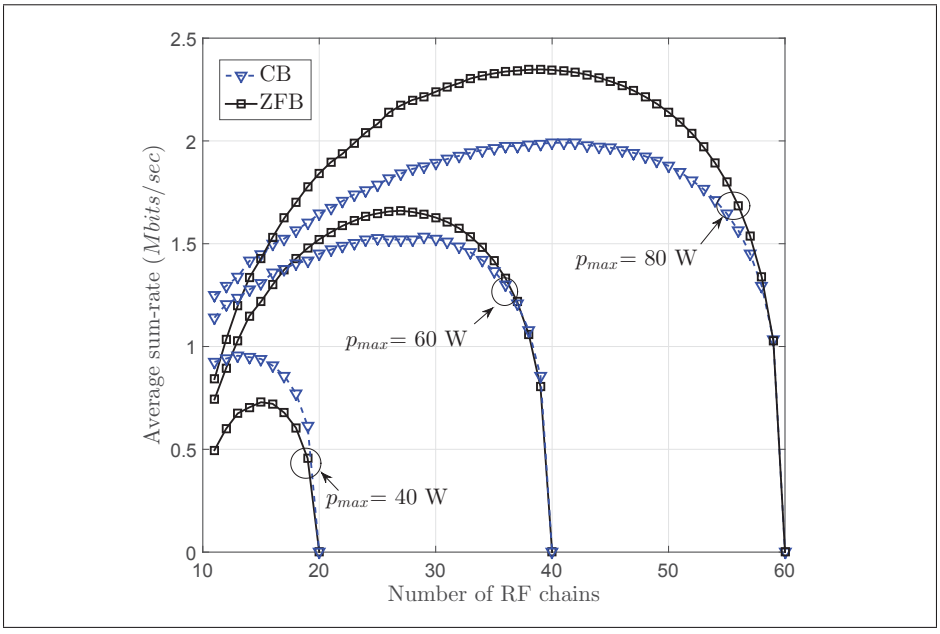

Figure 2.2 Average sum-rate in function of the number of activated RF chains assuming AAS and OPA.

Fig. 2.4 shows the maximum achievable sum-rate considering AAS for different power allocation strategies. The optimal user scheduling is given by BFS algorithm (i.e. an exhaustive

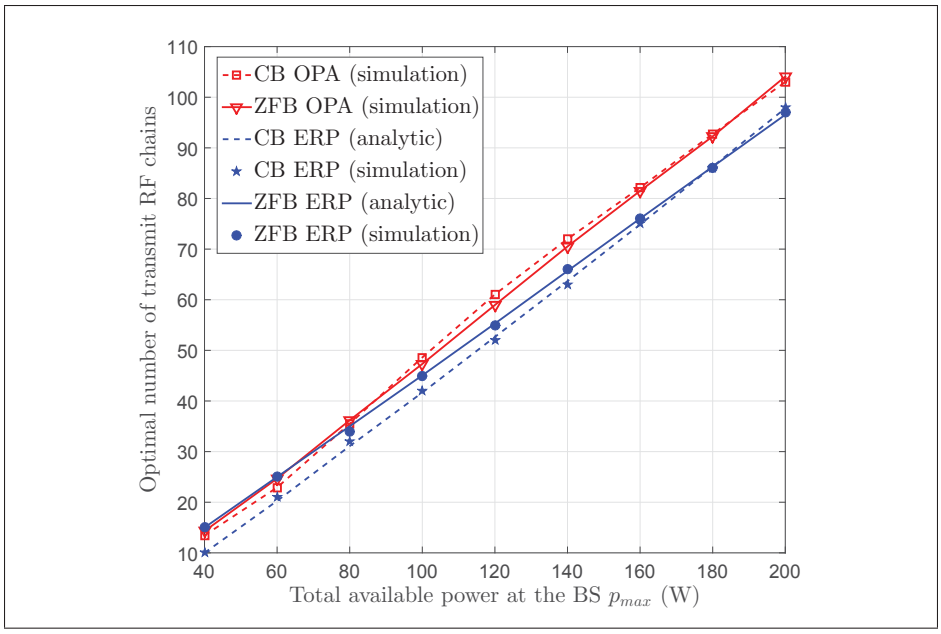

Figure 2.3 Number of activated transmit RF chains whith AAS.

search over all possible users' combinations). Under CB, it can be seen that the proposed user scheduling algorithms significantly ameliorate the performance compared to ERP. Also, user scheduling outperforms slightly OPA (except for very high p_{max}) since OPA has the constraint to schedule all the users. As expected, Algorithm 2.1 is less performant than Algorithm 2.2 since it aims to schedule the maximum number of users. It will be seen later that Algorithm 2.1 provides higher fairness. The achieved sum-rate by Algorithm 2.2 approaches the optimal user scheduling. Under ZFB, user scheduling algorithms can achieve higher performance than OPA because ZFB eliminates completely the multi-user interference. Therefore, when serving less users (i.e. scheduling only the users whose channel vectors are near-orthogonal), the system can achieve higher sum-rate. It is to be noted that OPA serves always all users whereas the optimal user scheduling applies optimal power allocation to a subset of adequately selected users.

The achieved sum-rate by the Algorithm 2.2 fits exactly with the optimal user scheduling. Also, we observe that the analytical expressions of the average sum-rate under ERP given in (2.25) and (2.30) fit with the simulations results. These figures corroborate that under ERP and

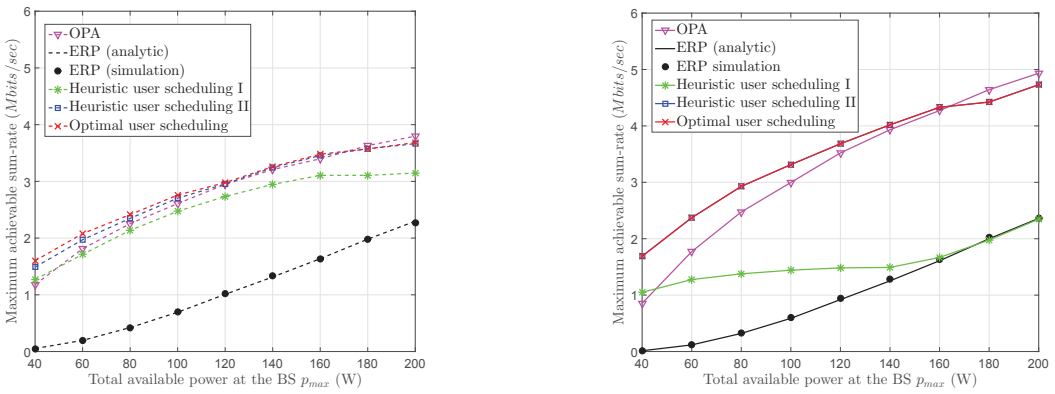

(a) CB (b) ZFB

Figure 2.4 Performance comparison of different algorithms considering AAS.

when the antenna selection is performed arbitrary, using CB provides higher system sum-rate than using ZFB for large p_{max} values (the crossing point of the two curves can be obtained by solving $\widetilde{\gamma}_{ERP}^{CB}(p_{max}) = \widetilde{\gamma}_{ERP}^{ZF}(p_{max})$).

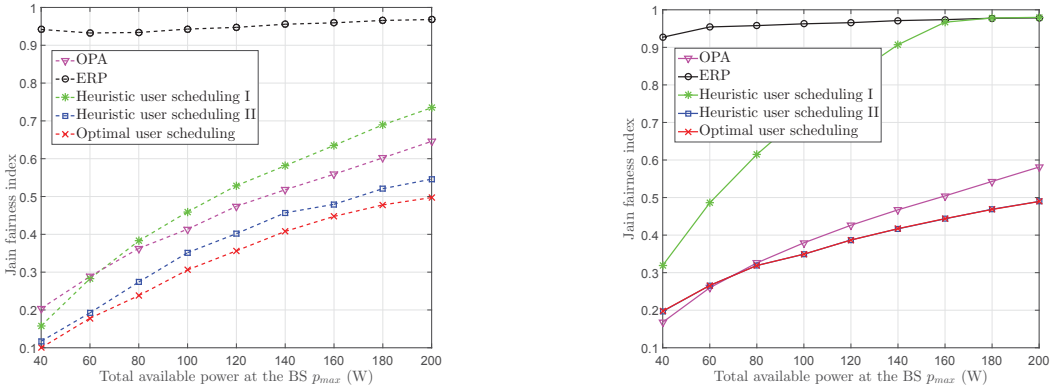

(a) CB (b) ZFB

Figure 2.5 Jain's fairness index considering AAS.

Fig. 2.5 shows the fairness level achieved by the proposed algorithms for AAS under CB and ZFB respectively. The used fairness metric is the well known Jain's fairness index Jain *et al.*

(1984) defined as $J(R) = \frac{(\sum_{k=1}^{K} R_k)^2}{K \sum_{k=1}^{K} R_k^2}$. Under equal received power, the Jain index is close to 1 due to channel estimation imperfection. Full and instantaneous fairness between users can be only achieved when considering perfect CSI at the BS. For the other algorithms, the Jain index increases when we increase the total available power at the BS. For both CB and ZBF, Algorithm 2.1 provides higher fairness than optimal user scheduling since it aims to schedule the maximum number of users with ERP. The fairness provided by Algorithm 2.2 is the same as optimal user scheduling for ZFB. On the other hand, these figures show also that the Jain fairness index given by optimal user scheduling is less than OPA. Also, it can be seen that CB provides higher fairness than ZFB when considering OPA.

In Fig. 2.6, we show the impact of the transmit spatial correlation on the maximum achieved sum-rate under ERP considering both beamforming techniques. In high p_{max} region and high spatial correlation factor, sensitivity to the spatial correlation increases and results in serious system performance degradation. Also, it can be seen in this figure that ZFB is more robust to the spatial correlation between transmit antennas than CB.

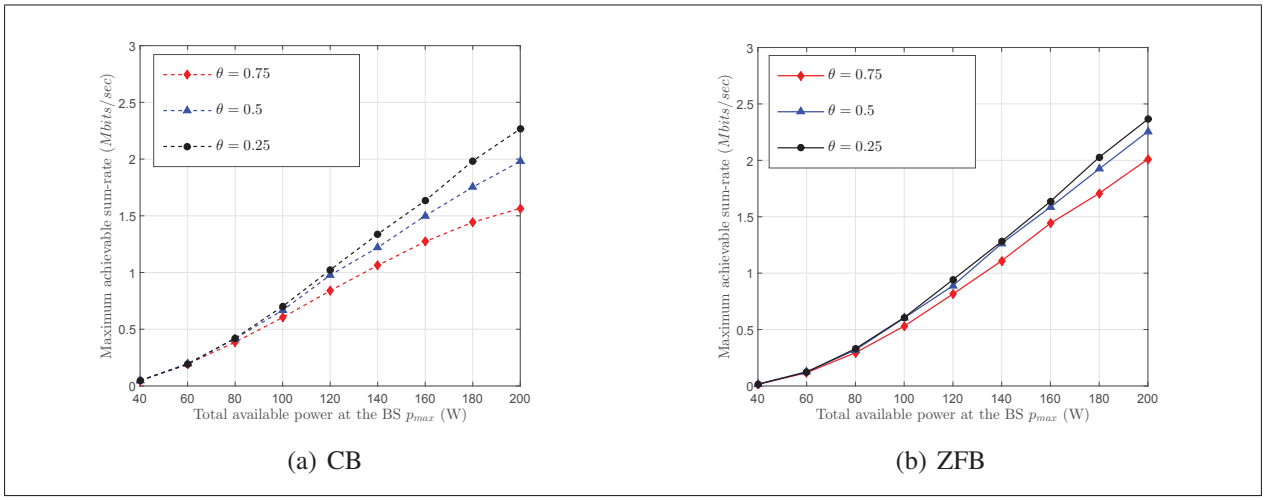

(a) CB (b) ZFB

Figure 2.6 Maximum achievable sum-rate under ERP in different spatially-correlated conditions.

Now, we investigate the energy efficiency and spectral efficiency tradeoff (SET) by considering the utility function given by Deng *et al.* (2013). The SET utility is expressed in function of the number of activated RF chains and the output power p_{out} as:

$$U(S, p_{out}) = \left(\frac{f_{SE}(S, p_{out})}{f_{SE}^{max}} \right)^{w} \cdot \left(\frac{f_{EE}(S, p_{out})}{f_{EE}^{max}} \right)^{1-w}, \tag{2.46}$$

where f_{SE} denotes the spectral efficiency that is given by the system sum rate, f_{SE}^{max} denotes the maximal spectral efficiency, f_{EE} denotes the energy efficiency, f_{EE}^{max} denotes the maximal energy efficiency and $w \in [0,1]$ denotes the preference for the spectral efficiency. The energy efficiency is given by the spectral efficiency divided by the total consumed power as $f_{EE}(S, p_{out}) = f_{SE}(S, p_{out})/(p_{out} + S \cdot p_c)$.

Considering ERP, the SET utility is optimized by deriving the optimal S^* and p_{out}^* for different values of w and shown in Fig. 2.7 for both CB and ZFB.

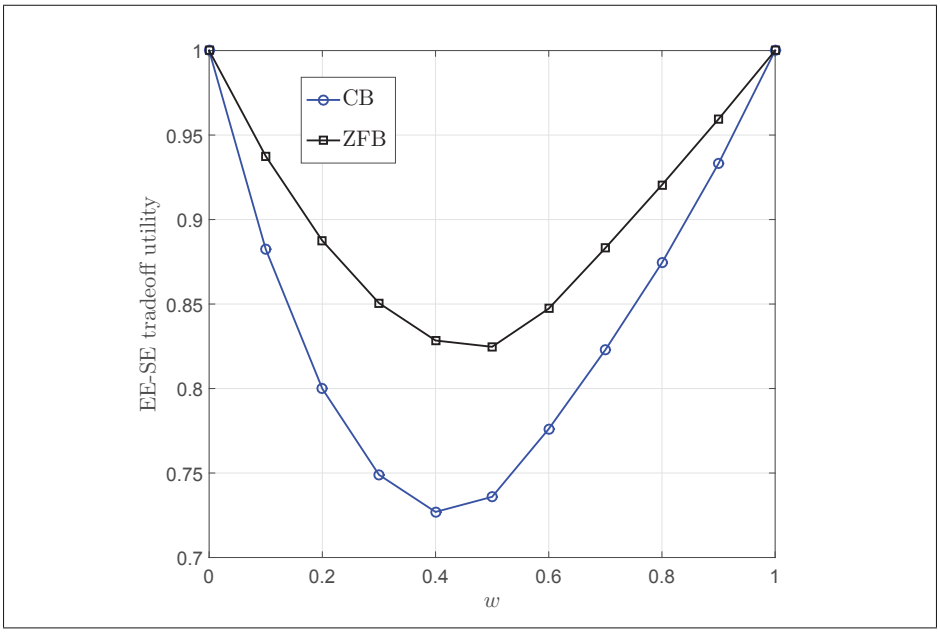

Figure 2.7 Energy efficiency and spectral efficiency tradeoff.

2.8.2 Iterative Antenna Selection

Fig. 2.8 plots the maximum achievable sum-rate under the proposed IAS algorithms and optimal antenna selection. Simulation results for optimal antenna selection are presented for limited number of antennas N and for $K = 3$ due to the extremely high exponential complexity of the optimal algorithm. As expected, the increase in the number of antennas offers more diversity and achieves higher sum-rate. The performance gap between the IAS and optimal antenna selection is tight and does not change too much when N increases.

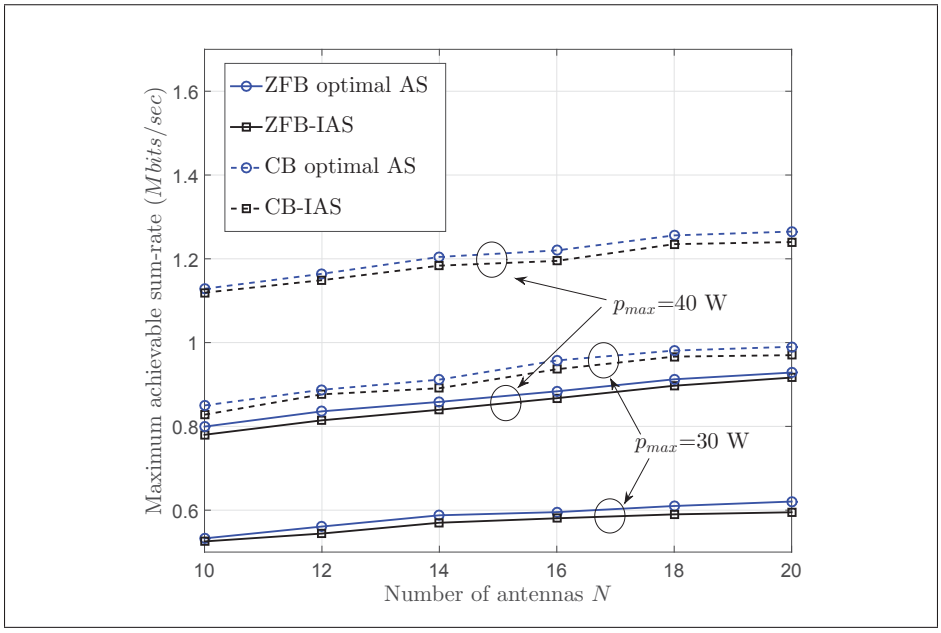

Figure 2.8 Maximum achievable sum-rate under optimal AS and IAS considering OPA ($K = 3$).

In Fig. 2.9, we compare the performance of the proposed IAS algorithms assuming OPA under different channel imperfection levels (i.e. different values of ξ). It is clear that the IAS algorithm under ZFB significantly outperforms IAS under CB for higher value of p_{max}. The opposite is true in low p_{max} region. The degradation of the performance of conjugate beamforming is due to the increase of multi-user interference. Also, the proposed CB low complexity IAS algorithm (Algorithm 2.4) outperforms the CB-IAS algorithm (Algorithm 2.3) in high p_{max} region. It is clear that the decrease of the reliability of the estimation (as ξ decreases) de-

grades the system performance. The IAS algorithms are more sensitive to channel estimation imperfection than AAS because this imperfection has effect on both power allocation and antenna selection. Under imperfect CSI, ZFB cannot perfectly mitigate multi-user interference. Therefore, CB is more robust to channel estimation imperfection than ZFB.

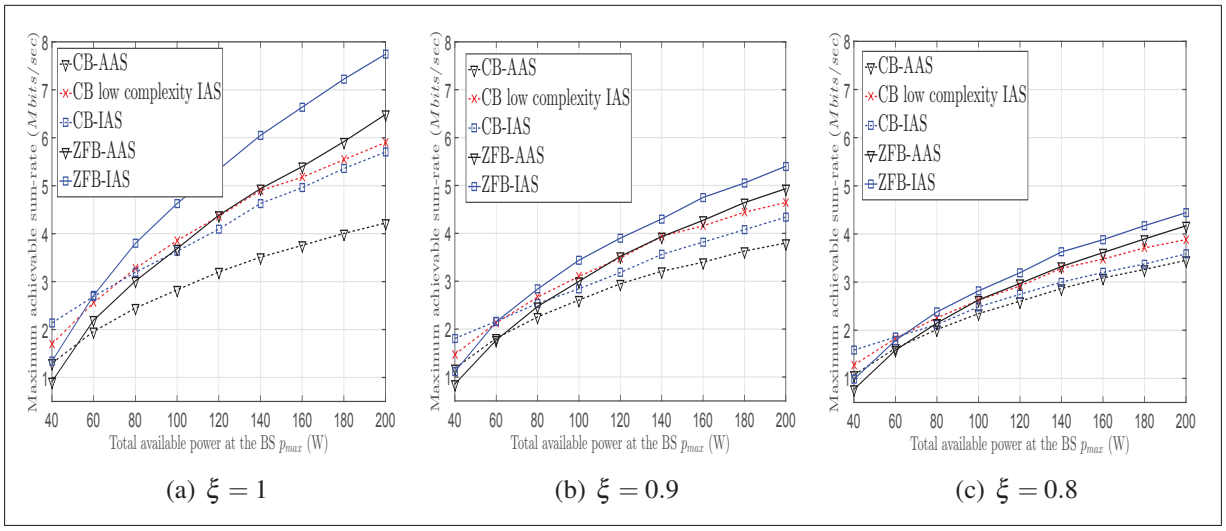

(a) $\xi = 1$ (b) $\xi = 0.9$ (c) $\xi = 0.8$

Figure 2.9 Performance comparison of different algorithms considering OPA under different channel imperfection levels.

Finally, we compare the proposed algorithm ZFB-IAS with a state-of-the-art algorithm, namely JASUS Benmimoune *et al.* (2015) after performing some minor adaptations according to our system model. In fact, JASUS takes as input the number of active RF chains and selects iteratively the best antennas that maximize the sum-rate under ZFB. Therefore, we have run JASUS taking as input the number of RF chains calculated under AAS. Fig. 2.10 shows that ZFB-IAS outperforms JASUS.

2.9 Conclusion

The downlink of large-scale MIMO systems is investigated in this paper considering a non negligible circuit power consumption. The studied resource allocation focuses on: (i) activating a subset of RF chains, (ii) activated antenna selection, (iii) power allocation and (iv) user

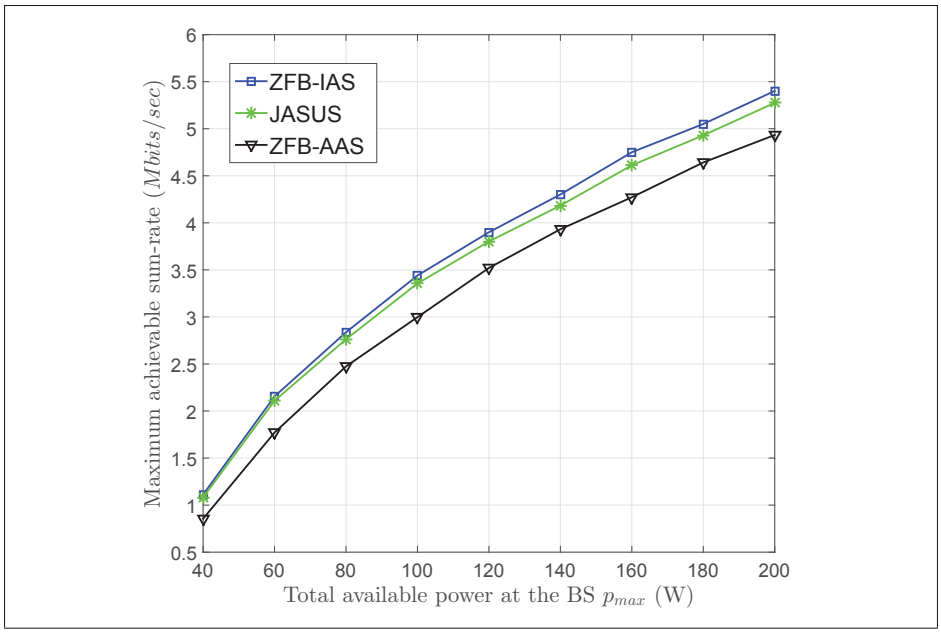

Figure 2.10 Comparison with JASUS.

scheduling considering two linear precoders CB and ZFB. Since the instantaneous sum-rate is considered as the objective function, we confirm that it isn't maximized by activating all RF chains. For this reason, we find the optimal number of RF chains to be activated that maximizes the sum-rate assuming firstly arbitrary antenna selection and considering either optimal power allocation or fair equal received SINR (denoted ERP). CB is shown to provide higher fairness than ZFB. However, ERP leads to low performance compared to optimal power allocation. Hence, scheduling only the users that are able to respect a minimum SINR requirement is investigated. Two user scheduling algorithms are proposed. The first one is shown to be fair and achieves acceptable sum-rate whereas the second one achieves the optimal system sum-rate. Next, we investigate instantaneous antenna selection that allows to improve the system sum-rate. Since the optimal antenna selection is highly complex, we propose two polynomial time iterative antenna selection algorithms that allow to find a near-to-optimal balance between the amount of power consumed at the RF chains and the transmit power.

Future work could be directed towards the design of low complexity beamforming schemes that outperform CB and ZFB considering a non-negligible circuit power consumption. Also,

the system model may be extended to intercell scenario where multi-cell interference and pilot contamination are taken into account for the design of resource allocation strategies.

CHAPTER 3

ENERGY MANAGEMENT IN HYBRID ENERGY LARGE-SCALE MIMO SYSTEMS

Rami Hamdi[1,2], Elmahdi Driouch[3], Wessam Ajib[1]

[1] Department of Computer Science, Université du Québec à Montréal (UQÀM), QC, Canada
[2] École de Technologie Supérieure,
1100 Notre-Dame Ouest, Montréal, Québec, Canada H3C 1K3
[3] Université de Moncton, NB, Canada

This article was published in IEEE Transactions on Vehicular Technology in November 2017 Hamdi *et al.* (2017b).

3.1 Abstract

This paper investigates the energy consumption of distributed large-scale MIMO systems made up of a set of remote radio heads (RRHs), each of which is powered by both an independent energy harvesting source and the grid. The grid energy source allows to compensate for the randomness and intermittency of the harvested energy. Hence, the problem of grid power consumption minimization has to be solved by efficiently managing the energy delivered from different sources while satisfying the system requirements in terms of users' quality of service demands. First, this paper solves the optimal off-line version of the problem using linear programming. In fact, the main problem is decomposed and heuristically solved in order to deal with the large number of constraints and variables. Since sometimes all the users cannot be served, an iterative link removal algorithm is devised ensuring the feasibility of the problem. Next, we investigate the on-line energy management problem. We first propose a dynamic programming approach to obtain the optimal on-line solution but with high complexity. Then, we develop and propose a low complexity heuristic solution based on using the maximal available energy at the batteries. Taking benefits of the characteristics of large-scale MIMO and the modeling of the harvested energy as Markov chains, we devise an efficient on-line energy management algorithm based on energy prediction. Finally, we propose a heuristic solution for

RRH on/off operation with the objective of improving the system energy efficiency. The performance of the proposed algorithms is evaluated by simulations and it is shown that the proposed energy management approaches offer efficient use of non-renewable energy to compensate the variability of renewable energy in large-scale MIMO systems.

3.2 Introduction

Large-scale multiple-input multiple-output (MIMO) (also known as massive MIMO) is seen as a key technology to be exploited in the next generations of wireless networks Andrews *et al.* (2014). It is based on multiplexing few hundred antennas to serve few tens of users at the same time-frequency, which allows to achieve high spectral efficiency using linear transmit and receive techniques Rusek *et al.* (2013). However, systems with co-located antennas may suffer from highly-correlated small-scale fading and identical large-scale fading. Also, the deployment of large number of antennas on the same base station presents many technical and implementation challenges Larsson *et al.* (2014). Alternatively, distributed large-scale MIMO systems can mitigate large-scale fading due to heterogeneous path-loss conditions. They are also shown to be more energy efficient than co-located antenna systems when taking exclusively into account the energy consumption of transmit and receive units He *et al.* (2014).

A distributed large-scale MIMO system consists of a set of remote radio heads (RRHs) distributed over a large area. Each RRH contains single or multiple antennas and RF chains and is reliably connected to a central unit. Such systems may be also seen as the so-called cloud radio access networks (C-RAN) Saxena *et al.* (2016). They may also incorporate energy harvesting that is a promising key technology for greening future wireless networks since it reduces network operation costs and carbon footprints Ku *et al.* (2016). Therefore, each RRH can be powered by both energy harvested from renewable sources such as thermal, wind or solar Prasad *et al.* (2017) and energy bought from the electrical grid.

The gains offered by distributed large-scale MIMO systems cannot be extracted without adequate resource management strategies as shown in Liu & Lau (2014); Joung *et al.* (2014);

Van Chien *et al.* (2016). In Liu & Lau (2014), the sum-rate is maximized using an efficient joint antenna selection and power allocation scheme in large C-RAN. The authors in Joung *et al.* (2014) investigate the energy efficiency in distributed large-scale antenna systems and propose efficient power control, antenna selection and user clustering algorithms. In Van Chien *et al.* (2016), the problem of transmit power minimization and user association is optimally solved for downlink multi-cell large-scale MIMO systems.

On the other hand, resource allocation in cellular systems powered by energy harvesting sources, exclusively or in conjunction with the grid, was also studied in the literature. The optimal base station on/off policy that minimizes the grid power consumption in such systems is obtained in Che *et al.* (2016). In Touzri *et al.* (2016), the BSs are assumed to be powered by multiple micro-grids. Efficient resource allocation techniques that minimize a power cost function are proposed. The capability of renewable energy to power cellular networks is investigated in Hu *et al.* (2016) in terms of coverage. A distributed deployment model of energy harvesting sources is proposed in order to cope with energy spatial random variations. In Yadav *et al.* (2016), the optimal off-line and on-line energy management settings are derived for small-cell access points.

The design of energy efficient communication systems is challenging when considering large-scale MIMO powered by energy harvesting due to the large number of antennas and to the intermittent characteristics of renewable energy sources. Even though resource allocation was extensively investigated for large-scale MIMO systems or for energy harvesting systems, very little attention was given to the design of energy management schemes that implement both technologies. In Zhou *et al.* (2014), a co-located point-to-point large-scale MIMO system powered by a single hybrid source was considered. Unlike the system presented in this paper, the authors of Zhou *et al.* (2014) consider only one user and one energy harvesting source. In Chia *et al.* (2014), cooperation between BSs powered by individual hybrid sources is proposed and investigated and the optimal energy cooperation policy is determined. The authors proposed an on-line energy management solution for conventional cellular system where large-scale MIMO was not considered. Therefore, our paper investigates distributed large-scale MIMO systems

where the RRHs are powered by energy bought from a grid source in addition to energy harvested from renewable sources. The objective is to propose efficient energy management solutions while satisfying the users requirements in terms of rate. In summary, this paper presents the following novel contributions:

- The problem of grid power consumption minimization in distributed hybrid energy large-scale MIMO system is formulated and the off-line energy management problem is optimally solved.
- Due to the large number of constraints and variables, the off-line problem is decomposed and heuristically solved.
- The feasibility problem is addressed by proposing an efficient link removal algorithm.
- Differently from Hamdi *et al.* (2017a) where the harvested energy is assumed to be independent over time, this work models the harvested energy as correlated time processes. Furthermore, the optimal on-line energy management policy is obtained and an efficient low complexity heuristic algorithm based on maximal available energy use is also proposed.
- An efficient on-line energy management algorithm based on energy prediction is proposed.
- For better energy efficiency, RRH on/off operation is investigated and a heuristic algorithm is proposed.

To clarify the new contributions of this paper relative to Hamdi *et al.* (2017a), it should be noted that the second point as well as the last three points of the above list are completely novel.

The rest of the paper is organized as follows. In Section 3.3, the system model is presented and the grid power consumption minimization problem is formulated. The optimal off-line energy management solution is presented in Section 3.4 and the on-line solutions are given in Section 3.5. RRH on/off operation is investigated in Section 3.6. Numerical results are presented and discussed in Section 3.7. Finally, we conclude this paper in Section 3.8.

3.3 System Model and Problem Formulation

3.3.1 Channel and Signal Model

The distributed large-scale MIMO system shown in Fig. 3.1 is considered. The central unit is connected via error-free links to N RRHs serving K single-antenna users where $N \gg K$. A given time interval is partitioned into L frames. The downlink channel coefficients between the RRHs and the users are represented by a complex matrix $\mathbf{G}(i) = [\mathbf{g}_1(i), \mathbf{g}_2(i), ..., \mathbf{g}_K(i)]$ where $\mathbf{g}_k(i) = [g_{n,k}(i)]_{n=1:N} \in \mathbb{C}^{1\times N}$ is the k^{th} channel vector for user k at frame i. Since non co-located antennas and non co-located users are assumed, the spatial correlation is neglected for both transmission and reception links. The channel coefficient $g_{n,k}(i)$ is given by $g_{n,k}(i) = \sqrt{\beta_{n,k}} h_{n,k}(i)$, where $h_{n,k}(i)$ is the small-scale fading channel coefficient at frame i, which is assumed to be quasi-static Gaussian independent and identically distributed (i.i.d.) slow fading channel and $\beta_{n,k}$ represents the large-scale fading channel coefficient between user k and RRH n. Considering only path loss, the large-scale fading component is expressed as $\beta_{n,k} = \zeta \frac{d_{n,k}^{-\nu}}{d_0^{-\nu}}$, where ν is the path loss exponent, $d_{n,k}$ is the distance between the RRH n and user k, d_0 is the reference distance and ζ is a constant related to the carrier frequency and reference distance. The central unit estimates the channel using the minimum mean square error (MMSE) and thus the estimated channel coefficient satisfies Rusek *et al.* (2013):

$$\widehat{g}_{n,k}(i) = \sqrt{\beta_{n,k}}(\xi h_{n,k}(i) + \sqrt{1-\xi^2} e), \tag{3.1}$$

where $0 \leq \xi \leq 1$ denotes the reliability of the estimate and e is an error component with Gaussian i.i.d. entries with zero mean and unit variance.

We denote by $\mathbf{w}_k(i) \in \mathbb{C}^{N\times 1}$ the k^{th} beamforming vector for user k. The low complexity maximum ratio transmission (MRT) is considered as beamforming technique for downlink transmission. The beamforming vector for user k is given by $\mathbf{w}_k(i) = \frac{\widehat{\mathbf{g}}_k(i)^H}{\eta(i)}$, where $\eta(i) = \| \widehat{\mathbf{G}}(i)^H \|_F$ is the normalization factor. Hence, the received signal-to-interference-plus-noise ratio (SINR) at user k is expressed as:

$$\gamma_k(i) = \frac{\frac{\sum_{n=1}^{N} p_{n,k}(i)}{\eta^2(i)} \mid \mathbf{g}_k(i)\widehat{\mathbf{g}}_k(i)^H \mid^2}{\sum_{m=1,m\neq k}^{K} \frac{\sum_{n=1}^{N} p_{n,m}(i)}{\eta^2(i)} \mid \mathbf{g}_k(i)\widehat{\mathbf{g}}_m(i)^H \mid^2 + \sigma^2}. \tag{3.2}$$

where $p_{n,k}(i)$ is the power allocated for user k on RRH n at frame i and σ^2 is the noise variance that is assumed to be additive white Gaussian noise (AWGN) with zero mean.

Finally, the uplink decoding is assumed to be performed at the central unit. Thus, the uplink data signal is received and transmitted to the central unit with fixed power on each RRH.

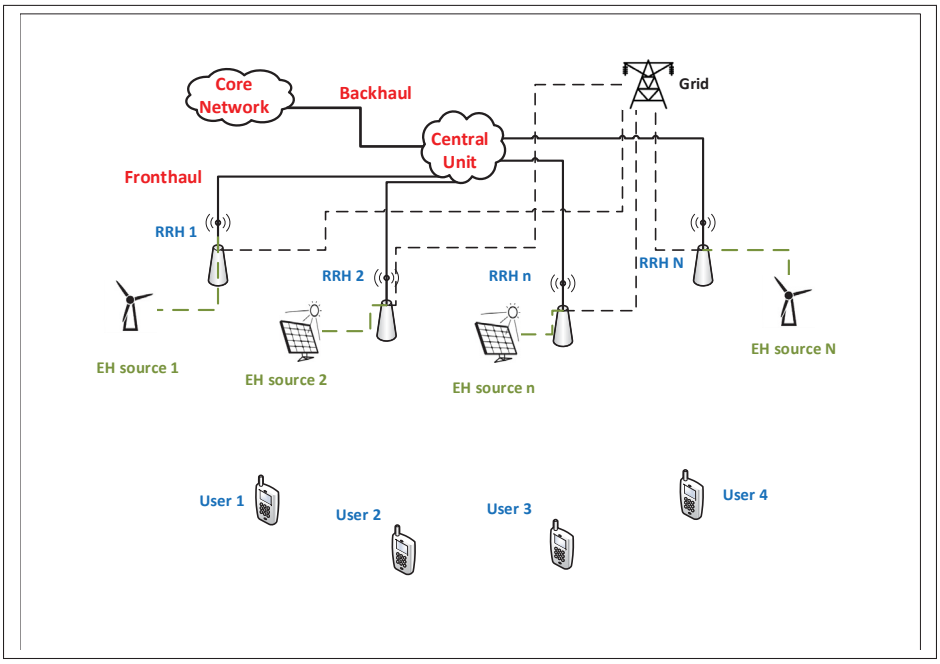

Figure 3.1 Distributed large-scale MIMO system with per-RRH energy harvesting.

3.3.2 Energy Harvesting Model

The harvested energy at each RRH is first stored in a battery with maximal capacity B_{max}. Let $A_n(i)$ and $X_n(i)$ denote respectively the amount of harvested energy and of consumed energy at RRH n during frame i. The amount of harvested energy is modeled as a correlated time process following a discrete-time Markov model as in Niyato *et al.* (2007); Blasco *et al.* (2013),

$A_n(i) \in \Omega \triangleq \{\omega_1, \omega_2, ..., \omega_M\}$ where Ω is the set of possible amount of harvested energy and $Q(\omega_m, \omega_j) = Pr(A_n(i+1) = \omega_m \mid A_n(i) = \omega_j)$ is the state transition probability.

The grid energy is required to compensate for the randomness and intermittence of the harvested energy, and hence enough power is always available which increases the feasibility of the problem (i.e., serving all users). We also consider that $p_{n,k}(i) = p^e_{n,k}(i) + p^g_{n,k}(i)$, where $p^e_{n,k}(i)$ and $p^g_{n,k}(i)$ denote the power drawn from the energy harvesting source and the power grid respectively. We also define E_{fix} for each RRH as the summation of the required energy to transmit (i) its current battery level, (ii) the received data signal and (iii) the received pilot signal to the central unit, and the energy consumed by the circuit. The latter includes the power consumed by the digital to analog converters, mixers and filters. Since the RRHs are powered by both renewable and grid sources, the required energy for the RRHs operation can be written as:

$$E_{fix} = E^e_n(i) + E^g_n(i),\ n = 1..N,\ i = 1..L, \tag{3.3}$$

where $E^e_n(i)$ and $E^g_n(i)$ are the energy drawn from the energy harvesting and the grid source respectively. Hence, the consumed energy per RRH n at frame i can be given by:

$$\begin{aligned} X_n(i) &= E_{fix} + \sum_{k=1}^{K} p_{n,k}(i) \cdot T \\ &= E^e_n(i) + E^g_n(i) + \sum_{k=1}^{K} p^e_{n,k}(i) \cdot T + \sum_{k=1}^{K} p^g_{n,k}(i) \cdot T \\ &= X^e_n(i) + E^g_n(i) + \sum_{k=1}^{K} p^g_{n,k}(i) \cdot T, \end{aligned} \tag{3.4}$$

where $X^e_n(i)$ denotes the total energy drawn from the energy harvesting source by RRH n at frame i and T denotes the duration of downlink transmission phase.

Let $B_n(i)$ denote the battery level of RRH n at frame i. The energy drawn from the energy harvesting source cannot exceed the battery level. Hence, the energy causality constraint is given by:

$$X_n^e(i) \leq B_n(i), \tag{3.5}$$

and the battery level update is expressed as:

$$B_n(i+1) = \min(B_{max}, B_n(i) - X_n^e(i) + A_n(i)). \tag{3.6}$$

We consider that the grid power consumption by RRH n at frame i is weighted by a factor $\alpha_{n,i}$ Che *et al.* (2016). Hence, the total grid power consumption is expressed as:

$$\Delta_{tot} = \sum_{i=1}^{L} \sum_{n=1}^{N} \alpha_{n,i} \cdot \Delta_{n,i}, \tag{3.7}$$

where $\Delta_{n,i} = \frac{E_{fix} - E_n^e(i)}{T} + \sum_{k=1}^{K} p_{n,k}^g(i)$.

3.3.3 Frame Structure

The considered system adopts, without loss of generality, time division duplex (TDD) for uplink/downlink communication. Each frame consists of 4 phases:

a. First, users send uplink pilot symbols to the RRHs;
b. second, each RRH sends reliably its current battery level and the received pilot signal to the central unit with fixed transmit energy;
c. third, the central unit performs channel estimation, beamforming, resource management and forwards its decisions towards the RRHs; and
d. finally uplink or downlink data transmission occurs.

3.3.4 Problem Formulation

The objective of this work is to minimize the total consumed grid energy while making use of the available harvested energy. We assume that each user requires a minimum received SINR to be satisfied. The energy management should take advantage of the grid power's weight variations by consuming more grid power when the associated weight is low while storing the renewable energy for future use, and by consuming less (or even zero) grid power when its weight is high. The main problem when channel coefficients, harvested energy arrivals and grid power weights are known, can be formulated as (3.8).

Constraints $(3.8.a)$ ensure a minimum received SINR, denoted γ_{th}, to each user. Constraints $(3.8.b)$ are related to the energy causality, i.e. the consumed harvested energy at RRH n can not exceed the energy harvested at RRH n. Constraints $(3.8.c)$ specify that the harvested energy at the current frame cannot exceed the maximal battery capacity. Constraints $(3.8.d)$ specify that the transmit power at each RRH is constrained due to the limited linear domain of the power amplifiers. Finally, constraints $(3.8.e)$ and $(3.8.f)$ ensure the non-negativity of the allocated amounts of power or energy.

The objective function and the constraints of problem (3.8) are clearly linear. Hence, the optimal energy management is obtained by solving a linear program as discussed in the next section.

Before delving into the details of the proposed solutions to the energy management, let's discuss a special case of the formulated problem. When the grid power's weights are all equal, i.e. $\alpha_{n,i} = \alpha \ \forall n, i$, we have no penalty to use the renewable energy once it is available. Hence, the optimal energy management is given by using all the harvested energy available at the batteries during the corresponding frame. The grid power is used when needed (i.e. when the battery is empty) to keep the users satisfied.

$$\underset{\substack{\{p^e_{n,k}(i),p^g_{n,k}(i),E^e_n(i)\}\\ k=1..K,n=1..N,i=1..L}}{\text{minimize}} \sum_{i=1}^{L}\sum_{n=1}^{N} \alpha_{n,i}\Delta_{n,i}$$

subject to

$$\begin{aligned}
&(3.8.a): \gamma_k(i) \geq \gamma_{th},\ k=1..K,\ i=1..L,\\
&(3.8.b): \sum_{i=1}^{l}\left(E^e_n(i)+\sum_{k=1}^{K} p^e_{n,k}(i)\cdot T\right) \leq \sum_{i=1}^{l} A_n(i),\ n=1..N,\ l=1..L,\\
&(3.8.c): \sum_{i=1}^{l} A_n(i) - \sum_{i=1}^{l-1}\left(E^e_n(i)+\sum_{k=1}^{K} p^e_{n,k}(i)\cdot T\right) \leq B_{max},\ n=1..N,\ l=2..L,\\
&(3.8.d): \sum_{k=1}^{K}(p^e_{n,k}(i)+p^g_{n,k}(i)) \leq p_{max},\ n=1..N,\ i=1..L,\\
&(3.8.e): p^e_{n,k}(i), p^g_{n,k}(i) \geq 0,\ k=1..K,\ n=1..N,\ i=1..L,\\
&(3.8.f): E_{fix} \geq E^e_n(i) \geq 0,\ n=1..N,\ i=1..L.
\end{aligned} \tag{3.8}$$

For better comprehension, the following reformulates problem (3.8) for a simple scenario of only two frames, a single user and a single RRH. Hence problem (3.8) becomes:

$$\underset{p^e_{1,1}(1),p^g_{1,1}(1),E^e_1(1),E^e_1(2),p^e_{1,1}(2),p^g_{1,1}(2)}{\text{minimize}} \alpha_{1,1}\Delta_{1,1}+\alpha_{1,2}\Delta_{1,2}$$

subject to

$$\begin{aligned}
&(3.9.a): \frac{p^e_{1,1}(1)+p^g_{1,1}(1)}{\sigma^2} \mid \mathbf{g}_1(1) \mid^2 = \gamma_{th},\\
&(3.9.b): \frac{p^e_{1,1}(2)+p^g_{1,1}(2)}{\sigma^2} \mid \mathbf{g}_1(2) \mid^2 = \gamma_{th},\\
&(3.9.c): E^e_1(1)+p^e_{1,1}(1)\cdot T \leq A_1(1),\\
&(3.9.d): E^e_1(1)+p^e_{1,1}(1)+E^e_1(1)+p^e_{1,1}(1)\cdot T \leq A_1(1)+A_1(2),\\
&(3.9.e): A_1(1)+A_1(2)-\left(E^e_1(1)+p^e_{1,1}(1)\cdot T\right) \leq B_{max},\\
&(3.9.f): E_{fix} \geq E^e_1(1) \geq 0,\\
&(3.9.g): E_{fix} \geq E^e_1(2) \geq 0.
\end{aligned} \tag{3.9}$$

It is to be noted that

Assuming $\gamma_{th} = 10$ dB, $B_{max} = 50$ J, $\alpha_1 = 0.2$ and $\alpha_2 = 0.6$, the optimal energy management is obtained while satisfying the user during both frames for a minimal grid power cost of 3.4 W.

3.4 Off-line Energy Management

In this section, we distinguish between the scenarios where (i) the harvested energy is large enough to serve all the users and there is no need for additional energy from the grid, (ii) the grid power is required but the problem is feasible (i.e., all the users can be satisfied) and finally (iii) some of the users cannot be satisfied. This section also discuss the problem decomposition allowing to obtain a heuristic solution with reduced complexity..

3.4.1 No Need for Grid Power

The power drawn from energy harvesting sources can be sufficient to ensure the QoS requirements for all users and there is no need for grid power, the energy drawn from the grid source for RRH operation is equal to zero, i.e. $E_n^g(i) = 0,\ n = 1..N,\ i = 1..L.$ Also, the portion of transmit power drawn from the grid source is equal to zero, i.e. $p_{n,k}^g(i) = 0,\ n = 1..N,\ k = 1..K,\ i = 1..L$, according to the following lemma.

Lemma 3.1: The consumption of grid power tends to zero if the following inequality, related to the amount of stored energy at the batteries and to the channel coefficients, is verified:

$$l \cdot E_{fix} + \sum_{i=1}^{l} \sum_{k=1}^{K} \frac{|\ \widehat{g}_{n,k}^H(i)\ |^2}{\eta(i)^2} p_k^*(i) \cdot T \leq \sum_{i=1}^{l} A_n(i),\ n = 1..N,\ l = 1..L, \tag{3.10}$$

where

$$p_k^*(i) = \left(\frac{N\sigma_d^2 + \sigma^2 \eta(i)^2}{\frac{1}{\gamma_{th} \sum_{m=1}^{K} \frac{1}{|\mathbf{g}_m(i) \widehat{\mathbf{g}}_m(i)^H|^2}} - 1} N\sigma_d^2 + \sigma^2 \eta(i)^2 \right) \cdot \frac{\gamma_{th}}{|\ \mathbf{g}_k(i) \widehat{\mathbf{g}}_k(i)^H\ |^2} \tag{3.11}$$

and $\sigma_d^2 = \mathbf{E}\{\mid g_{n,k}(i) \mid^2\}$ is the variance of the channel $g_{n,k}(i)$.

Proof: given in Appendix I.

Similarly to the main problem, we reformulate this lemma for a simple scenario of only two frames, a single user and a single RRH. The consumption of grid power tends to zero if the following inequalities are verified:

$$\begin{aligned} &E_{fix} + p_1^*(1) \cdot T \leq A_1(1), \\ &2E_{fix} + p_1^*(1) \cdot T + p_1^*(2) \cdot T \leq A_1(1) + A_1(2). \end{aligned} \tag{3.12}$$

3.4.2 Linear Programming

The optimal energy management can be obtained by linear programming when problem (3.8) is feasible as discussed in Hamdi *et al.* (2017a) using interior point method (IPM) implemented in numerical tools such as CVX. This linear program has $L \cdot K + N(4L-1)$ constraints and $N \cdot L(1+2K)$ variables and can be solved in polynomial-time using IPM with complexity order Boyd & Vandenberghe (2004) expressed as:

$$f(N,K,L) = O\left(\left(N \cdot L(1+2K)\right)^2 \left(L \cdot K + N(4L-1)\right) \right). \tag{3.13}$$

3.4.3 Link Removal

The multi-user interference present in constraints $(3.8.a)$ as well as the limitations imposed by constraints $(3.8.d)$ on the maximum transmit power at each RRH, involve that, in some cases, it may be impossible to ensure the SINR required by all the users at each frame Le & Hossain (2008). Hence, the problem may be infeasible even though the availability of grid power. Therefore, some users have to be denied service in some frames in order to overcome the infeasibility. More precisely, users with bad channel conditions in a particular frame have

higher probabilities to violate the SINR constraint, and hence they could not be satisfied in that frame.

A link removal solution may be proposed in order to overcome the infeasibility problem. We mean by link a particular (user, frame) pair. The formulated problem (3.8) becomes to jointly minimize the weighed consumed power and to minimize the number of removed links. A simplified version of this problem is to maximize the number of activated links while satisfying the required SINRs which is demonstrated to be an NP-complete problem in Andersin *et al.* (1996). Hence, the optimal link removal solution can be obtained only by high complex brute force search algorithm.

We propose in this section a link removal algorithm to solve heuristically the infeasibility problem. The proposed algorithm starts by removing one link based on fixed power allocation and re-tests the problem feasibility. This procedure is repeated until we obtain a set of links that ensures feasibility. By definition, the worst link is the one that violates the required SINR constraints the most. Alternatively, assuming a fixed power allocation, the worst link is the one that experiences the lowest SINR. The proposed link removal algorithm removes in each step the worst link. Such a link is characterized either by being in a noise-limited region or suffering from high interference caused by other transmissions. Therefore, the link removal algorithm chooses the link that experiences the least SINR. Note that similar removal policy has been previously proposed in different scenarios such as in Andersin *et al.* (1996); Le & Hossain (2008). The removal criterion can be applied as follows:

$$(k,l)^* \leftarrow \underset{(k,l)\in\{1,\ldots,K\}\times\{1,\ldots,L\}}{\operatorname{argmin}} \psi_{k,l} \tag{3.14}$$

where

$$\psi_{k,l} = \left[\frac{|\,\widehat{\mathbf{g}}_k(l)\widehat{\mathbf{g}}_k(l)^H\,|^2}{\sum_{i=1,i\neq k}^{K} |\,\widehat{\mathbf{g}}_k(l)\widehat{\mathbf{g}}_i(l)^H\,|^2 + \sigma^2\eta^2(l)} \right]. \tag{3.15}$$

This iterative procedure terminates once the problem becomes feasible by potentially removing the least number of links from the system. The proposed low complexity iterative link removal algorithm is given in Algorithm 3.1.

Another important factor for performance evaluation, that could replace SINR for the removing algorithm, is the signal-to-leakage-plus-noise ratio (SLNR) which is based on user's leakage power to others Cheng *et al.* (2010). Anyhow, since MRT is considered as beamforming in the system model, the SLNR metric has the same expression as the SINR metric. It is to be noted that the perfect channel state information (CSI) at the base station is not available, the removal criterion can be computed only with imperfect CSI.

Removing a single link by iteration may cause long running time for high number of links. Hence, to reduce the running time, multiple links could be removed in each iteration even though the algorithm may remove more links than needed.

Algorithm 3.1 Iterative Link Removal Algorithm

Computation of matrix $\mathbf{LR} = [\psi_{k,l}]_{k=1:K,l=1:L}$, // initialization (all links are scheduled);
$\Omega \leftarrow \{\}$, // set of removed links;
$feas \leftarrow$ **false**, // boolean variable for feasibility test;
$r1 \leftarrow 0$, // number of links already removed;
while $r1 < L \cdot K - R$ ***and Not*** $feas$ **do**
    $r1 \leftarrow r1 + R$, R is the number of links to be removed in each iteration;
    for $r2 = 1 : R$ **do**
        $(k,l)^* \leftarrow \underset{(k,l)\in\{1,\ldots,K\}\times\{1,\ldots,L\}}{\text{argmin}} \mathbf{LR}$;
        $\Omega \leftarrow \Omega \cup \{(k,l)^*\}$, // remove link $(k,l)^*$;
        update matrix **LR**;
    end
    solve linear program (3.8);
    if *problem (3.8) is feasible* **then**
        $feas \leftarrow$ **true**;
    end
end

Since the optimal link removal is obtained with the brute-force search algorithm, the number of possible combinations of sets of links is $\sum_{l=L}^{L}\sum_{k=1}^{K}\mathbf{C}_K^k\mathbf{C}_L^l$. Hence, its computational complexity is given by:

$$C_{lr}^{opt} = \sum_{l=L}^{L}\sum_{k=1}^{K}\binom{K}{k}\binom{L}{l}f(N,k,l). \tag{3.16}$$

For the iterative link removal algorithm, the computational complexity is given by:

$$C_{lr}^{ite} = \sum_{l=L}^{L}\sum_{k=1}^{K}f(N,k,l). \tag{3.17}$$

3.4.4 Problem Decomposition

Since the number of variables and constraints in problem (3.8) is very large and the complexity of the IPM depends on this number Renegar (1988), we propose to decompose the main problem and to heuristically solve it. First, the problem of user QoS satisfaction at frame i is formulated as:

$$\begin{aligned}
&\underset{\substack{\{p_{n,k}(i)\}\\ k=1..K,n=1..N}}{\text{minimize}} \sum_{n=1}^{N}\alpha_{n,i}\cdot\sum_{k=1}^{K}p_{n,k}(i)\\
&\text{subject to}\\
&(3.18.a): \gamma_k(i) \geq \gamma_{th},\ k=1..K,\\
&(3.18.b): \sum_{k=1}^{K}p_{n,k}(i) \leq p_{max},\ n=1..N,\\
&(3.18.c): p_{n,k}(i) \geq 0,\ k=1..K,\ n=1..N.
\end{aligned} \tag{3.18}$$

The problem (3.18) may be solved for each $i \in \{1,...,L\}$ in order to determine the required energy at each RRH given by $E_n^{req}(i) = E_{fix} + \sum_{k=1}^{K} p_{n,k}^{*}(i) \cdot T,,\ n = 1..N,\ i = 1..L$. Hence, the harvested energy management problem is reformulated as:

$$\begin{aligned}
&\underset{\substack{\{X_n^e(i)\} \\ n=1..N, i=1..L}}{\text{minimize}} \sum_{i=1}^{L} \sum_{n=1}^{N} \alpha_{n,i} \frac{E_n^{req}(i) - X_n^e(i)}{T} \\
&\text{subject to} \\
&(3.19.a): \sum_{i=1}^{l} X_n^e(i) \leq \sum_{i=1}^{l} A_n(i),\ n = 1..N,\ l = 1..L, \\
&(3.19.b): \sum_{i=1}^{l} A_n(i) - \sum_{i=1}^{l-1} X_n^e(i) \leq B_{max},\ n = 1..N,\ l = 2..L, \\
&(3.19.c): E_n^{req}(i) \geq X_n^e(i) \geq 0,\ n = 1..N,\ i = 1..L.
\end{aligned} \tag{3.19}$$

The number of variables in problem (3.8) is $N \cdot L(1+2K)$ while it is only $N \cdot L$ in problem (3.19). Also, the number of constraints is $L \cdot K + N(4L-1)$ in problem (3.8) compared to $N(3L-1)$ in problem (3.19). Hence, the problem decomposition allows to reduce the computational complexity of the off-line energy management to $O\left((N \cdot L)^2 N(3L-1) + L(N \cdot K)^2 (K+N)\right)$.

3.5 On-line Energy Management

In this section, we propose to solve problem (3.8) by an on-line energy management. The central unit is assumed to know the channel coefficients, the harvested energy at different RRHs only at the current frame *i*.

3.5.1 Optimal Setting

The optimal on-line solution to problem (3.8) i.e., without knowing the CSI values, harvested energy and batteries levels in the future frames, could be found by solving the well-known Bellman equation using dynamic programming (DP) Puterman (2014). The system state at frame *i* is defined by the current batteries levels in addition to the harvested energy amounts

as $s_i = \{B_n(i) + A_n(i)\}_{n=1..N}$, and the decision at frame i is defined by the energy drawn from the energy harvesting sources as $a(s_i) = \{X_n^e(i)\}_{n=1..N}$. Since future CSI values are not known, we define a penalty function as the expected minimal grid power consumption over channel realizations $U_a(s_i) = \mathbf{E}_{\mathbf{H}}\{u_{\mathbf{H}}(s_i, a)\}$, where

$$
\begin{aligned}
u_{\mathbf{H}}(s_i, a) = & \underset{\substack{\{E_n^e(i), p_{n,k}^e(i), p_{n,k}^g(i)\} \\ k=1..K, n=1..N}}{\text{minimize}} \sum_{n=1}^{N} \alpha_{n,i} \cdot \Delta_{n,i} \\
& \text{subject to} \\
& (3.20.a) : \gamma_k(i) \geq \gamma_{th},\ k = 1..K, \\
& (3.20.b) : E_n^e(i) + \sum_{k=1}^{K} p_{n,k}^e(i) \cdot T = X_n^e(i),\ n = 1..N, \\
& (3.20.c) : \sum_{k=1}^{K} p_{n,k}^e(i) + p_{n,k}^g(i) \leq p_{max},\ n = 1..N, \\
& (3.20.d) : p_{n,k}^e(i), p_{n,k}^g(i) \geq 0,\ k = 1..K,\ n = 1..N, \\
& (3.20.e) : E_{fix} \geq E_n^e(i) \geq 0,\ n = 1..N.
\end{aligned}
\tag{3.20}
$$

Given the current system state s_i, the optimal on-line decision a^* has to verify the Bellman's equation of optimality Puterman (2014):

$$
J^{a^*}(s_i) = \min_{a \in \varphi(s_i)} \{U_a(s_i) + \sum_{s' \in \phi(s_{i+1})} Pr(s_{i+1} = s' \mid s_i, a) J^{a^*}(s_{i+1} = s')\}, \tag{3.21}
$$

where $\varphi(s_i)$ denotes the set of all feasible decisions at state s_i and $\phi(s_{i+1})$ denotes the set of possible states at frame $i+1$.

The optimal on-line energy management can be determined by solving (3.21) using DP. The DP method suffers from high computational complexity due to very large number of system states and decisions.

3.5.2 Maximal Harvested Energy Utilization

In this section, we propose an on-line algorithm (Max-ON) that uses the maximal available harvested energy at each frame. Hence, the following problem could be solved at each frame i:

$$\begin{aligned}
&\underset{\substack{\{E^e_n(i),p^e_{n,k}(i),p^g_{n,k}(i)\}\\ k=1..K,n=1..N}}{\text{minimize}} \sum_{n=1}^{N} \alpha_{n,i}\cdot\Delta_{n,i}\\
&\text{subject to}\\
&(3.22.a): \gamma_k(i) \geq \gamma_{th},\ k=1..K,\\
&(3.22.b): E^e_n(i) + \sum_{k=1}^{K} p^e_{n,k}(i)\cdot T \leq B_n(i),\ n=1..N,\\
&(3.22.c): \sum_{k=1}^{K} p^e_{n,k}(i) + p^g_{n,k}(i) \leq p_{max},\ n=1..N,\\
&(3.22.d): p^e_{n,k}(i), p^g_{n,k}(i) \geq 0,\ k=1..K,\ n=1..N,\\
&(3.22.e): E_{fix} \geq E^e_n(i) \geq 0,\ n=1..N.
\end{aligned} \tag{3.22}$$

The on-line energy management algorithm described in Algorithm 3.2 solves the linear program (3.22) using IPM at each frame i.

Algorithm 3.2 Max-ON Algorithm

```
1  B_n(1) ← A_n(1), n = 1..N, // initialization;
2  Δ_tot ← 0, // initial grid power consumption;
3  for i = 1 : L do
4  |   solve linear program (3.22);
5  |   Δ_tot ← Δ_tot + Σ_{n=1}^{N} α_{n,i} · Δ_{n,i};
6  |   for n = 1 : N do
7  |   |   X^e_n(i) ← E^e_n(i) + Σ_{k=1}^{K} p^e_{n,k}(i) · T, n = 1..N, // Consumed harvested energies
   |   |     computation;
8  |   |   B_n(i+1) ← min(B_max, B_n(i) − X^e_n(i) + A_n(i)), n = 1..N, // batteries level
   |   |     update;
9  |   end
10 end
```

The linear program formulated in (3.22) using IPM with complexity order $f(N,K,1)$ when assuming $L=1$ can be solved. Hence, the computational complexity Max-ON Algorithm is given by:

$$C^{mo} = L \cdot f(N,K,1). \tag{3.23}$$

3.5.3 Harvested Energy Prediction

Prediction models that allow to predict the future harvested energy amount, were proposed based on real traces where Pro-Energy model Cammarano *et al.* (2016) is shown to be the most accurate. In Saidi *et al.* (2016), the future harvested energy is predicted using Kalman filter with high computational complexity. In our work, we propose to use the characteristic of the Markov chain that models the harvested energy over time in order to predict it and improve its management. We define the matrix $\mathbf{Q} = [Q(\omega_m, \omega_j)]_{m,j=1:M} \in \mathbb{C}^{M \times M}$ which contains the transition probabilities between the various states. Given the initial state of harvested energy $\pi_n(0)$, the vector $\pi_n(i) = [\pi_n^m(i)]_{m=1:M} \in \mathbb{C}^{1 \times M}$ of harvested energy distribution at RRH n during frame i is given by:

$$\pi_n(i) = \pi_n(0)\mathbf{Q}^i. \tag{3.24}$$

Hence, the predicted energy at RRH n during frame i is found as:

$$\widehat{A}_n(i) = \sum_{m=1}^{M} \pi_n^m(i)\omega_m. \tag{3.25}$$

Since the batteries levels and the harvested energy are known only in the current frame i, the future harvested energy at different RRHs could be predicted using (3.25). The different values of path loss are known at the central unit and assumed to be static during the L frames. Since the

Algorithm 3.3 Pred-ON Algorithm

$B_n(1) \leftarrow A_n(1),\ n = 1..N$, // initialization;
$\Delta_{tot} \leftarrow 0$, // initial grid power consumption;
for $i = 1 : L$ **do**
  $\pi_n(l) \leftarrow \pi_n(i)\mathbf{Q}^{l-i},\ n = 1..N,\ l = i+1..L$, // harvested energy distribution;
  $\widehat{A}_n(l) \leftarrow \sum_{m=1}^{M} \pi_n^m(i)\omega_m,\ n = 1..N,\ l = i+1..L$, // energy prediction;
  solve linear program (3.27);
  $\Delta_{tot} \leftarrow \Delta_{tot} + \sum_{n=1}^{N} \alpha_{n,i} \cdot \Delta_{n,i}$;
  for $n = 1 : N$ **do**
    $X_n^e(i) \leftarrow E_n^e(i) + \sum_{k=1}^{K} p_{n,k}^e(i) \cdot T,\ n = 1..N$, // computation of the consumed harvested energy;
    $B_n(i+1) \leftarrow \min(B_{max}, B_n(i) - X_n^e(i) + A_n(i)),\ n = 1..N$, // batteries level update;
  end
end

effect of small-scale fading vanishes in large-scale MIMO systems Rusek *et al.* (2013), small-scale fading coefficients of future frames are randomly generated as Gaussian random variables with zero mean and unit variance. We denote by $\widehat{\gamma}_k(l),\ k = 1..K,\ l = i+1..L$ the SINRs at future frames that are computed using estimated path loss values and randomly generated small-scale fading coefficients. In this context, while taking into account the predicted future harvested energies, the grid power consumption minimization problem at frame i is formulated as (3.27).

Next, we propose an on-line energy management algorithm (Pred-ON) described in Algorithm 3.3 that solves the linear program (3.27). The prediction is repeated at each frame which allows to improve the system performance. The computation of $\mathbf{Q}^i,\ i = 2..L$ may be done only once and stored into a lookup table.

The computational complexity of the Pred-ON Algorithm is given by:

$$C^{po} = \sum_{l=L}^{L} f(N, K, L-l+1). \tag{3.26}$$

3.6 RRH On/Off Operation

In this section, we investigate RRH on/off operation. RRHs with bad channel conditions at a given frame may transmit with very low power and thus have limited contribution on the users' SINRs. This causes unnecessary energy consumption by the circuit. Hence, it may be judicious to turn off some RRHs according to the time-varying channel and harvested energy in order to save power and thus to reduce the weighted grid power consumption.

Including RRH on/off operation to the energy management given by (3.8) makes the resulting problem a mixed-integer linear program (MILP). Antenna selection in MIMO wireless communication is known to be an NP-hard problem Dua *et al.* (2006); Luo & Zhang (2008). The optimal solution to this new problem can be obtained with Branch and Bound approaches. However, in the context of large-scale MIMO, such solution is inconceivable due to its high computational complexity that depends on the large number of RRHs.

$$
\begin{aligned}
&\underset{\substack{\{p^e_{n,k}(l),p^g_{n,k}(l),E^e_n(l)\}\\ k=1..K,n=1..N,l=i..L}}{\text{minimize}} \sum_{l=i}^{L}\sum_{n=1}^{N} \alpha_{n,i}\Delta_{n,i} \\
&\text{subject to} \\
&(3.27.a): \gamma_k(i) \geq \gamma_{th}, \widehat{\gamma}_k(l) \geq \gamma_{th},\ k=1..K,\ l=i+1..L, \\
&(3.27.b): \sum_{l=i}^{l'}\left(E^e_n(l)+\sum_{k=1}^{K} p^e_{n,k}(l)\cdot T\right) \leq B_n(i)+\sum_{l=i+1}^{l'}\widehat{A}_n(l),\ n=1..N,\ l'=i..L, \\
&(3.27.c): B_n(i)+\sum_{l=i+1}^{l'}\widehat{A}_n(l)-\sum_{l=i}^{l'-1}(E^e_n(l)+\sum_{k=1}^{K} p^e_{n,k}(l)\cdot T) \leq B_{max},\ n=1..N,\ l'=i+1..L, \\
&(3.27.d): \sum_{k=1}^{K}(p^e_{n,k}(l)+p^g_{n,k}(l)) \leq p_{max},\ n=1..N,\ l=i..L, \\
&(3.27.e): p^e_{n,k}(l), p^g_{n,k}(l) \geq 0,\ k=1..K,\ n=1..N,\ l=i..L, \\
&(3.27.f): E_{fix} \geq E^e_n(l) \geq 0,\ n=1..N,\ l=i..L.
\end{aligned}
\tag{3.27}
$$

We propose an efficient heuristic algorithm to solve the problem of RRH on/off operation and save unnecessary consumed energy by the circuit. The optimal off-line energy management is firstly solved considering that all RRHs are active during all frames. Next, the RRHs to be deactivated are those given by the set:

$$\Gamma = \{(n,l) \in \{1,...,N\} \times \{1,...,L\} | \sum_{k=1}^{K} (p_{n,k}^{e}(l) + p_{n,k}^{g}(l)) \leq \varepsilon\}. \tag{3.28}$$

Finally, we force the set of RRHs with low transmit power to be deactivated and thus we solve problem (3.8) taking as input the set $\overline{\Gamma} = \{1,...,N\} \times \{1,...,L\} \setminus \Gamma$ as the set of RRHs to be activated. It is worth noting that although the RRHs may be deactivated iteratively one by one starting by the one with less transmit power, such approach may lead to computational complexity increase due to the large number of RRHs in the considered system.

The optimal RRH On/Off operation is obtained with the brute-force search algorithm, the number of possible combinations of sets of links is $\sum_{l=L}^{L} \sum_{n=1}^{N} \mathbf{C}_N^n \mathbf{C}_L^L$. Hence, its computational complexity is given by:

$$C_{rrh}^{opt} = \sum_{l=L}^{L} \sum_{n=1}^{N} \binom{N}{n} \binom{L}{l} f(n,K,l). \tag{3.29}$$

The computational complexity of the heuristic RRH On/Off algorithm is given by:

$$C_{lr}^{ite} = \sum_{l=L}^{L} \sum_{n=1}^{N} f(n,K,l). \tag{3.30}$$

3.7 Numerical Results

In this section, monte carlo simulations are used to evaluate the performance of the proposed algorithms. The simulation parameters used in this section unless otherwise mentioned are

summarized in Table 3.1. We consider that the distributed large-scale array system adopts a circular topology. The RRHs are uniformly deployed along a circle of radius r_a and the users are uniformly distributed within the circular cell of radius r_c with $r_a < r_c$. The grid power consumption weights $\alpha_{n,i}$ are randomly generated according to a uniform standard uniform distribution.

Table 3.1 Simulation Parameters.

Symbol	Description	Value
p_c	circuit power per RF chain	30 dBm Kumar & Gurugubelli (2011)
ν	path loss exponent	3.7
r_a	antenna array radius	40 m
r_c	cell radius	500 m
p_{max}	max transmit power per-RRH	1 W
B_{max}	max battery capacity	50 J
N	number of RRHs	80
K	number of users	8
L	number of frames	5
	noise PSD	-174 dBm/Hz

In Fig. 3.2, we compare the grid power cost under different off-line and on-line energy management strategies versus SINR target. The performance gap between the optimal and heuristic off-line solutions increases as the SINR target increases. The on-line energy management algorithm with energy prediction performs very well compared to the on-line energy management algorithm with maximal available harvested energy utilization but with higher computational complexity. Moreover, the performance gap between the two proposed on-line solutions and the optimal off-line solution keeps almost unchanged when the SINR target increases.

Fig. 3.3 shows the impact of the number of RRHs on the performance of the proposed energy management algorithms. The grid power cost satisfying the system requirement starts decreasing since the total harvested energy increases by increasing the number of RRHs. Then, the grid power cost starts increasing at certain point due to the increase of the energy required by the circuits when the number of RRHs increases.

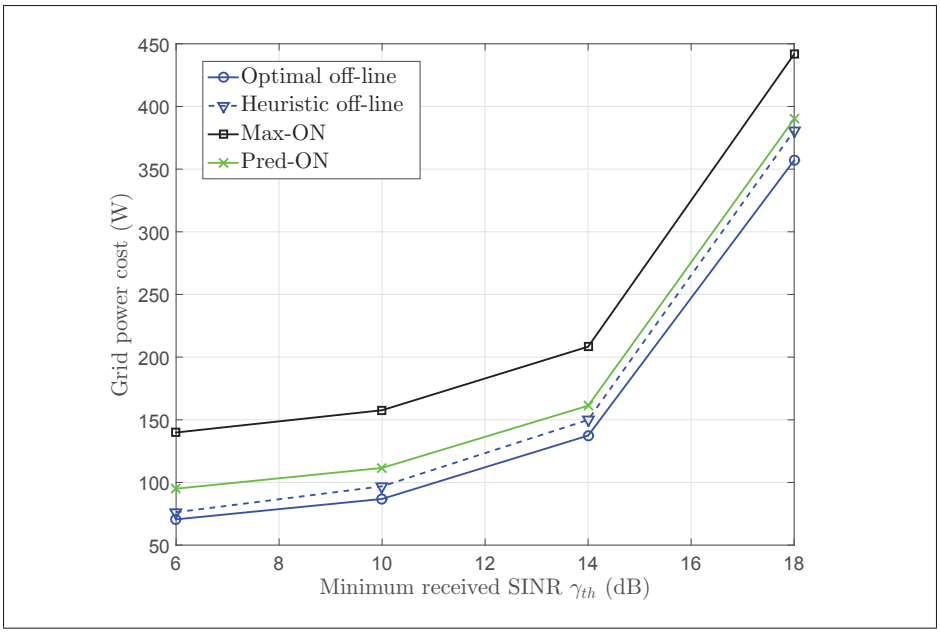

Figure 3.2 Grid power cost versus SINR target with off-line and on-line energy management.

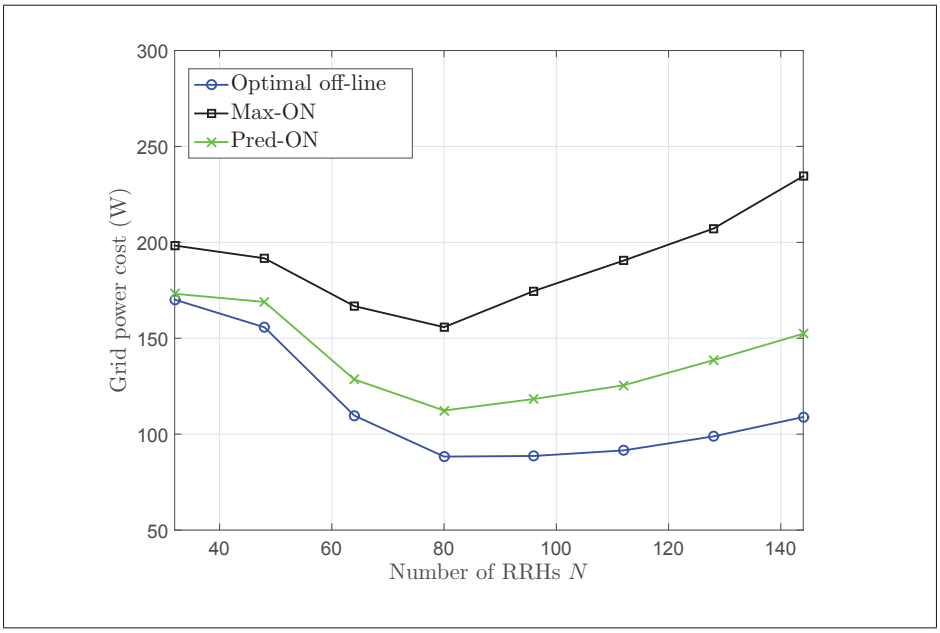

Figure 3.3 Grid power cost versus number of RRHs with off-line and on-line energy management.

In Fig. 3.4, we investigate the performance of the iterative link removal algorithm by showing the percentage of removed links versus the minimum received SINR. The optimal values are shown for only limited number of users $K = 4$ and frames $L = 2$ due to the high complexity of the exhaustive search optimal algorithm. The performance gap between the proposed algorithm and optimal link removal is tight and does not change too much when the SINR target increases. As expected, the percentage of removed links is higher when the QoS constraints are more stringent. Increasing per-RRH maximal transmit power p_{max} allows to increase the total transmit power and thus to admit more links. Hence, the percentage of removed links decreases particularly at low SINR targets. However, this performance gain vanishes at high SINR targets due to the increase of multi-user interference.

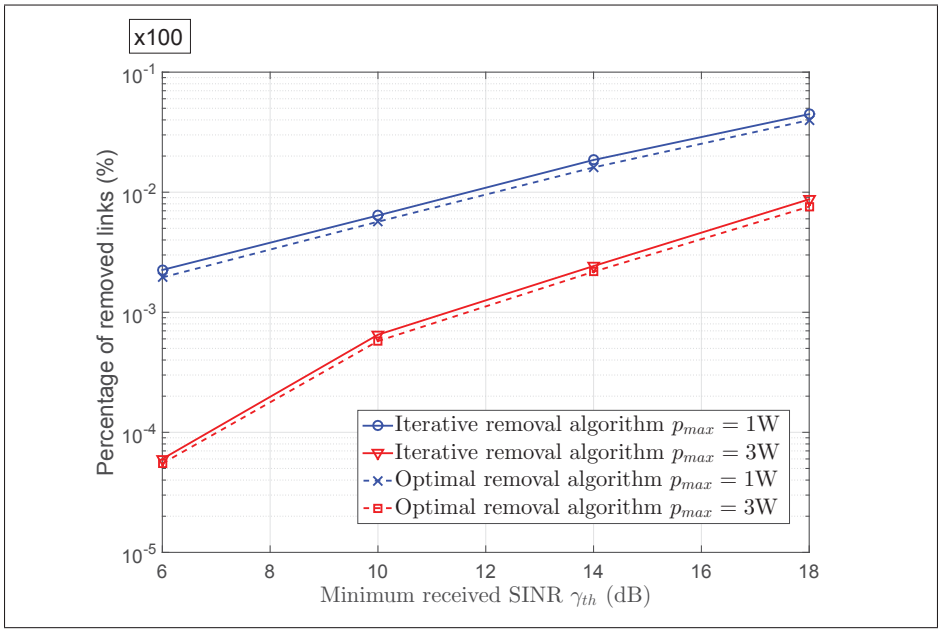

Figure 3.4 Percentage of removed links under iterative and optimal link removal algorithms($K = 4, L = 2$).

Removing links one by one may result in high computational complexity. We investigate in Table 3.2 the performance of the iterative link removal algorithm when R links are removed at each step considering a SINR target $\gamma_{th} = 10$ dB. The execution time of the multiple links removal algorithm is normalized by the execution time when removing links one by one. It is

clear that increasing the number of removed links at each step involves some performance loss. However, the gain in execution time may seem interesting for practical implementations.

Table 3.2 Multiple links removal($\gamma_{th} = 10$ dB).

R	Percentage of removed links (%)		Normalized execution time	
	L=5,K=8	L=7,K=10	L=5,K=8	L=7,K=10
1	6.8	14.79	-	-
5	9	17.34	0.27	0.29
10	12.95	20.16	0.19	0.19

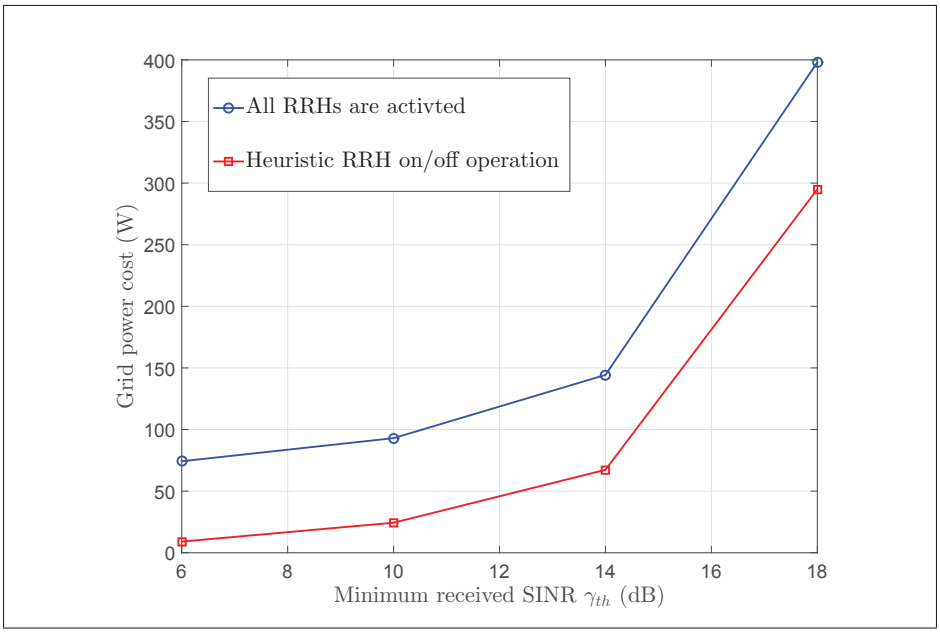

Figure 3.5 Grid power cost under heuristic RRH on/off operation.

In Fig. 3.5, we show the achieved grid power cost under the heuristic RRH on/off operation algorithm. All the users are satisfied. The grid power cost decreases significantly. Hence, the system performance is improved by deactivating the RRHs with low transmit power that causes unnecessary consumed circuit power.

3.8 Conclusion

This paper investigated energy efficient distributed large-scale MIMO systems while the RRHs are powered by energy bought from a grid source in addition to energy harvested from renewable sources. A minimization problem of grid power consumption subject to quality of service constraint per user was formulated as linear program. The off-line energy management was optimally and heuristically solved. The formulated problem could be infeasible due to the users requirement and per-antenna power constraints. Hence, an iterative link removal algorithm was proposed in order to overcome the feasibility problem. The optimal on-line energy management algorithm was also discussed for solving the problem and efficient on-line energy management algorithm based on energy prediction was proposed. RRH on/off operation was investigated in order to decrease the consumed energy. Furthermore, the proposed approach allows efficient use of non-renewable energy in hybrid energy large-scale MIMO systems.

Future works will focus on developing distributed energy management approaches inspired by game theory.

CHAPTER 4

NEW EFFICIENT TRANSMISSION TECHNIQUE FOR HETNETS WITH MASSIVE MIMO WIRELESS BACKHAUL

Rami Hamdi[1,2], Elmahdi Driouch[3], Wessam Ajib[1]

[1] Department of Computer Science, Université du Québec à Montréal (UQÀM), QC, Canada
[2] École de Technologie Supérieure,
1100 Notre-Dame Ouest, Montréal, Québec, Canada H3C 1K3
[3] Université de Moncton, NB, Canada

This article was submitted to IEEE Transactions on Wireless Communications in December 2017 and revised (Major revision) in April 2018.

4.1 Abstract

In order to cope with the rapid increase in power consumption of heterogeneous cellular networks, this paper proposes a new efficient transmission technique for heterogeneous networks with massive MIMO wireless backhaul with the objective of minimizing power consumption cost. We assume that transmissions on the backhaul link and the access link occur simultaneously on the same frequency band (in-band) thanks to MIMO spatial multiplexing. On the other hand, we consider that uplink and downlink transmissions are separated in time. In order to prevent multi-user and inter-tier interference, block diagonalization beamforming is considered at the macro base station (MBS) and the signal from the small base station (SBS) to the MBS is transmitted orthogonally to the channel of the SBS's users. The problem of minimizing the transmit power of base stations under users minimum-rate constraints is formulated. We first derive analytically the optimal time splitting parameter and the allocated transmit power considering that the inter-SBS interference is generated by fixed power. Next, we solve the power allocation problem when the generated inter-SBS interference is no longer considered fixed by proposing an efficient iterative power allocation algorithm. A heuristic user scheduling algorithm is devised in order to deal with the problem feasibility. Finally, simulations validate our analysis and show that the proposed transmission technique outperforms the conventional

reverse time division duplex with bandwidth splitting (out-band) in terms of transmit power consumption.

4.2 Introduction

Heterogenous networks (HetNets) and massive multiple-input multiple-output (MIMO) are key technologies that will allow next generation wireless networks to support the increasing data traffic Andrews *et al.* (2014). HetNets are based on the deployment of low-power small base stations (SBSs) geographically distributed within the macro cell. These base stations have the capability to increase the data rate and to enhance the network reliability Ghosh *et al.* (2012). However, the backhauling of huge amount of data traffic is challenging especially when the SBSs are densely deployed. Moreover, the massive implementation of wired backhauling may become infeasible for next generation wireless networks. In this context, wireless backhauling was proposed as an alternative solution that enable low-cost connection between the SBSs and the macro base station (MBS) Siddique *et al.* (2015). On the other hand, massive MIMO systems are based on using few hundreds of antennas to serve at the same time-frequency few tens of users Rusek *et al.* (2013). In consequence of the law of large numbers, the diversity of large number of antennas implies quasi-orthogonality between the users' channels. Thus, linear transmitters and receivers are able to achieve high performance Yang & Marzetta (2013). The coexistence of massive MIMO, HetNets and wireless backhauling is a promising research direction since massive MIMO is a suitable solution to enable wireless backhauling Zhang *et al.* (2015b). The gains offered by the coexistence between the two technologies absolutely require adequate resource allocation and interference management strategies. Specifically, it is very challenging to manage the interference between the wireless backhaul links and the access links.

4.2.1 Related Work

In HetNets with wireless backhaul, reverse time division duplex (RTDD) with bandwidth splitting was investigated in Sanguinetti *et al.* (2015); Wang *et al.* (2016a); Xia *et al.* (2017); Niu

et al. (2018); Feng & Mao (2017); Nguyen *et al.* (2016) for managing interference between backhaul and access links. In RTDD (as shown in Fig.4.1, the interference between the backhaul link and the access link is managed as follows: first the bandwidth is orthogonally split between backhaul downlink (DL) transmissions (MBS $\rightarrow$ SBS) and access uplink (UL) transmissions (SBS $\leftarrow$ users), then the bandwidth is orthogonally split in the next time slot between backhaul UL transmissions (MBS $\leftarrow$ SBS) and access DL transmissions (SBS $\rightarrow$ users). On another hand, investigating massive MIMO systems in wireless backhauling was done in, for instance, Sanguinetti *et al.* (2015); Wang *et al.* (2016a); Xia *et al.* (2017); Niu *et al.* (2018); Feng & Mao (2017). A large system analysis is performed in Sanguinetti *et al.* (2015) to find the asymptotic power allocation and beamforming vectors. An efficient cell association and bandwidth allocation algorithm that maximizes wireless backhaul link sum-rate was proposed in Wang *et al.* (2016a). In Xia *et al.* (2017), the authors optimize the bandwidth division between access and backhaul links based on statistical channel information. An efficient iterative resource allocation algorithm that maximizes the throughput based on primal decomposition is developed in Niu *et al.* (2018). In Feng & Mao (2017), the authors proposed a distributed pilot allocation and user association algorithm that maximizes the sum rate of all users. The optimal bandwidth splitting is derived in Nguyen *et al.* (2016) for conventional wireless backhaul systems.

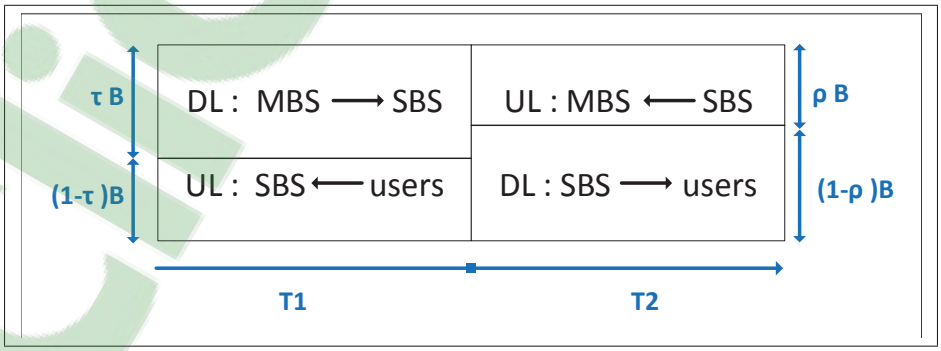

Figure 4.1 RTDD with bandwidth splitting.

Other works Li *et al.* (2015); Tabassum *et al.* (2016); Chen *et al.* (2016b) investigated wireless backhauling enabled by full duplex SBSs where the backhaul as well as the access links share

the same spectrum band. In Li *et al.* (2015), the authors demonstrate that these systems have the potential to improve the sum-rate. In Tabassum *et al.* (2016), the portion of SBSs working on full duplex mode is optimized in order to improve several performance metrics. In addition of considering wireless backhaul communication enabled by full duplex, the authors of Chen *et al.* (2016b) assume that the SBSs are powered by energy harvesting sources. Efficient power allocation and user association algorithms are proposed in order to optimize the energy efficiency. Unfortunately, full duplex communication systems may suffer from self interference which lead to poor system performance, unless implementing high complexity interference cancellation techniques.

Also, the access and backhaul spectrum bands could be separated in order to eliminate the inter-tier interference which was the focus of Zhao *et al.* (2015). The authors proposed efficient iterative algorithms to manage the inter-SBS interference and hence to maximize the number of active SBSs. Moreover, millimeter wave systems were incorporated in HetNets in order to eliminate the inter-tier interference Gao *et al.* (2015). An architecture based on millimeter wave communications is proposed in Hao & Yang (2018) and an efficient iterative power allocation algorithm is designed. However, these systems are vulnerable to severe pathloss attenuation compared to conventional spectrum band.

4.2.2 Contribution

The interference in HetNets between the access links and the backhaul should be efficiently managed especially when the wireless backhaul is using massive MIMO systems. Novel efficient inter-tier interference management scheme have to be designed to ensure an efficient network operation in terms of power consumption Li *et al.* (2016). Therefore, this paper proposes a new transmission technique (named spatial time division duplexing or spatial TDD) for HetNets based on MIMO spatial multiplexing and time splitting. We consider that the SBSs are able to communicate with the MBS and serve their associated users thanks to MIMO while the DL and UL transmissions are separated in time. In particular, block diagonalization beamforming is considered at MBS and the signal from the SBS to the MBS is transmitted

orthogonally to the channel of the SBS's users. In summary, this paper presents the following novel contributions:

- A new efficient interference management scheme for HetNets is proposed based on MIMO spatial multiplexing and time splitting.
- The problem of optimizing a general utility function (and in particular the base stations transmit power consumption) subject to users minimum-rate requirements is formulated as a non-linear optimization problem.
- The optimal time splitting parameter and the allocated transmit power are derived. The proposed transmission technique is shown to be more efficient in terms of transmit power consumption than RTDD with bandwidth splitting.
- An iterative power allocation algorithm adapted to our transmission technique is devised to provide close-to-optimal solution and the convergence of this algorithm is proven.
- The problem feasibility is addressed by proposing an efficient user scheduling algorithm.

4.2.3 Organization

The rest of the paper is organized as follows. The system model is presented in Section 4.3 and the proposed transmission technique is presented in Section 4.4. We investigate the transmit power minimization problem in Section 4.5. We investigate the optimal time splitting parameter and power allocation in Section 4.6. User scheduling is investigated in Section 4.7. Numerical results are presented and discussed in Section 4.8. Finally, conclusions are provided in Section 4.9.

4.3 System Model

We consider a HetNet as depicted in Fig. 4.2 where a single massive MIMO MBS coexists with S MIMO SBSs. The MBS is equipped with a large number of antennas N and each SBS s is equipped with M_s antennas where $N > \sum_{s=1}^{S} M_s$. The MBS communicates with the SBSs via

wireless backhaul and each SBS could serve one or multiple single-antenna users. We denote by Λ_s the set of users associated with SBS s and K_s the cardinal of Λ_s. Also, we consider that the MBS serves F macro users equipments(MUEs).

The wireless backhaul channel between the MBS and SBS s undergoes a Rician fading and is represented by $\mathbf{H}_s \in \mathbb{C}^{M_s \times N}$ whose elements are complex Gaussian variables with nonzero mean. Perfect channel knowledge is assumed in order to make the problem tractable. The assumption of perfect channel knowledge is widely used in the literature Li *et al.* (2016); Wang *et al.* (2016a); Feng & Mao (2017); Wang *et al.* (2017). In addition, obtaining perfect channel knowledge is hard in practice, we illustrate the impact of channel estimation on the performance of the studied and proposed techniques in simulation results section.

The access link channel between user $k \in \Lambda_s$ and SBS s is represented by vector $\mathbf{g}_{s,k} = \sqrt{\alpha_{s,k}}\mathbf{l}_{s,k} \in \mathbb{C}^{M_s \times 1}$. The $M_s \times 1$ vector $\mathbf{l}_{s,k}$ is the small-scale fading channel vector between user k and SBS s, which is assumed to be quasi-static complex Gaussian i.i.d. slow fading channel and $\alpha_{s,k}$ represents the large-scale fading channel coefficient. The whole channel matrix is defined as $\mathbf{G}_s = [\mathbf{g}_{s,k}]_{k=1:K_s} \in \mathbb{C}^{M_s \times K_s}$. We use the following notation $(.)^{a,b}$, where a is either *ac* for access link or *bh* for backhaul link, whereas b is either *ul* for uplink or *dl* for downlink.

4.4 Spatial TDD transmission technique

In our proposed spatial TDD transmission technique illustrated in Fig. 4.3, we consider time division duplex (TDD) to exploit the channel reciprocity for UL/DL and facilitate the channel state information (CSI) acquisition. However, in contrast to RTDD, our proposed technique considers that the UL and DL transmissions occur on the same frequency band since no orthogonal splitting is assumed. The time slot with duration T is dynamically divided into two frames. In the first frame with duration $\lambda \cdot T$, the SBSs are on receive mode. Hence, DL transmissions (MBS $\rightarrow$ SBS) and UL transmissions (SBS $\leftarrow$ users) occur on the same frequency band. In the second frame with duration $(1-\lambda) \cdot T$, blue the SBSs are on transmit mode, and once again transmissions to the MBS and the users are performed on the same frequency band.

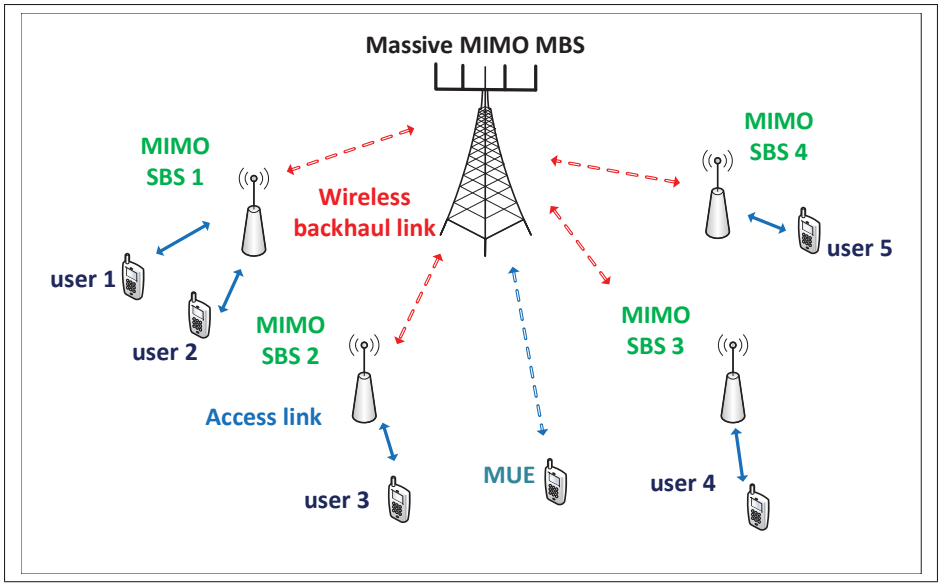

Figure 4.2 HetNet with MIMO SBSs and massive MIMO wireless backhaul.

The coefficient $\lambda \in [0,1]$, called the time splitting parameter, has to be dynamically optimized for maximal performance.

4.4.1 1st Frame: SBS on Receive Mode

Linear beamforming techniques such as zero forcing (ZF) beamforming are shown to achieve near-optimal performance in massive MIMO systems Rusek *et al.* (2013). ZF beamforming is suitable for downlink transmission when the receivers are equipped with single antenna. Moreover, multi-user interference, when receivers have multiple antennas, could be suppressed using the low complexity block diagonalization (BD), which is known to achieve near-optimal capacity in conventional MIMO Spencer *et al.* (2004). Also, BD was investigated in Ni & Dong (2016) and was shown to be suitable for massive MIMO systems. Thus, our proposed technique considers BD as a beamforming technique for downlink transmission from the MBS to the SBSs.

We denote by $\mathbf{W}_s^{bh,dl}$ the beamforming matrix for SBS s. This matrix is designed in order to satisfy the constraints blue$\mathbf{H}_i \mathbf{W}_s^{bh,dl^H} = \mathbf{0}_{M_i \times L_s}$ and $\mathbf{W}_s^{bh,dl^H} \mathbf{W}_s^{bh,dl} = \mathbf{I}_N$ for all $i \neq s$. Follow-

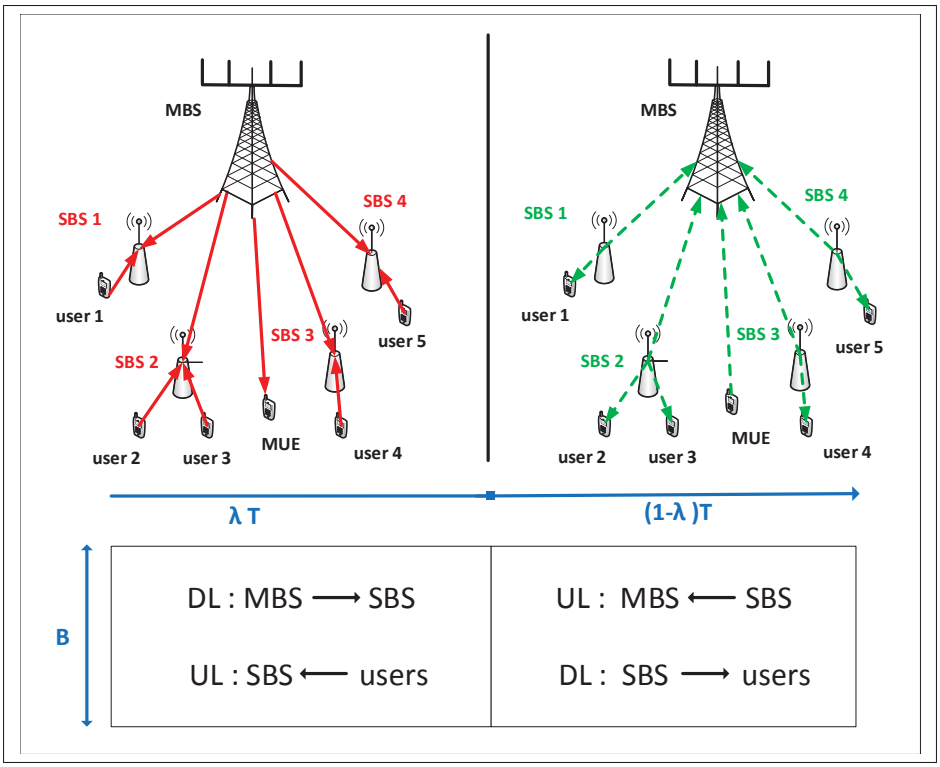

Figure 4.3 Proposed transmission technique.

ing Spencer *et al.* (2004), $\mathbf{W}_s^{bh,dl}$ lies in the null space of matrix $\overline{\mathbf{H}}_s$ which is defined as $\overline{\mathbf{H}}_s = [\mathbf{H}_1^T ... \mathbf{H}_{s-1}^T \mathbf{H}_{s+1}^T ... \mathbf{H}_S^T]^T$. The beamforming matrix for SBS s is obtained as $\mathbf{W}_s^{bh,dl} = \overline{\mathbf{V}}_s^{(0)} \mathbf{V}_s^{(1)}$, where $\overline{\mathbf{V}}_s^{(0)}$ is composed of the last $N - \overline{L}_s$ right singular vectors of $\overline{\mathbf{H}}_s$, $\mathbf{V}_s^{(1)}$ represents the first L_s right singular vectors of $\overline{\mathbf{H}}_s \overline{\mathbf{V}}_s^{(0)}$, $\overline{L}_s = \text{rank}(\overline{\mathbf{H}}_s)$ and $L_s = \text{rank}(\overline{\mathbf{H}}_s \overline{\mathbf{V}}_s^{(0)})$.

Let $p_s^{bh,dl}$ denote the portion of power allocated to SBS s and $p^{ac,ul}$ denote the fixed transmit power by the users. Hence, the received signal by SBS s can be written as:

$$\mathbf{y}_s^{sbs} = \mathbf{H}_s \mathbf{W}_s^{bh,dl^H} \mathbf{B}_s \mathbf{a}_s^{bh,dl} \sqrt{\frac{p_s^{bh,dl}}{U_s}} + \sum_{k=1}^{K_s} \mathbf{g}_{s,k} \sqrt{p^{ac,ul}} a_{s,k}^{ac,ul} + \sum_{i=1, i \neq s}^{S} \sum_{j=1}^{K_i} \mathbf{f}_{i,j}^{s} \sqrt{p^{ac,ul}} a_{i,j}^{ac,ul} + \mathbf{n}_s^{sbs}, \tag{4.1}$$

where $U_s = M_s - K_s$ is the number of beams for SBS s, $\mathbf{a}_s^{bh,dl} \in \mathbb{C}^{U_s \times 1}$ is the data symbol vector, $\mathbf{B}_s = \begin{bmatrix} \mathbf{I}_{U_s} \\ \mathbf{0}_{L_s - U_s \times U_s} \end{bmatrix} \in \mathbb{C}^{L_s \times U_s}$, $a_{s,k}^{ac,ul}$ is a data symbol with unit energy, $\mathbf{f}_{i,j}^{s}$ denotes the channel vector from user j associated with SBS i to SBS s and $\mathbf{n}_s^{sbs}$ denotes the noise vector which is assumed to be additive white Gaussian noise (AWGN) with zero mean and variance σ^2.

Our proposed technique assumes the utilisation of ZF detectors at the SBSs. Hence, the decoder matrix $\mathbf{Z}_s$ of SBS s is given by $\mathbf{Z}_s = \mathbf{F}_s(\mathbf{F}_s^H \mathbf{F}_s)^{-1}$, where blue $\mathbf{F}_s = [\mathbf{G}_s \, \mathbf{H}_s \mathbf{W}_s^{bh,dl^H} \mathbf{B}_s]$. blue We have $\text{rank}(\mathbf{G}_s) = K_s$ and $\text{rank}(\mathbf{H}_s \mathbf{W}_s^{bh,dl^H} \mathbf{B}_s) \leq U_s = M_s - K_s$. Hence, we obtain $\text{rank}(\mathbf{F}_s) \leq K_s + U_s = M_s$. Hence, the number of antennas M_s at the SBS s is larger than the rank of matrix $\mathbf{F}_s$. The received signals from the MBS and the users are separated as $\mathbf{r}_s^{sbs} = \mathbf{Z}_s^H \mathbf{y}_s^{sbs}$. Consequently, the rate for SBS s is expressed as Shi *et al.* (2009):

$$r_s^{bh,dl} = \lambda \cdot \sum_{u=1}^{U_s} \log_2 \left(1 + \frac{\frac{p_s^{bh,dl}}{U_s}}{\varphi_s^u + \sigma^2 \left[(\mathbf{F}_s^H \mathbf{F}_s)^{-1} \right]_{K_s+u, K_s+u}} \right), \tag{4.2}$$

where $\varphi_s^u = \sum_{i=1, i \neq s}^{S} \sum_{j=1}^{K_i} p^{ac,ul} \mid \mathbf{z}^{sH}_{K_s+u} \mathbf{f}_{i,j}^{s} \mid^2$ represents interference from the users associated with others SBSs.

The rate for user k associated with SBS s is given by:

$$r_{s,k}^{ac,ul} = \lambda \cdot \log_2 \left(1 + \frac{p^{ac,ul}}{\mu_{s,k} + \sigma^2 \left[(\mathbf{F}_s^H \mathbf{F}_s)^{-1} \right]_{k,k}} \right), \tag{4.3}$$

where $\mu_{s,k} = \sum_{i=1, i \neq s}^{S} \sum_{j=1}^{K_i} p^{ac,ul} \mid \mathbf{z}_k^{sH} \mathbf{f}_{i,j}^{s} \mid^2$ represents the interference from the users associated with other SBSs.

Since we consider that MUEs are served directly by the MBS, the MUEs are also on receive mode in this frame using BD and the rate $r_f^{mu,dl}$ for MUE f is similar to (4.2).

Finally, p_{max}^{mbs} denotes the maximal transmit power of the MBS. Thus, the following constraint should hold:

$$\sum_{s=1}^{S} p_s^{bh,dl} + \sum_{f=1}^{F} p_f^{mu,dl} \leq p_{max}^{mbs}. \tag{4.4}$$

4.4.2 2nd Frame: SBS on Transmit Mode

In this frame, the SBSs are in transmit mode. Each SBS transmits simultaneously to the MBS and to its associated users. First, the transmit signals to the users are precoded using ZF which eliminate the inter-user interference. The beamforming matrix is given by $\mathbf{W}_s^{ac,dl} = \mathbf{G}_s(\mathbf{G}_s^H\mathbf{G}_s)^{-1}/\sqrt{\mathbf{Tr}\{(\mathbf{G}_s^H\mathbf{G}_s)^{-1}\}}$. We denote by $\mathbf{w}_{s,k}^{ac,dl} \in \mathbb{C}^{M_s\times 1}$ the beamforming vector for user k associated with SBS s.

Since the MBS is equipped with large number of antennas, the signal intended to the MBS is transmitted orthogonally to the channel of the users in order to prevent excessive interference at the users. The beamforming vector $\mathbf{w}_s^{bh,ul} \in \mathbb{C}^{M_s\times 1}$ for the MBS is a projection vector based on the null space of the users channel matrix using Gram–Schmidt orthonormalization Matsumura & Ohtsuki (2011) and has to verify $\mathbf{G}_s^H\mathbf{w}_s^{bh,ul} = \mathbf{0}_{K_s\times 1}$. Hence, the transmitted signal of SBS s is expressed as:

$$\mathbf{x}_s^{sbs} = \mathbf{w}_s^{bh,ul}\sqrt{p_s^{bh,ul}}a_s^{bh,ul} + \sum_{k=1}^{K_s} \mathbf{w}_{s,k}^{ac,dl}\sqrt{p_{s,k}^{ac,dl}}a_{s,k}^{ac,dl}, \tag{4.5}$$

where $a_s^{bh,ul}$ and $a_{s,k}^{ac,dl}$ denote the data symbols with unit energy intended respectively to the MBS and to user k, $p_s^{bh,ul}$ denotes the portion of power allocated for the MBS and $p_{s,k}^{ac,dl}$ denotes the power allocated for user $k \in \Lambda_s$.

The rate for user k associated with SBS s is expressed as:

$$r_{s,k}^{ac,dl} = (1-\lambda)\cdot \log_2\left(1+\frac{p_{s,k}^{ac,dl}}{\frac{\mathbf{Tr}\{(\mathbf{G}_s^H\mathbf{G}_s)^{-1}\}}{\varpi_s+\sigma^2}}\right), \tag{4.6}$$

where the interference from the other SBSs is expressed as:

$$\varpi_s = \sum_{i=1,i\neq s}^{S} p_i^{bh,ul} \mid \mathbf{f}_{s,k}^{iH}\mathbf{w}_i^{bh,ul} \mid^2 + \sum_{i=1,i\neq s}^{S}\sum_{j=1}^{K_i} p_{i,j}^{ac,dl} \mid \mathbf{f}_{s,k}^{iH}\mathbf{w}_{i,j}^{ac,dl} \mid^2 . \tag{4.7}$$

On the other hand, the received signal at the MBS is given by:

$$\mathbf{y}^{mbs} = \sum_{s=1}^{S}\mathbf{H}_s^H\mathbf{w}_s^{bh,ul}\sqrt{p_s^{bh,ul}}a_s^{bh,ul} + \sum_{s=1}^{S}\sum_{k=1}^{K_s}\mathbf{H}_s^H\mathbf{w}_{s,k}^{ac,dl}\sqrt{p_{s,k}^{ac,dl}}a_{s,k}^{ac,dl} + \mathbf{n}^{mbs}, \tag{4.8}$$

where $\mathbf{n}^{mbs}$ denotes the noise vector which is assumed to be AWGN with zero mean and variance σ^2.

The proposed technique assumes that the signals received at the MBS from the SBSs are separated using a ZF detector as $\mathbf{r}^{mbs} = \mathbf{Q}^H\mathbf{y}^{mbs}$, where the detection matrix is given by $\mathbf{Q} = \mathbf{D}(\mathbf{D}^H\mathbf{D})^{-1}$ and $\mathbf{D} = [\mathbf{H}_1^H\mathbf{w}_1^{bh,ul}... \ \mathbf{H}_S^H\mathbf{w}_S^{bh,ul}] \in \mathbb{C}^{N\times S}$. However, the signals intended to the users are considered as interference. Hence, the rate for the MBS from SBS s is expressed as:

$$r_s^{bh,ul} = (1-\lambda)\cdot \log_2\left(1+\frac{p_s^{bh,ul}}{\upsilon_s+\sigma^2\left[(\mathbf{D}^H\mathbf{D})^{-1}\right]_{s,s}}\right), \tag{4.9}$$

where the interference caused by the signals intended to the users is expressed as:

$$\upsilon_s = \sum_{i=1}^{S}\sum_{j=1}^{K_i} p_{i,j}^{ac,dl} \mid \mathbf{q}_s^H\mathbf{H}_i^H\mathbf{w}_{i,j}^{ac,dl} \mid^2 . \tag{4.10}$$

The MUEs are also on transmit mode in this frame and the rate $r_f^{mu,ul}$ for MUE f can be given similarly to (4.9).

Finally, p_{max}^{sbs} denotes the maximal transmit power at each SBS. Thus, the following constraint should hold:

$$p_s^{bh,ul} + \sum_{k=1}^{K_s} p_{s,k}^{ac,dl} \leq p_{max}^{sbs}. \tag{4.11}$$

The important notations are summarized in Table 4.1.

Table 4.1 Summary of Important Notations.

Symbol	Description
N, M_s	Number of antennas at the MBS and SBS s respectively
S	Number of SBSs
Λ_s	Set of users associated with SBS s
$p_{max}^{mbs}, p_{max}^{sbs}$	Maximal transmit power of the MBS and the SBSs respectively
$p^{ac,ul}$	Transmit power of each user
$p_s^{bh,dl}, p_s^{bh,ul}$	Portion of power allocated to SBS s on DL and UL respectively
$p_{s,k}^{ac,dl}$	Power allocated for user k associated with SBS s
$p_f^{mu,dl}$	Portion of power allocated to MUE f on DL
$\mathbf{H}_s$	Channel matrix between the MBS and SBS s
$\mathbf{g}_{s,k}$	Channel vector between user $k \in \Lambda_s$ and SBS s
λ	Time splitting parameter
$r_{s,k}^{ac,ul}, r_{s,k}^{ac,dl}$	Rate for user $k \in \Lambda_s$ on UL and DL respectively
$r_s^{bh,ul}, r_s^{bh,dl}$	Rate for SBS s on UL and DL respectively

4.5 Total Transmit Power Minimization

4.5.1 Problem Formulation

The objective here is to optimize a system utility function while ensuring a minimum rate for each user at UL and DL and performing optimal power allocation. Also, the frame duration

must be optimally split between the two transmit frames. Hence, the main problem can be formulated as (4.13).

We seek to optimize the system utility function $U(\mathbf{p},\lambda)$ which is convex and depends on the portions of allocated power and on time splitting parameter. A common used choice for a linear system utility is the total consumed power Li *et al.* (2016); Wang *et al.* (2017):

$$U(\mathbf{p},\lambda)=\sum_{s=1}^{S}\left(p_s^{bh,dl}+p_s^{bh,ul}+\sum_{k=1}^{K_s}(p_{s,k}^{ac,dl}+p_{s,k}^{ac,ul})\right)+\sum_{f=1}^{F}p_f^{mu,dl}. \tag{4.12}$$

It is important to note that, to make the problem tractable analytically, we assume that the transmit powers of the users $p^{ac,ul}$ are fixed. Anyhow, these powers are too small compared to the transmit power of the base stations i.e., $p_s^{bh,dl}$ and $p_s^{bh,ul}$. Also, it may be challenging in practice to implement a centralized power control for the base stations and for the users.

We denote by $\mathbf{p}$ the vector containing the portions of allocated power. Constraints $(4.13.a)$ and $(4.13.b)$ ensure that the backhaul transmission rate is at least larger than the access transmission rate for both UL and DL. Constraints $(4.13.c)$ and $(4.13.d)$ impose a minimum rate to the users denoted $r_{th}^{ac,ul}$ for UL and $r_{th}^{ac,dl}$ for DL. Constraints $(4.13.e)$ and $(4.13.f)$ impose a maximum transmit power to the MBS and the SBSs.

The backhaul and access links cannot be all simultaneously active due to inter-SBS interference, multi-user interference and maximal power constraint. Hence, SBS and user scheduling schemes may be devised to maximize the number of served users that ensure their minimum rate requirements. Scheduling schemes may be designed jointly with optimal power control.

UL and DL transmissions are coupled by the parameter λ. Also, $\mathbf{p}$ and λ are coupled by all constraints which make it difficult to decouple the problem into independent sub-problems. Moreover, the problem is non-convex since constraints $(4.13.a)-(4.13.d)$ are non-convex due to inter-SBS interference. Hence, it is extremely difficult to obtain the optimal global solution.

Users association to SBSs may greatly affect the overall power consumption of the system. In fact, user association has a clear impact on the power allocation, which may cause many changes in the perceivable interference at the receivers. However, solving user association in conjunction with resource allocation (i.e. power allocation and time splitting), although it may improve the system performance, makes the joint optimization very hard to solve as shown in Liu *et al.* (2016) where the joint optimization is performed iteratively with high computational complexity. Therefore for simplification purposes, we propose to separate these two problems and mainly focus on resource allocation (i.e. power allocation and time splitting) for our novel transmission technique.

$$
\begin{aligned}
&\underset{\mathbf{p},\lambda}{\text{minimize}}\ U(\mathbf{p},\lambda)\\
&\text{subject to}\\
&(4.13.a): r_s^{bh,dl} \geq \sum_{k=1}^{K_s} r_{s,k}^{ac,dl},\ s=1..S,\\
&(4.13.b): r_s^{bh,ul} \geq \sum_{k=1}^{K_s} r_{s,k}^{ac,ul},\ s=1..S,\\
&(4.13.c): r_{s,k}^{ac,ul}, r_f^{mu,ul} \geq r_{th}^{ac,ul},\ s=1..S,\ k=1..K_s,\ f=1..F,\\
&(4.13.d): r_{s,k}^{ac,dl}, r_f^{mu,dl} \geq r_{th}^{ac,dl},\ s=1..S,\ k=1..K_s,\ f=1..F,\\
&(4.13.e): \sum_{s=1}^{S} p_s^{bh,dl} + \sum_{f=1}^{F} p_f^{mu,dl} \leq p_{max}^{mbs},\\
&(4.13.f): p_s^{bh,ul} + \sum_{k=1}^{K_s} p_{s,k}^{ac,dl} \leq p_{max}^{sbs},\ s=1..S,\\
&(4.13.i): 0<\lambda<1,\\
&(4.13.j): \mathbf{p} \geq 0.
\end{aligned}
\tag{4.13}
$$

4.5.2 RTDD with Bandwidth Splitting

In this case, the bandwidth is divided between the backhaul and the access transmissions where θ is the bandwidth fraction. Since all BSs are equipped with multiple antennas, block diag-

onalization is assumed in the wireless backhaul of the RTDD scheme whereas zero-forcing beamforming is considered in the access link. The interference between backhaul links and access links is thus completely eliminated. The ZF decoder at the SBSs matrix becomes: $\mathbf{Z}_s^0 = \mathbf{G}_s(\mathbf{G}_s^H\mathbf{G}_s)^{-1}$. Hence, the UL rate for user k associated with SBS s becomes:

$$r_{s,k}^{ac,ul,bs} = \frac{\theta}{2}\cdot\log_2\left(1+\frac{p^{ac,ul}}{\mu_{s,k}^0+\theta\cdot\sigma^2\left[(\mathbf{G}_s^H\mathbf{G}_s)^{-1}\right]_{k,k}}\right), \tag{4.14}$$

where $\mu_{s,k}^0 = \sum_{i=1,i\neq s}^{S}\sum_{j=1}^{K_i} p^{ac,ul} \mid \mathbf{z}_k^{s,0H}\mathbf{f}_{i,j}^{s} \mid^2$, and the DL rate becomes:

$$r_{s,k}^{ac,dl,bs} = \frac{1-\theta}{2}\cdot\log_2\left(1+\frac{\frac{p_{s,k}^{ac,dl,bs}}{\mathbf{Tr}\{(\mathbf{G}_s^H\mathbf{G}_s)^{-1}\}}}{\varpi_s^0+(1-\theta)\sigma^2}\right), \tag{4.15}$$

where $\varpi_s^0 = \sum_{i=1,i\neq s}^{S}\sum_{j=1}^{K_i} p_{i,j}^{ac,dl,bs} \mid \mathbf{f}_{s,k}^{iH}\mathbf{w}_{i,j}^{ac,dl} \mid^2$.

The signal intended to the users is no longer seen as interference by the MBS, and the rate between the MBS and SBS s becomes:

$$r_s^{bh,ul,bs} = \frac{1-\theta}{2}\cdot\log_2\left(1+\frac{p_s^{bh,ul,bs}}{(1-\theta)\sigma^2\left[(\mathbf{D}^H\mathbf{D})^{-1}\right]_{s,s}}\right). \tag{4.16}$$

Therefore, the optimal transmit power from SBS s to the MBS is given by:

$$p_s^{bh,ul,bs} = (1-\theta)\sigma^2\left[(\mathbf{D}^H\mathbf{D})^{-1}\right]_{s,s}(2^{\frac{\theta\cdot\phi_s}{(1-\theta)}}-1). \tag{4.17}$$

The optimal transmit power from SBS s to user k is given by:

$$p_{s,k}^{ac,dl,bs} = (\varpi_s^0+(1-\theta)\sigma^2)\mathbf{Tr}\{(\mathbf{G}_s\mathbf{G}_s^H)^{-1}\}(2^{\frac{2r_{th}^{ac,dl}}{1-\theta}}-1). \tag{4.18}$$

4.6 Time Splitting and Power Allocation

In order to investigate the formulated problem considering the proposed transmission technique, and derive the optimal time splitting parameter and power allocation that minimize the sum SBS transmit power when the problem is feasible, we first consider fixed power allocation and second we relax this assumption and consider iterative power allocation.

4.6.1 Fixed Power Allocation

The problem is non-convex since the constraints are non-convex due to inter-SBS interference. Hence, it is extremely difficult to obtain the optimal global solution. We relax the problem by assuming fixed uplink users transmit powers. However, the transmit power of the MBS $p_s^{bh,dl},\ s=1..S$ and the SBSs $p_{s,k}^{ac,dl}, p_s^{bh,ul},\ s=1..S,\ k=1..K_s$ have to be optimized in order to satisfy the constraints of problem (4.13). The interference terms ϖ_s and υ_s generated by the SBSs are assumed to be fixed Shen & Yu (2016) by considering that these terms are generated by fixed transmit power. Thus, the constraints of problem (4.13) become all convex.

Under the new assumptions, the optimal power allocation and time splitting parameter can be jointly derived. In order to minimize the sum SBS transmit power, the users may be served with their minimum required rate and the allocated power is thus given by:

$$p_{s,k}^{ac,dl} = (\varpi_s + \sigma^2)\mathbf{Tr}\{(\mathbf{G}_s\mathbf{G}_s^H)^{-1}\}(2^{\frac{r_{th}^{ac,dl}}{1-\lambda}} - 1). \tag{4.19}$$

The backhaul link is assigned with the same rate as the access link for both UL and DL. Hence, we obtain the allocated power for DL from constraints $(4.13.a)$ by solving the following polynomial equation:

$$\prod_{u=1}^{U_s}\left(1 + \frac{p_s^{bh,dl}}{U_s(\varphi_s^u + \sigma^2\left[(\mathbf{F}_s^H\mathbf{F}_s)^{-1}\right]_{K_s+u,K_s+u})}\right) = 2^{\frac{K_s r_{th}^{ac,dl}}{\lambda}}. \tag{4.20}$$

The allocated power for UL can be expressed as a function of the time splitting parameter λ from constraints $(4.13.b)$ as:

$$p_s^{bh,ul} = (\upsilon_s + \sigma^2 \left[(\mathbf{D}^H\mathbf{D})^{-1}\right]_{s,s})(2^{\frac{\lambda\phi_s}{1-\lambda}} - 1), \tag{4.21}$$

where $\phi_s = \sum_{k=1}^{K_s} \log_2(1+\gamma_{s,k}^{ac,ul})$.

The portions of allocated power are expressed as a function of the time splitting parameter. We replace their expressions in problem (4.13) and the optimal time splitting parameter could be obtained by solving the following problem:

$$\begin{aligned}
&\underset{\lambda}{\text{minimize}}\ f(\lambda) = \sum_{s=1}^{S} \kappa_s(2^{\frac{\lambda\phi_s}{1-\lambda}} - 1) + \xi_s(2^{\frac{r_{th}^{ac,dl}}{1-\lambda}} - 1)\\
&\text{subject to}\\
&(4.22.a): \lambda \geq \frac{r_{th}^{ac,ul}}{\log_2(1+\gamma_{s,k}^{ac,ul})},\ s = 1..S,\ k = 1..K_s,\\
&(4.22.b): \sum_{s=1}^{S} p_s^{bh,dl} \leq p_{max}^{mbs},\\
&(4.22.c): \kappa_s(2^{\frac{\lambda\phi_s}{1-\lambda}} - 1) + \xi_s(2^{\frac{r_{th}^{ac,dl}}{1-\lambda}} - 1) \leq p_{max}^{sbs},\ s = 1..S,\\
&(4.22.d): 0 < \lambda < 1,
\end{aligned} \tag{4.22}$$

where $\kappa_s = \upsilon_s + \sigma^2 \left[(\mathbf{D}^H\mathbf{D})^{-1}\right]_{s,s}$ and $\xi_s = \sum_{k=1}^{K_s}(\varpi_s + \sigma^2)\mathbf{Tr}\{(\mathbf{G}_s\mathbf{G}_s^H)^{-1}\}$.

The derivative of the objective function is given by:

$$f'(\lambda) = \sum_{s=1}^{S} \kappa_s \frac{\ln(2)\phi_s 2^{\frac{\lambda\phi_s}{1-\lambda}}}{(1-\lambda)^2} + \xi_s \frac{\ln(2) r_{th}^{ac,dl} 2^{\frac{r_{th}^{ac,dl}}{1-\lambda}}}{(1-\lambda)^2}. \tag{4.23}$$

The derivative is positive on the interval $[0,1[$. Hence, the objective function $f(\lambda)$ is an increasing function. Also, constraints $(4.22.b)$ and $(4.22.c)$ represent upper bounds for λ.

Hence, the optimal time splitting parameter is equal to the lower bound given by $(4.22.a)$ when the problem is feasible:

$$\lambda^* = \frac{r_{th}^{ac,ul}}{\log_2(1+\min\limits_{s=1:S,k=1:K_s}\gamma_{s,k}^{ac,ul})}. \tag{4.24}$$

4.6.2 Iterative Power Allocation

Here, we consider that the inter-SBS interference is no longer fixed. It is extremely difficult to obtain the optimal global solution due to the non-convexity and non-linearity of constraints $(4.13.a-d)$. The literature has shown that the iterative power allocation can be an efficient low complexity solution for different network architectures (e.g. Rashid-Farrokhi *et al.* (1998); Zhao *et al.* (2017)). Motivated by this, we design an adapted iterative power allocation solution for our transmission technique based on the results obtained in Section 4.6.1.

We denote by $\mathbf{p}^{ac,dl,(n)}$ the vector that contains the power portions allocated to the users, (i.e. the vector containing $p_{s,k}^{ac,dl,(n)},\ s=1..S,\ k=1..K_s$) and by $\mathbf{p}^{bh,ul,(n)}$ the vector that contains the portions of power allocated to the MBS (i.e. the vector containing $p_s^{bh,ul,(n)},\ s=1..S$) at iteration n. Starting from fixed initial power allocation, we consider that the inter-SBS interference at iteration $n+1$ is computed based on the allocated power at iteration n as follows:

$$\varpi_s^{(n+1)} = \sum_{i=1,i\neq s}^{S} p_i^{bh,ul,(n)} \mid \mathbf{f}_{s,k}^{iH}\mathbf{w}_i^{bh,ul} \mid^2 + \sum_{i=1,i\neq s}^{S}\sum_{j=1}^{K_i} p_{i,j}^{ac,dl,(n)} \mid \mathbf{f}_{s,k}^{iH}\mathbf{w}_{i,j}^{ac,dl} \mid^2 . \tag{4.25}$$

Hence, the allocated power to the users at iteration $n+1$ is given by:

$$p_{s,k}^{ac,dl,(n+1)} = (\varpi_s^{(n+1)} + \sigma^2)\mathbf{Tr}\{(\mathbf{G}_s\mathbf{G}_s^H)^{-1}\}(2^{\frac{r_{th}^{ac,dl}}{1-\lambda}} - 1). \tag{4.26}$$

The interference at the MBS at iteration $n+1$ can be computed as follows:

$$\upsilon_s^{(n+1)} = \sum_{i=1}^{S} \sum_{j=1}^{K_i} p_{i,j}^{ac,dl,(n+1)} \mid \mathbf{q}_s^H \mathbf{H}_i^H \mathbf{w}_{i,j}^{ac,dl} \mid^2 . \tag{4.27}$$

Hence, the power allocated to the MBS at iteration $n+1$ is given by:

$$p_s^{bh,ul,(n+1)} = (\upsilon_s^{(n+1)} + \sigma^2 \left[(\mathbf{D}^H \mathbf{D})^{-1}\right]_{s,s})(2^{\frac{\lambda \phi_s}{1-\lambda}} - 1). \tag{4.28}$$

We define the function $\nu(n)$ that is used for convergence test as:

$$\nu(n) = \sum_{s=1}^{S} \left(p_s^{bh,ul,(n+1)} - p_s^{bh,ul,(n)} + \sum_{k=1}^{K_s} (p_{s,k}^{ac,dl,(n+1)} - p_{s,k}^{ac,dl,(n)}) \right). \tag{4.29}$$

Theorem 4.1: The sequence of allocated power to the users $\mathbf{p}^{ac,dl,(n)}$ and to the MBS $\mathbf{p}^{bh,ul,(n)}$ converges to a fixed point.

Proof: We define the function g that generates the sequence of portions of allocated power vectors as:

$$\mathbf{p}^{ac,dl,(n+1)} = g(\mathbf{p}^{ac,dl,(n)}). \tag{4.30}$$

We start by proving that the sequence of allocated power to the users $\mathbf{p}^{ac,dl,(n)}$ is increasing starting from an initial point $\mathbf{p}^{ac,dl,(0)} = \mathbf{0}_{K \cdot S \times 1}$. We note that any two power vectors $\mathbf{p}_1$ and $\mathbf{p}_2$ such as $\mathbf{p}_1 \leq \mathbf{p}_2$ verify $g(\mathbf{p}_1) \leq g(\mathbf{p}_2)$ since the coefficients of g are positive. Hence, starting from $\mathbf{p}^{ac,dl,(0)} \leq \mathbf{p}^{ac,dl,(1)}$ and by applying g we obtain $\mathbf{p}^{ac,dl,(n)} = g(\mathbf{p}^{ac,dl,(n-1)}) \leq \mathbf{p}^{ac,dl,(n+1)} = g(\mathbf{p}^{ac,dl,(n)})$.

Similar to the sequence of allocated power to the users $\mathbf{p}^{ac,dl,(n)}$, the sequence of allocated power to the MBS $\mathbf{p}^{bh,ul,(n)}$ can be proven to be increasing starting from an initial point $\mathbf{p}^{bh,ul,(0)} = \mathbf{0}_{S \times 1}$. Since these generated sequences $\mathbf{p}^{ac,dl,(n)}$ and $\mathbf{p}^{bh,ul,(n)}$ are bounded by con-

straints $(4.13.f)$, the convergence is ensured as $\lim_{n\to\infty} \mathbf{p}^{ac,dl,(n)} = \mathbf{p}^{ac,dl,*}$ and $\lim_{n\to\infty} \mathbf{p}^{bh,ul,(n)} = \mathbf{p}^{bh,ul,*}$ ■

Hence, based on this result, we build an iterative power allocation algorithm described in Algorithm 4.1 with the objective of finding a sub-optimal power allocation solution of problem (4.13).

Algorithm 4.1 Iterative Power Allocation Algorithm

```
Compute p_{s,k}^{ac,dl,(0)}, s = 1..S, k = 1..K_s using (4.19), // initialization;
Compute p_s^{bh,ul,(0)}, s = 1..S using (4.21);
Compute λ using (4.24);
n ← 0, // number of iterations;
while |ν(n)| > ε do
    n ← n + 1;
    for s = 1 : S do
        Compute ϖ_s^{(n+1)} using (4.25);
        for k = 1 : K_s do
            Compute p_{s,k}^{ac,dl,(n+1)} using (4.26);
        end
    end
    for s = 1 : S do
        Compute υ_s^{(n+1)} using (4.27);
        Compute p_s^{bh,ul,(n+1)} using (4.28);
    end
    Compute ν(n) using (4.29);
end
```

4.7 User Scheduling

The SBSs and their associated users cannot be all simultaneously scheduled when they are requiring a minimum rate due to inter-SBS interference, multi-user interference and maximal power constraints. A user scheduling has to be implemented in order to deal with the infea-

sibility problem. Hence, this section presents a user scheduling scheme that serves as many users as possible while satisfying the minimum rate requirement.

We define a boolean variable χ_s^{sbs} that is set to 1 if SBS s is scheduled for both backhaul and access transmission and to 0 otherwise. In addition, we define $\chi_{s,k}^{us}$ that is set to 1 if user k associated with SBS s is scheduled for UL and DL transmissions and to 0 otherwise. It is to be noted that when SBS s is unscheduled, i.e. $\chi_s^{sbs} = 0$, all its associated users in Λ_s are automatically unscheduled $\chi_{s,k}^{us} = 0,\ k = 1..K_s$. We denote by χ the vector that contains the variables $\chi_{s,k}^{us}$ and χ_s^{sbs}. Hence, the problem of maximizing the number of scheduled users can be formulated as:

$$
\begin{aligned}
&\underset{\chi,\mathbf{p},\lambda}{\text{maximize}} \sum_{s=1}^{S}\sum_{k=1}^{K_s} \chi_{s,k}^{us} \\
&\text{subject to} \\
&(4.31.a): r_s^{wl,dl} \geq \sum_{k=1}^{K_s} r_{s,k}^{al,dl},\ s = 1..S, \\
&(4.31.b): r_s^{wl,ul} \geq \sum_{k=1}^{K_s} r_{s,k}^{al,ul},\ s = 1..S, \\
&(4.31.c): r_{s,k}^{al,ul} \geq \chi_{s,k}^{us} \cdot r_{th}^{al,ul},\ s = 1..S,\ k = 1..K_s, \\
&(4.31.d): r_{s,k}^{al,dl} \geq \chi_{s,k}^{us} \cdot r_{th}^{al,dl},\ s = 1..S,\ k = 1..K_s, \\
&(4.31.e): \sum_{s=1}^{S} \chi_s^{sbs} \cdot p_s^{wl,dl} \leq p_{max}^{mbs}, \\
&(4.31.f): \chi_s^{sbs} \cdot p_s^{wl,ul} + \sum_{k=1}^{K_s} \chi_{s,k}^{us} \cdot p_{s,k}^{al,dl} \leq p_{max}^{sbs},\ s = 1..S, \\
&(4.31.g): \chi_s^{sbs} = \max_{k=1..K_s} \chi_{s,k}^{us},\ s = 1..S, \\
&(4.31.h): 0 < \lambda < 1, \\
&(4.31.i): \chi_s^{sbs}, \chi_{s,k}^{us} \in \{0,1\},\ s = 1..S,\ k = 1..K_s, \\
&(4.31.j): \mathbf{p} \geq 0.
\end{aligned}
\tag{4.31}
$$

Compared to problem (4.13), we include constraints $(4.31.g)$ which force the SBSs to be turned off when all their associated users are unscheduled. A special case of problem (4.31) is the problem of maximizing the number of scheduled users while satisfying the required SINRs. This special case has been proven to be an NP-complete problem in Andersin *et al.* (1996). Hence, the user scheduling problem (4.31) is also NP-hard and its optimal solution can be obtained only by high complexity brute force search algorithm.

Therefore, we propose in this section a low complexity heuristic user scheduling algorithm to overcome the infeasibility problem. The proposed algorithm is initialized by scheduling all users. The users are removed one by one at each iteration until the problem becomes feasible.

We define the worst user at each iteration as the one that violates constraint $(4.31.c)$ the most, i.e the user that experiences the least SINR. This procedure is repeated until we obtain a time splitting parameter (given by (4.24)) that is less than 1. First, the removal criterion is applied as follows:

$$(s,k)^* \leftarrow \underset{(s,k)\in\Omega}{\operatorname{argmin}} \gamma_{s,k}^{ac,ul}, \tag{4.32}$$

where Ω is the set of scheduled users.

Next, in addition to satisfying a set of scheduled users with minimal rate, the constraints $(4.31.f)$ related to maximal transmit power per-SBS need to be verified. The user that has to be removed in each iteration is the one that requires the maximal transmit power. Hence, the following removal criterion is applied:

$$(s,k)^* \leftarrow \underset{(s,k)\in\Omega}{\operatorname{argmax}} p_{s,k}^{ac,dl}. \tag{4.33}$$

This iterative procedure terminates once the problem becomes feasible by potentially removing the least number of users from the network. The proposed low complexity heuristic user scheduling algorithm is given in Algorithm 4.2.

Algorithm 4.2 Heuristic User Scheduling Algorithm

Compute $\gamma_{s,k}^{ac,ul},\ s=1..S,\ k=1..K_s$ using (4.3), // initialization (all users are scheduled);
Compute λ using (4.24);
$r1 \leftarrow 0$, // number of unscheduled users;
while $\lambda \geq 1$ ***and*** $r1 < \sum_{s=1}^{S} K_s$ **do**
    $(s,k)^* \leftarrow \underset{(s,k)\in\Omega}{\text{argmin}}\ \gamma_{s,k}^{ac,ul}$;
    $\Omega \leftarrow \Omega - \{(s,k)^*\}$, // unscheduled user $(s,k)^*$;
    $r1 \leftarrow r1+1$;
    update $\gamma_{s,k}^{ac,ul},\ (s,k)\in\Omega$;
    update λ;
end
Compute $p_{s,k}^{ac,dl},\ (s,k)\in\Omega$ using (4.19);
Compute $p_s^{bh,ul}$ using (4.21);
while *Constraint* $(4.31.f)$ *is not satisfied* ***and*** $r1 < \sum_{s=1}^{S} K_s$ **do**
    $(s,k)^* \leftarrow \underset{(s,k)\in\Omega}{\text{argmax}}\ p_{s,k}^{ac,dl}$;
    $\Omega \leftarrow \Omega - \{(s,k)^*\}$, // unscheduled user $(s,k)^*$;
    $r1 \leftarrow r1+1$;
    update $p_{s,k}^{ac,dl},\ (s,k)\in\Omega$;
end

The optimal user scheduling is obtained with the brute-force search algorithm. The number of possible combinations of sets of users is $\sum_{s=1}^{S}\sum_{k=1}^{K_s}\binom{S}{s}\binom{K_s}{k}$. Hence, its computational complexity is given by:

$$C_{us}^{opt} = \sum_{s=1}^{S}\sum_{k=1}^{K_s}\binom{S}{s}\binom{K_s}{k} f(s,k), \tag{4.34}$$

where $f(s,k)$ is a polynomial function that represents the computational complexity of the verification of the problem feasibility. For the heuristic user scheduling algorithm, the computational complexity is given by:

$$C_{us}^{hr} = \sum_{s=1}^{S} \sum_{k=1}^{K_s} f(s,k). \tag{4.35}$$

4.8 Numerical Results

In this section, monte carlo simulations are used to evaluate the performance of the proposed transmission technique. We assume a circular coverage of the macrocell where the MBS is positioned at the center and the SBSs are uniformly placed within the considered coverage. Also, we assume two users randomly scattered across each small cell. The correlation among the antennas is following the Kronecker spatial correlation model represented by $\Sigma[i,j] = a^{|i-j|}, \forall i,j = 1...N$, where a is a correlation coefficient such that $a = 0$ (resp. $a = 1$) corresponds to the uncorrelated (resp. fully correlated) conditions. The simulation parameters are summarized in Table 4.2.

Table 4.2 Simulation Parameters.

Symbol	Description	Value
N	Number of antennas at the MBS	128
S	Number of SBSs	8
M_s	Number of antennas at each SBS	4
F	Number of MUEs	4
ν	Path loss exponent	3.7
	Coverage radius of each SBS	20 m
	Coverage radius of the MBS	200 m
p_{max}^{sbs}	Max. trans. power of an SBS	50 W
p_{max}^{mbs}	Max. trans. power of the MBS	100 W
$p^{ac,ul}$	Transmit power of a user	1 W
B	Bandwidth	10 MHz
	Noise PSD	-174 dBm/Hz

In Fig. 4.4, we show the optimal time splitting parameter as a function of the minimum transmission rate. The curve is obtained by averaging (4.24) over 100000 channels realizations. We confirm that the optimal sum SBS transmit power is not achieved when the 1st and 2nd frames

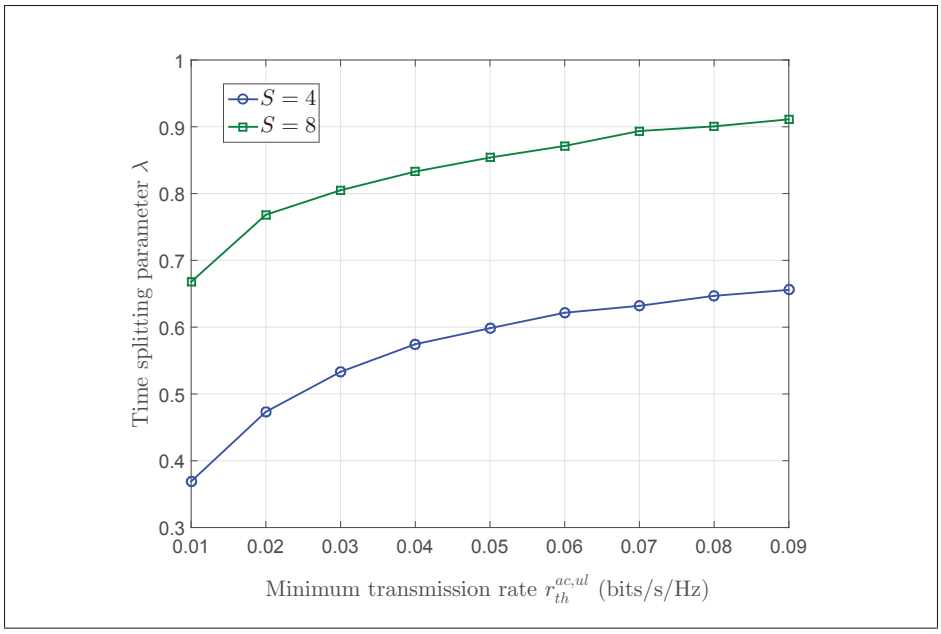

Figure 4.4 Optimal time splitting parameter.

have equal duration. The time splitting parameter tends to zero when the minimum transmission rate tends to zero and it tends to infinity when the minimum transmission rate becomes large.

Fig. 4.5 shows the achieved BSs transmit power as a function of the number of SBSs when using the optimal time splitting parameter λ^* and when considering $\lambda = 1/2$. It is clear that significant power can be saved when the transmission time is optimally divided.

In Fig. 4.6, we compare the achieved total transmit power between our proposed transmission technique and RTDD with bandwidth splitting. The proposed technique significantly outperforms RTDD with bandwidth splitting thanks to the efficient management of the interference between access and backhaul links. Also, the performance gap remains significant for large minimum users transmission rate requirements.

Clearly, increasing the number of users in the system requires the increase of the BSs transmit power in order to satisfy the required users minimum rate as shown in Fig. 4.7.

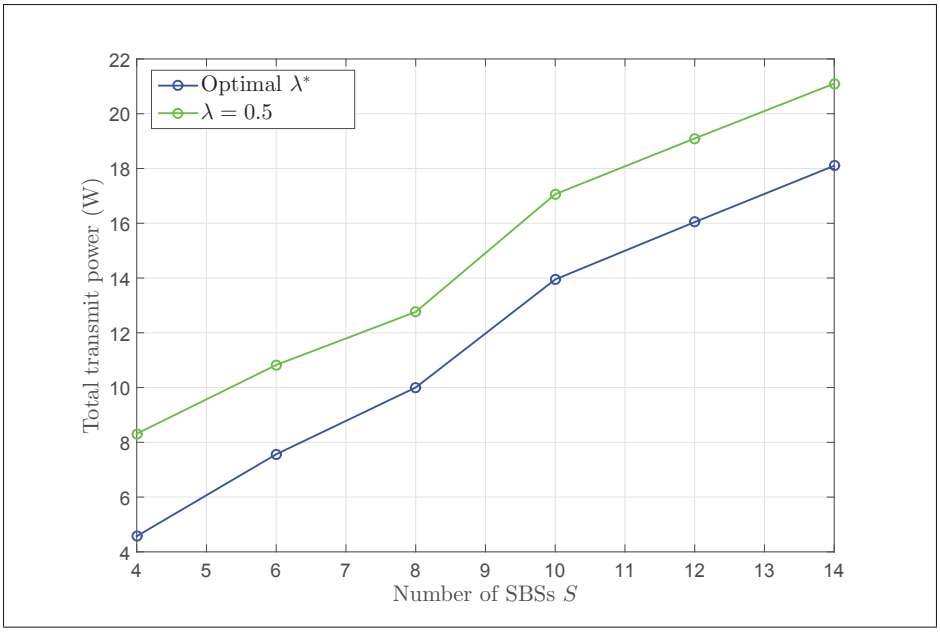

Figure 4.5 Total transmit power under optimal λ^* and $\lambda = 1/2$.

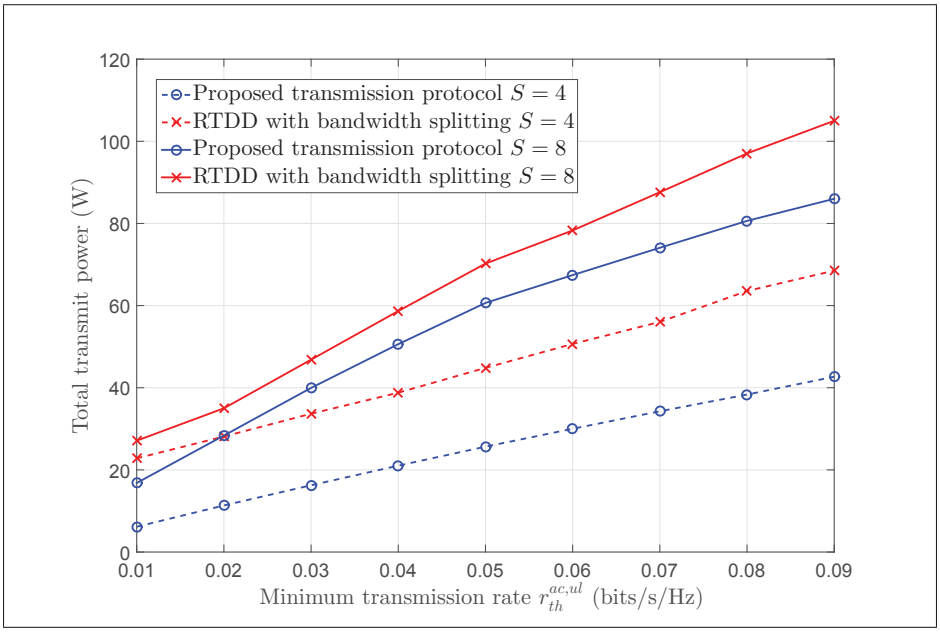

Figure 4.6 Total transmit power under the proposed transmission technique and RTDD with bandwidth splitting.

Also, the total transmit power decreases slightly by increasing the number of antennas at the MBS and the SBSs thanks to MIMO spatial multiplexing as shown in Fig. 4.8 and Fig. 4.9.

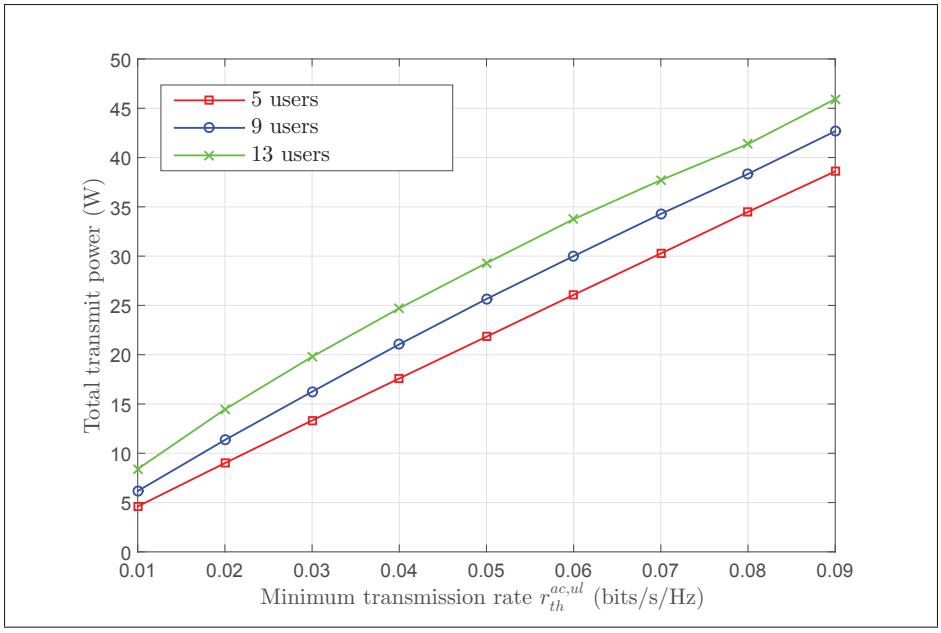

Figure 4.7 Impact of the number of users.

Specifically, increasing the number of antennas at the MBS allows to decrease the MBS transmit power and increasing the number of antennas at the SBSs allows to decrease the transmit power at the SBSs.

In Fig. 4.10, we show the impact of the channel estimation reliability ξ on the system performance. Clearly, the total transmit power increases when the channel estimation degrades.

In Fig. 4.11, we show the performance of the proposed iterative power allocation algorithm compared to the performance achieved when considering fixed inter-SBS interference in terms of transmit power consumption. Also, the proposed iterative algorithm allows to significantly reduce the transmit power consumption even though it is important to remind that the iterative algorithm requires much higher computational complexity.

Fig. 4.12 shows the percentage of unscheduled users as a function of the minimum transmission rate under the proposed heuristic and optimal user scheduling algorithms. The performance gap between the proposed algorithm and optimal user scheduling is tight and does not change too much when the minimum transmission rate increases. As expected, the percentage of

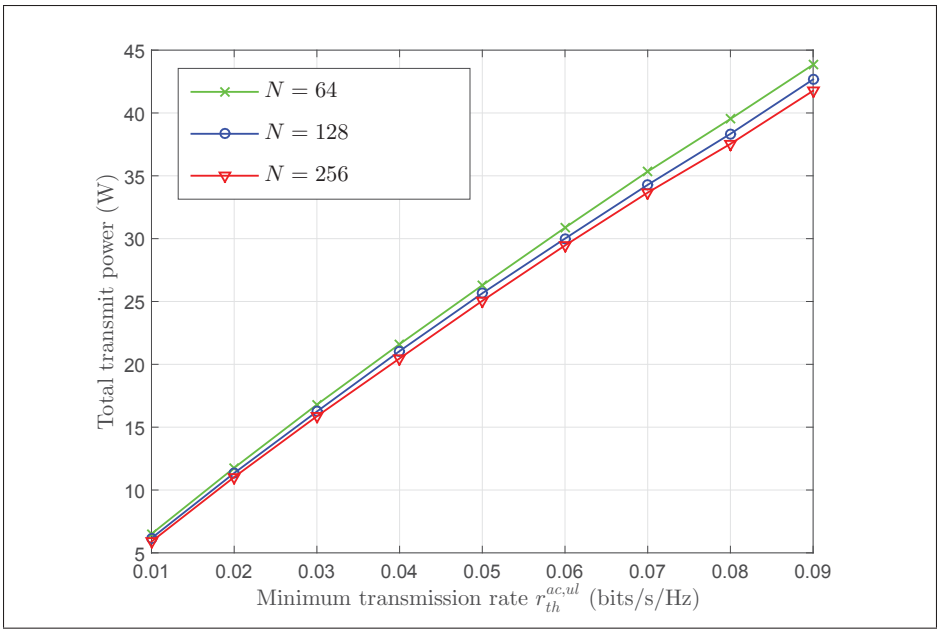

Figure 4.8 Impact of the number of antennas at the MBS.

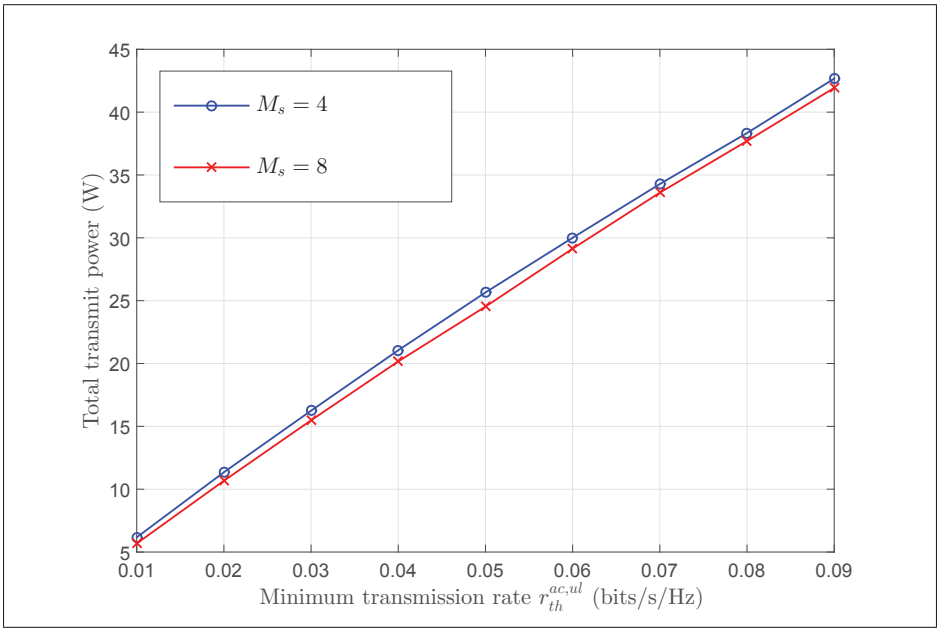

Figure 4.9 Impact of the number of antennas at the SBSs.

unscheduled users is higher when the minimum rate constraints are more stringent. Also, the percentage of unscheduled users increases with the decrease of maximal transmit power per-SBS specially for higher transmission rate.

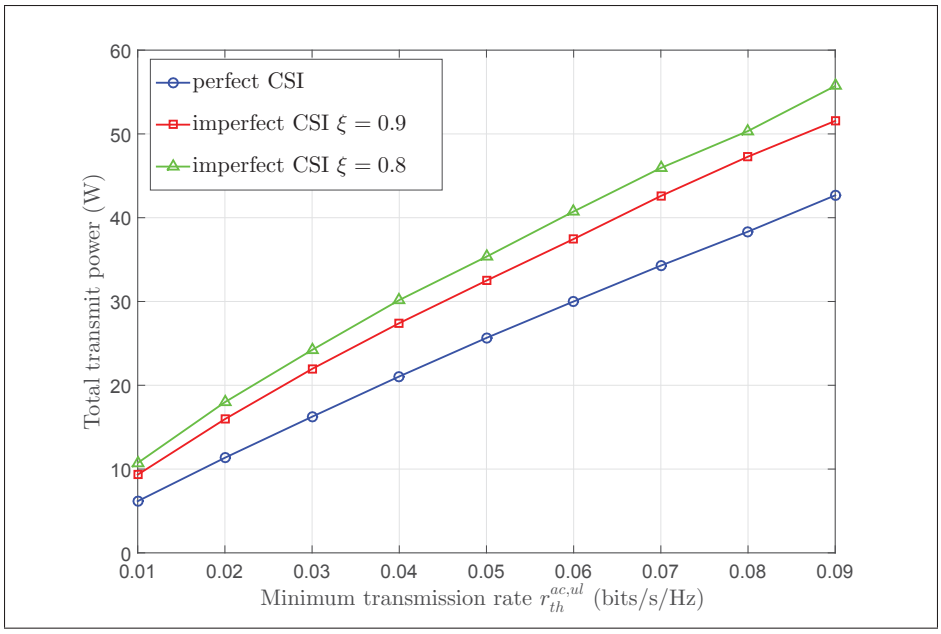

Figure 4.10 Impact of the channel estimation reliability.

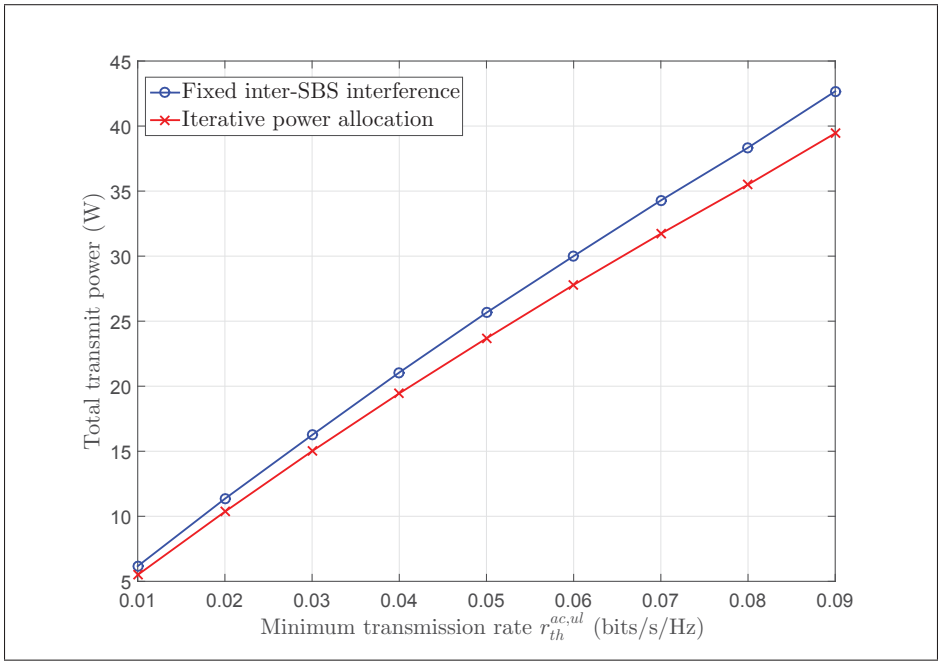

Figure 4.11 Performance of the iterative power allocation algorithm.

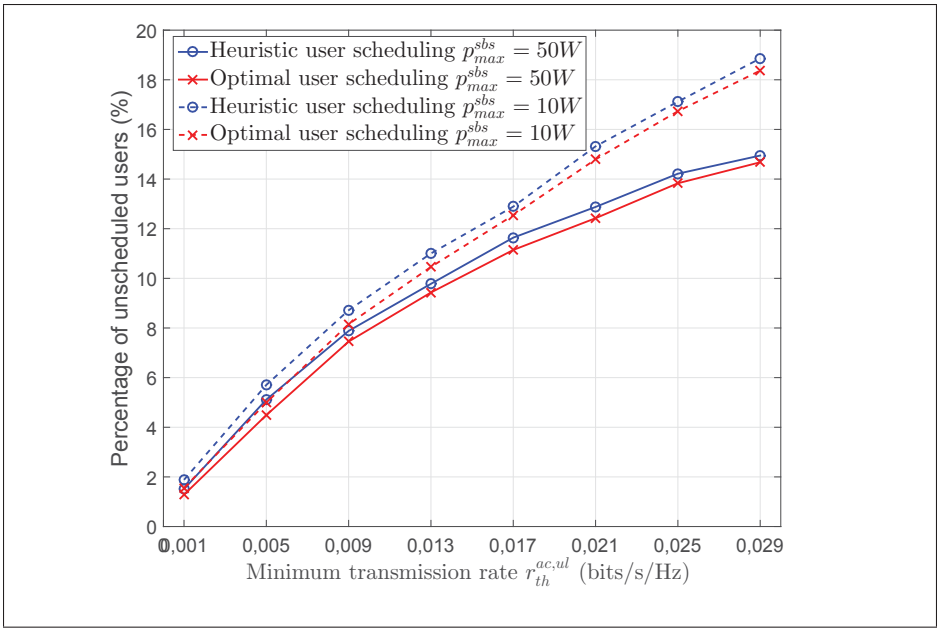

Figure 4.12 Percentage of unscheduled users under heuristic and optimal user scheduling algorithms.

Fig. 4.13 shows the impact of user association on system performance. The different cell size user association algorithm allows to reduce the power consumption compared to the closest SBS user association algorithm since the inter-SBS interference is reduced.

4.9 Conclusion

This paper proposed a new interference management scheme for HetNets with massive MIMO wireless backhaul based on MIMO spatial multiplexing and time splitting. We formulate a sum BSs transmit power minimization problem under user minimum rate constraints and we derive the optimal time splitting parameter. Since the power allocation problem is NP-hard, we proposed an efficient iterative power allocation algorithm to obtain a sub-optimal solution. The formulated problem could be infeasible due to the users requirement and per-SBS power constraints. Hence, a heuristic user scheduling algorithm was proposed in order to overcome the feasibility problem. Furthermore, we show that the proposed transmission technique is more efficient than RTDD with bandwidth splitting in term of transmit power consumption.

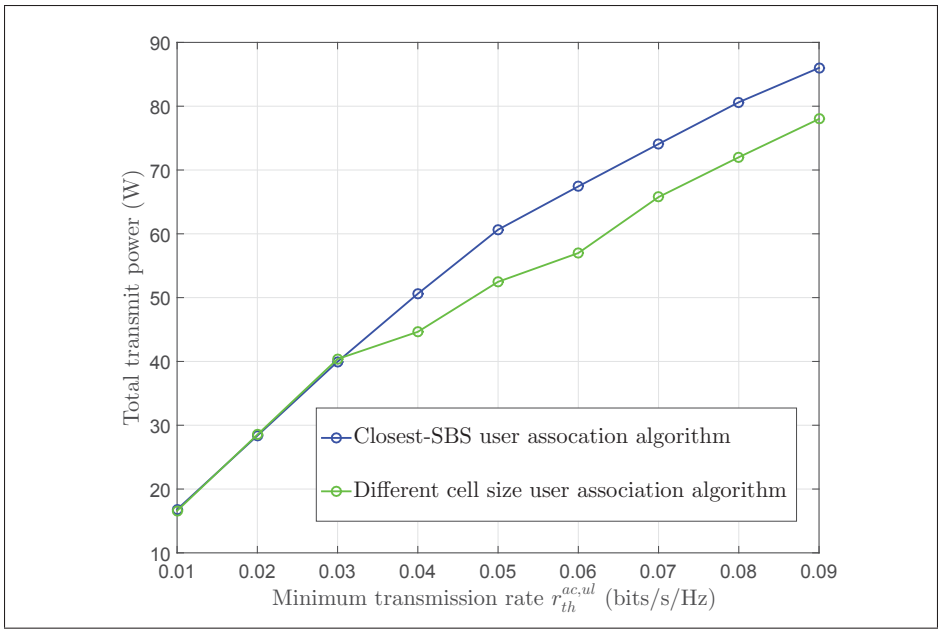

Figure 4.13 Impact of user association on system performance.

Future works will focus on designing distributed resource allocation techniques considering our proposed transmission technique for HetNets based on learning tools.

CONCLUSION AND RECOMMENDATIONS

This dissertation investigated resource allocation problem related to energy consumption in wireless communication systems that incorporate large-scale MIMO. We show that large-scale MIMO systems could coexist with other wireless technologies such as HetNet and energy harvesting in order to improve the system performance. After presenting the state of the art, motivations, objectives and contributions of this work in the first chapter, Chapter 2 proposed efficient heuristic algorithms for downlink large-scale MIMO systems considering a non negligible circuit power consumption. The studied resource allocation focuses on: (i) activating a subset of RF chains, (ii) activated antenna selection, (iii) power allocation and (iv) user scheduling considering two linear precoders CB and ZFB. Chapter 3 investigated energy efficient distributed large-scale MIMO systems while the RRHs are powered by energy bought from a grid source in addition to energy harvested from renewable sources. Efficient energy management strategies are designed. The proposed approach allows efficient use of non-renewable energy in hybrid energy large-scale MIMO systems. Chapter 4 proposed a new transmission scheme for HetNets with massive MIMO wireless backhaul based on MIMO spatial multiplexing and time splitting. The proposed transmission technique is shown to be more efficient than RTDD with bandwidth splitting in term of transmit power consumption.

Future works could be directed towards the design of low complexity beamforming schemes that outperform CB and ZFB considering a non-negligible circuit power consumption. Also, the system model may be extended to inter-cell scenario where multi-cell interference and pilot contamination are taken into account for the design of resource allocation strategies. Furthermore, distributed resource management approaches inspired by game theory may be developed for hybrid energy distributed large-scale MIMO systems. In addition, distributed resource allocation techniques may be designed considering our proposed transmission technique for HetNets based on learning tools. Finally, resource allocation in secure wireless systems and

wireless energy transfer systems that incorporate large-scale MIMO are promising research directions.

APPENDIX I

APPENDIX FOR CHAPTER 3

1. Proof of Lemma 3.1

Considering the case where energy harvesting is sufficient to ensure the SINR requirements for each user at each frame, the allocated power drawn from energy harvesting sources for user k at frame i verifies:

$$\frac{p_k^*(i) \mid \mathbf{g}_k(i)\widehat{\mathbf{g}}_k(i)^H \mid^2}{\sum_{m=1,m\neq k}^{K} p_m^*(i) \mid \mathbf{g}_k(i)\widehat{\mathbf{g}}_m(i)^H \mid^2 + \sigma^2\eta^2(i)} = \gamma_{th}. \tag{A I-1}$$

The interference term in large-scale MIMO systems can be asymptotically approximated when K and N are large but finite, Zhao *et al.* (2013) as:

$$\begin{aligned}\sum_{m=1,m\neq k}^{K} p_m^*(i) \mid \mathbf{g}_k(i)\widehat{\mathbf{g}}_m(i)^H \mid^2 N &\rightarrow p_{out}(i)\mathbf{E}\{\mid \mathbf{g}_k(i)\widehat{\mathbf{g}}_m(i)^H \mid^2\} \\ &\approx N p_{out}(i)\sigma_d^2,\end{aligned} \tag{A I-2}$$

where $p_{out}(i)$ is the total transmitted power at frame i and $\sigma_d^2 = \mathbf{E}\{\mid g_{n,k}(i) \mid^2\}$ is the variance of the channel $g_{n,k}(i)$. Hence, we obtain:

$$p_k^*(i) = \frac{\gamma_{th}}{\mid \mathbf{g}_k(i)\widehat{\mathbf{g}}_k(i)^H \mid^2}(N p_{out}(i)\sigma_d^2 + \sigma^2\eta^2(i)) \tag{A I-3}$$

Using $p_{out}(i) = \sum_{k=1}^{K} p_k^*(i)$ and $(AI-3)$, we obtain the expression of $p_{out}(i)$ as:

$$p_{out}(i) = \frac{N\sigma_d^2 + \sigma^2\eta^2(i)}{\frac{1}{\gamma_{th}\sum_{k=1}^{K}\frac{1}{|\mathbf{g}_k(i)\widehat{\mathbf{g}}_k(i)^H|^2}} - 1}. \tag{A I-4}$$

By replacing the expression of $p_{out}(i)$ in $(AI-3)$, we obtain $p_k^*(i)$ that ensure the SINR requirements for each user. Then, we replace $p_k^*(i)$ in the energy causality constraints $(3.8.b)$ and we obtain the relation (3.10). This completes the proof of *Lemma 3.1*.

BIBLIOGRAPHY

Amadori, P. V. & Masouros, C. (2016). Interference-driven antenna selection for massive multiuser mimo. *Ieee transactions on vehicular technology*, 65(8), 5944–5958.

Amadori, P. V. & Masouros, C. (2017). Large scale antenna selection and precoding for interference exploitation. *Ieee transactions on communications*, 65(10), 4529–4542.

Andersin, M., Rosberg, Z. & Zander, J. (1996). Gradual removals in cellular pcs with constrained power control and noise. *Wireless networks*, 2(1), 27–43.

Andrews, J. G., Buzzi, S., Choi, W., Hanly, S. V., Lozano, A., Soong, A. C. & Zhang, J. C. (2014). What will 5g be? *Ieee journal on selected areas in communications*, 32(6), 1065–1082.

Benmimoune, M., Driouch, E., Ajib, W. & Massicotte, D. (2015). Joint transmit antenna selection and user scheduling for massive mimo systems. *Proc. ieee wireless communications and networking conference (wcnc)*, pp. 381–386.

Bjornson, E., Matthaiou, M. & Debbah, M. (2014). Circuit-aware design of energy-efficient massive mimo systems. *Proc. international symposium on communications, control and signal processing (isccsp)*, pp. 101–104.

Blasco, P., Gunduz, D. & Dohler, M. (2013). A learning theoretic approach to energy harvesting communication system optimization. *Ieee transactions on wireless communications*, 12(4), 1872–1882.

Boccardi, F., Heath, R. W., Lozano, A., Marzetta, T. L. & Popovski, P. (2014). Five disruptive technology directions for 5g. *Ieee communications magazine*, 52(2), 74–80.

Boyd, S. & Vandenberghe, L. (2004). *Convex optimization*. Cambridge university press.

Caire, G. & Shamai, S. (2003). On the achievable throughput of a multiantenna gaussian broadcast channel. *Ieee transactions on information theory*, 49(7), 1691–1706.

Cammarano, A., Petrioli, C. & Spenza, D. (2016). Online energy harvesting prediction in environmentally powered wireless sensor networks. *Ieee sensors journal*, 16(17), 6793–6804.

Che, Y. L., Duan, L. & Zhang, R. (2016). Dynamic base station operation in large-scale green cellular networks. *Ieee journal on selected areas in communications*, 34(12), 3127–3141.

Chen, J., Chen, X., Gerstacker, W. H. & Ng, D. W. K. (2016a). Resource allocation for a massive mimo relay aided secure communication. *Ieee transactions on information forensics and security*, 11(8), 1700–1711.

Chen, L., Yu, F. R., Ji, H., Rong, B., Li, X. & Leung, V. C. (2016b). Green full-duplex self-backhaul and energy harvesting small cell networks with massive mimo. *Ieee journal on selected areas in communications*, 34(12), 3709–3724.

Chen, X., Ng, D. W. K., Gerstacker, W. & Chen, H.-H. (2017). A survey on multiple-antenna techniques for physical layer security. *Ieee communications surveys & tutorials*.

Cheng, P., Tao, M. & Zhang, W. (2010). A new slnr-based linear precoding for downlink multi-user multi-stream mimo systems. *Ieee communications letters*, 14(11), 1008–1010.

Chia, Y.-K., Sun, S. & Zhang, R. (2014). Energy cooperation in cellular networks with renewable powered base stations. *Ieee transactions on wireless communications*, 13(12), 6996–7010.

Chuah, C.-N., Tse, D. N. C., Kahn, J. M. & Valenzuela, R. A. (2002). Capacity scaling in mimo wireless systems under correlated fading. *Ieee transactions on information theory*, 48(3), 637–650.

Deng, L., Rui, Y., Cheng, P., Zhang, J., Zhang, Q. & Li, M. (2013). A unified energy efficiency and spectral efficiency tradeoff metric in wireless networks. *Ieee communications letters*, 17(1), 55–58.

Driouch, E. & Ajib, W. (2012). Efficient scheduling algorithms for multiantenna cdma systems. *Ieee transactions on vehicular technology*, 61(2), 521–532.

Dua, A., Medepalli, K. & Paulraj, A. J. (2006). Receive antenna selection in mimo systems using convex optimization. *Ieee transactions on wireless communications*, 5(9), 2353–2357.

Feng, M. & Mao, S. (2017). Adaptive pilot design for massive mimo hetnets with wireless backhaul. *Proc. ieee international conference on sensing, communication, and networking (secon)*, pp. 1–9.

Feng, W., Chen, Y., Shi, R., Ge, N. & Lu, J. (2016). Exploiting macrodiversity in massively distributed antenna systems: a controllable coordination perspective. *Ieee transactions on vehicular technology*, 65(10), 8720–8724.

Gao, X., Edfors, O., Liu, J. & Tufvesson, F. (2013). Antenna selection in measured massive mimo channels using convex optimization. *Proc. ieee global communications conference workshops (globecom wkshps)*, pp. 129–134.

Gao, Z., Dai, L., Mi, D., Wang, Z., Imran, M. A. & Shakir, M. Z. (2015). Mmwave massive-mimo-based wireless backhaul for the 5g ultra-dense network. *Ieee wireless communications*, 22(5), 13–21.

Garcia-Rodriguez, A., Masouros, C. & Rulikowski, P. (2017). Reduced switching connectivity for large scale antenna selection. *Ieee transactions on communications*, 65(5), 2250–2263.

Gaur, S. & Ingram, M. A. (2005). Transmit/receive antenna selection for mimo systems to improve error performance of linear receivers. *Proc. itg/ieee international workshop on smart antennas*.

Ghosh, A., Mangalvedhe, N., Ratasuk, R., Mondal, B., Cudak, M., Visotsky, E., Thomas, T. A., Andrews, J. G., Xia, P., Jo, H. S. et al. (2012). Heterogeneous cellular networks: From theory to practice. *Ieee communications magazine*, 50(6), 54–64.

Gkizeli, M. & Karystinos, G. N. (2014). Maximum-snr antenna selection among a large number of transmit antennas. *Ieee journal of selected topics in signal processing*, 8(5), 891–901.

Guozhen, X., An, L., Wei, J., Haige, X. & Wu, L. (2014). Joint user scheduling and antenna selection in distributed massive mimo systems with limited backhaul capacity. *China communications*, 11(5), 17–30.

Gupta, A. & Jha, R. K. (2015). A survey of 5g network: Architecture and emerging technologies. *Ieee access*, 3, 1206–1232.

Ha, D., Lee, K. & Kang, J. (2013). Energy efficiency analysis with circuit power consumption in massive mimo systems. *Proc. ieee international symposium on personal indoor and mobile radio communications (pimrc)*, pp. 938–942.

Hamdi, R. & Ajib, W. (2015a). Joint optimal number of rf chains and power allocation for downlink massive mimo systems. *Proc. ieee vehicular technology conference (vtc-fall)*, pp. 1-5.

Hamdi, R. & Ajib, W. (2015b). Sum-rate maximizing in downlink massive mimo systems with circuit power consumption. *Proc. ieee international conference on wireless and mobile computing, networking and communications (wimob)*, pp. 437–442.

Hamdi, R., Driouch, E. & Ajib, W. (2016a). Resource allocation in downlink large-scale mimo systems. *Ieee access*, 4, 8303–8316.

Hamdi, R., Driouch, E. & Ajib, W. (2016b). Large-scale mimo systems with practical power constraints. *Proc. ieee vehicular technology conference (vtc-fall)*, pp. 1–5.

Hamdi, R., Driouch, E. & Ajib, W. (2017a). Energy management in large-scale mimo systems with per-antenna energy harvesting. *Ieee international conference on communications (icc)*, pp. 1–6.

Hamdi, R., Driouch, E. & Ajib, W. (2017b). Energy management in hybrid energy large-scale mimo systems. *Ieee transactions on vehicular technology*, 66(11), 10183–10193.

Hamdi, R., Driouch, E. & Ajib, W. (2018). On the resource allocation in hetnets with massive mimo wireless backhaul. *Proc. ieee vehicular technology conference (vtc-fall)*, pp. 1-5.

Hao, W. & Yang, S. (2018). Small cell cluster-based resource allocation for wireless backhaul in two-tier heterogeneous networks with massive mimo. *Ieee transactions on vehicular technology*, 67(1), 509–523.

He, C., Sheng, B., Zhu, P., Wang, D. & You, X. (2014). Energy efficiency comparison between distributed and co-located mimo systems. *International journal of communication systems*, 27(1), 81–94.

Hu, S., Zhang, Y., Wang, X. & Giannakis, G. B. (2016). Weighted sum-rate maximization for mimo downlink systems powered by renewables. *Ieee transactions on wireless communications*, 15(8), 5615–5625.

Jain, R., Chiu, D.-M. & Hawe, W. R. (1984). *A quantitative measure of fairness and discrimination for resource allocation in shared computer system*. Eastern Research Laboratory, Digital Equipment Corporation Hudson, MA.

Jose, J., Ashikhmin, A., Marzetta, T. L. & Vishwanath, S. (2011). Pilot contamination and precoding in multi-cell tdd systems. *Ieee transactions on wireless communications*, 10(8), 2640–2651.

Joung, J., Chia, Y. K. & Sun, S. (2014). Energy-efficient, large-scale distributed-antenna system (l-das) for multiple users. *Ieee journal of selected topics in signal processing*, 8(5), 954–965.

Ku, M.-L., Li, W., Chen, Y. & Liu, K. R. (2016). Advances in energy harvesting communications: Past, present, and future challenges. *Ieee communications surveys & tutorials*, 18(2), 1384–1412.

Kumar, R. R. & Gurugubelli, J. (2011). How green the lte technology can be? *Proc. international conference on wireless communication, vehicular technology, information theory and aerospace & electronic systems technology (wireless vitae)*, pp. 1–5.

Larsson, E. G., Edfors, O., Tufvesson, F. & Marzetta, T. L. (2014). Massive mimo for next generation wireless systems. *Ieee communications magazine*, 52(2), 186–195.

Le, L. B. & Hossain, E. (2008). Resource allocation for spectrum underlay in cognitive radio networks. *Ieee transactions on wireless communications*, 7(12), 5306–5315.

Li, B., Zhu, D. & Liang, P. (2015). Small cell in-band wireless backhaul in massive mimo systems: A cooperation of next-generation techniques. *Ieee transactions on wireless communications*, 14(12), 7057–7069.

Li, H., Song, L. & Debbah, M. (2014). Energy efficiency of large-scale multiple antenna systems with transmit antenna selection. *Ieee transactions on communications*, 62(2), 638–647.

Li, Y., Sheng, M., Sun, Y. & Shi, Y. (2016). Joint optimization of bs operation, user association, subcarrier assignment, and power allocation for energy-efficient hetnets. *Ieee journal on selected areas in communications*, 34(12), 3339–3353.

Liu, A. & Lau, V. K. (2014). Joint power and antenna selection optimization in large cloud radio access networks. *Ieee transactions on signal processing*, 62(5), 1319–1328.

Liu, P., Jin, S., Jiang, T., Zhang, Q. & Matthaiou, M. (2017a). Pilot power allocation through user grouping in multi-cell massive mimo systems. *Ieee transactions on communications*, 65(4), 1561–1574.

Liu, Y., Lu, L., Li, G. Y., Cui, Q. & Han, W. (2016). Joint user association and spectrum allocation for small cell networks with wireless backhauls. *Ieee wireless communications letters*, 5(5), 496–499.

Liu, Z., Du, W. & Sun, D. (2017b). Energy and spectral efficiency tradeoff for massive mimo systems with transmit antenna selection. *Ieee transactions on vehicular technology*, 66(5), 4453–4457.

Luo, Z.-Q. & Zhang, S. (2008). Dynamic spectrum management: Complexity and duality. *Ieee journal of selected topics in signal processing*, 2(1), 57–73.

Lütkepohl, H. Handbook of matrices. 1996. *John wiley&sons*.

Makki, B., Svensson, T., Eriksson, T. & Alouini, M.-S. (2016). On the required number of antennas in a point-to-point large-but-finite mimo system: Outage-limited scenario. *Ieee transactions on communications*, 64(5), 1968–1983.

Makki, B., Ide, A., Svensson, T., Eriksson, T. & Alouini, M.-S. (2017). A genetic algorithm-based antenna selection approach for large-but-finite mimo networks. *Ieee transactions on vehicular technology*, 66(7), 6591–6595.

Matsumura, K. & Ohtsuki, T. (2011). Orthogonal beamforming using gram-schmidt orthogonalization for multi-user mimo downlink system. *Eurasip journal on wireless communications and networking*, 2011(1), 41.

Nam, Y.-H., Ng, B. L., Sayana, K., Li, Y., Zhang, J., Kim, Y. & Lee, J. (2013). Full-dimension mimo (fd-mimo) for next generation cellular technology. *Ieee communications magazine*, 51(6), 172–179.

Ng, D. W. K. & Schober, R. (2012). Spectral efficiency in large-scale mimo-ofdm systems with per-antenna power cost. *Proc. asilomar conference on signals, systems and computers (asilomar)*, pp. 289–294.

Ng, D. W. K., Lo, E. S. & Schober, R. (2012a). Energy-efficient resource allocation in ofdma systems with large numbers of base station antennas. *Ieee transactions on wireless communications*, 11(9), 3292–3304.

Ng, D. W. K., Lo, E. S. & Schober, R. (2012b). Energy-efficient resource allocation for secure ofdma systems. *Ieee transactions on vehicular technology*, 61(6), 2572–2585.

Ngo, H. Q., Larsson, E. G. & Marzetta, T. L. (2013a). The multicell multiuser mimo uplink with very large antenna arrays and a finite-dimensional channel. *Ieee transactions on communications*, 61(6), 2350–2361.

Ngo, H. Q., Larsson, E. G. & Marzetta, T. L. (2013b). Energy and spectral efficiency of very large multiuser mimo systems. *Ieee transactions on communications*, 61(4), 1436–1449.

Ngo, H. Q., Matthaiou, M. & Larsson, E. G. (2014). Massive mimo with optimal power and training duration allocation. *Ieee wireless communications letters*, 3(6), 605–608.

Nguyen, T. M., Ha, V. N. & Le, L. B. (2015). Resource allocation optimization in multi-user multi-cell massive mimo networks considering pilot contamination. *Ieee access*, 3, 1272–1287.

Nguyen, T. M., Yadav, A., Ajib, W. & Assi, C. (2016). Resource allocation in two-tier wireless backhaul heterogeneous networks. *Ieee transactions on wireless communications*, 15(10), 6690–6704.

Ni, W. & Dong, X. (2016). Hybrid block diagonalization for massive multiuser mimo systems. *Ieee transactions on communications*, 64(1), 201–211.

Niu, J., Li, G. Y., Chen, X., Zheng, J., Fang, D. & Li, X. (2018). Resource allocation in reverse tdd wireless backhaul hetnets with 3d massive antennas. *Ieee wireless communications letters*, 7(1), 30–33.

Niyato, D., Hossain, E. & Fallahi, A. (2007). Sleep and wakeup strategies in solar-powered wireless sensor/mesh networks: Performance analysis and optimization. *Ieee transactions on mobile computing*, 6(2), 221–236.

Pei, Y., Pham, T.-H. & Liang, Y.-C. (2012). How many rf chains are optimal for large-scale mimo systems when circuit power is considered? *Proc. ieee global communications conference (globecom)*, pp. 3868–3873.

Pitarokoilis, A., Mohammed, S. K. & Larsson, E. G. (2012). On the optimality of single-carrier transmission in large-scale antenna systems. *Ieee wireless communications letters*, 1(4), 276–279.

Prasad, K. S. V., Hossain, E. & Bhargava, V. K. (2017). Energy efficiency in massive mimo-based 5g networks: Opportunities and challenges. *Ieee wireless communications*.

Puterman, M. L. (2014). *Markov decision processes: discrete stochastic dynamic programming*. John Wiley & Sons.

Rashid-Farrokhi, F., Tassiulas, L. & Liu, K. R. (1998). Joint optimal power control and beamforming in wireless networks using antenna arrays. *Ieee transactions on communications*, 46(10), 1313–1324.

Renegar, J. (1988). A polynomial-time algorithm, based on newton's method, for linear programming. *Mathematical programming*, 40(1), 59–93.

Rusek, F., Persson, D., Lau, B. K., Larsson, E. G., Marzetta, T. L., Edfors, O. & Tufvesson, F. (2013). Scaling up mimo: Opportunities and challenges with very large arrays. *Ieee signal processing magazine*, 30(1), 40–60.

Saidi, K., Ajib, W. & Boukadoum, M. (2016). Adaptive transmitter load size using receiver harvested energy prediction by kalman filter. *Proc. international symposium on communication systems, networks and digital signal processing (csndsp)*, pp. 1–5.

Sanguinetti, L., Moustakas, A. L. & Debbah, M. (2015). Interference management in 5g reverse tdd hetnets with wireless backhaul: A large system analysis. *Ieee journal on selected areas in communications*, 33(6), 1187–1200.

Saxena, N., Roy, A. & Kim, H. (2016). Traffic-aware cloud ran: a key for green 5g networks. *Ieee journal on selected areas in communications*, 34(4), 1010–1021.

Shen, K. & Yu, W. (2016). Load and interference aware joint cell association and user scheduling in uplink cellular networks. *Proc. ieee international workshop on signal processing advances in wireless communications (spawc)*, pp. 1–5.

Shi, C., Schmidt, D. A., Berry, R. A., Honig, M. L. & Utschick, W. (2009). Distributed interference pricing for the mimo interference channel. *Ieee international conference on communications (icc)*, pp. 1–5.

Siddique, U., Tabassum, H., Hossain, E. & Kim, D. I. (2015). Wireless backhauling of 5g small cells: challenges and solution approaches. *Ieee wireless communications*, 22(5), 22–31.

Spencer, Q. H., Swindlehurst, A. L. & Haardt, M. (2004). Zero-forcing methods for downlink spatial multiplexing in multiuser mimo channels. *Ieee transactions on signal processing*, 52(2), 461–471.

Tabassum, H., Sakr, A. H. & Hossain, E. (2016). Analysis of massive mimo-enabled downlink wireless backhauling for full-duplex small cells. *Ieee transactions on communications*, 64(6), 2354–2369.

Touzri, T., Ghorbel, M. B., Hamdaoui, B., Guizani, M. & Khalfi, B. (2016). Efficient usage of renewable energy in communication systems using dynamic spectrum allocation and collaborative hybrid powering. *Ieee transactions on wireless communications*, 15(5), 3327–3338.

Van Chien, T., Björnson, E. & Larsson, E. G. (2016). Joint power allocation and user association optimization for massive mimo systems. *Ieee transactions on wireless communications*, 15(9), 6384–6399.

Wang, B., Kong, Q., Liu, W. & Yang, L. T. (2017). On efficient utilization of green energy in heterogeneous cellular networks. *Ieee systems journal*, 11(2), 846–857.

Wang, C.-X., Haider, F., Gao, X., You, X.-H., Yang, Y., Yuan, D., Aggoune, H., Haas, H., Fletcher, S. & Hepsaydir, E. (2014). Cellular architecture and key technologies for 5g wireless communication networks. *Ieee communications magazine*, 52(2), 122–130.

Wang, N., Hossain, E. & Bhargava, V. K. (2016a). Joint downlink cell association and bandwidth allocation for wireless backhauling in two-tier hetnets with large-scale antenna arrays. *Ieee transactions on wireless communications*, 15(5), 3251–3268.

Wang, Y., Li, C., Huang, Y., Wang, D., Ban, T. & Yang, L. (2016b). Energy-efficient optimization for downlink massive mimo fdd systems with transmit-side channel correlation. *Ieee transactions on vehicular technology*, 65(9), 7228–7243.

Xia, W., Zhang, J., Jin, S., Wen, C.-K., Gao, F. & Zhu, H. (2017). Large system analysis of resource allocation in heterogeneous networks with wireless backhaul. *Ieee transactions on communications*, 65(11), 5040–5053.

Yadav, A., Nguyen, T. M. & Ajib, W. (2016). Optimal energy management in hybrid energy small cell access points. *Ieee transactions on communications*, 64(12), 5334–5348.

Yang, G., Ho, C. K., Zhang, R. & Guan, Y. L. (2015). Throughput optimization for massive mimo systems powered by wireless energy transfer. *Ieee journal on selected areas in communications*, 33(8), 1640–1650.

Yang, H. & Marzetta, T. L. (2013). Performance of conjugate and zero-forcing beamforming in large-scale antenna systems. *Ieee journal on selected areas in communications*, 31(2), 172–179.

Yang, S. & Hanzo, L. (2015). Fifty years of mimo detection: The road to large-scale mimos. *Ieee communications surveys & tutorials*, 17(4), 1941–1988.

Yuan, F., Jin, S., Huang, Y., Wong, K.-K., Zhang, Q. & Zhu, H. (2015). Joint wireless information and energy transfer in massive distributed antenna systems. *Ieee communications magazine*, 53(6), 109–116.

Zhang, Q., Jin, S., McKay, M., Morales-Jimenez, D. & Zhu, H. (2015a). Power allocation schemes for multicell massive mimo systems. *Ieee transactions on wireless communications*, 14(11), 5941–5955.

Zhang, Z., Wang, X., Long, K., Vasilakos, A. V. & Hanzo, L. (2015b). Large-scale mimo-based wireless backhaul in 5g networks. *Ieee wireless communications*, 22(5), 58–66.

Zhao, J., Quek, T. Q. & Lei, Z. (2015). Heterogeneous cellular networks using wireless backhaul: Fast admission control and large system analysis. *Ieee journal on selected areas in communications*, 33(10), 2128–2143.

Zhao, L., Zhao, H., Hu, F., Zheng, K. & Zhang, J. (2013). Energy efficient power allocation algorithm for downlink massive mimo with mrt precoding. *Proc. ieee vehicular technology conference (vtc-fall)*, pp. 1–5.

Zhao, L., Riihonen, T., Xiang, W., Kuang, Y. & Zheng, K. (2017). Resource optimization of wireless information and energy supply control systems with massive mimo. *Ieee communications letters*, 21(12), 2734–2737.

Zheng, K., Zhao, L., Mei, J., Shao, B., Xiang, W. & Hanzo, L. (2015). Survey of large-scale mimo systems. *Ieee communications surveys & tutorials*, 17(3), 1738–1760.

Zhou, Z., Zhou, S., Gong, J. & Niu, Z. (2014). Energy-efficient antenna selection and power allocation for large-scale multiple antenna systems with hybrid energy supply. *Proc. ieee global communications conference (globecom)*, pp. 2574–2579.

Zuo, J., Zhang, J., Yuen, C., Jiang, W. & Luo, W. (2017). Energy-efficient downlink transmission for multicell massive das with pilot contamination. *Ieee transactions on vehicular technology*, 66(2), 1209–1221.